

Aus der Kinderchirurgischen Klinik und Poliklinik
im Dr. von Haunerschen Kinderspital
der Ludwig-Maximilians-Universität München
Direktor: Prof. Dr. med. Dietrich von Schweinitz

Neurokinin-1 receptor as a therapeutic target in hepatoblastoma

Dissertation
zum Erwerb des Doktorgrades der Humanbiologie
an der Medizinischen Fakultät der
Ludwig-Maximilians-Universität zu München

vorgelegt von

Agnès Garnier

aus Poitiers, Frankreich

2016

Mit Genehmigung der Medizinischen Fakultät
der Universität München

Berichterstatter: Prof. Dr. rer. nat. Roland Kappler

Mitberichterstatter: Prof. Dr. rer. nat. Andreas Jung
Priv. Doz. Dr. Andreas Herbst
Prof. Dr. rer. nat. Olivier Gires

Mitbetreuung durch den
promovierten Mitarbeiter: PD Dr. med. Michael Berger

Dekan: Prof. Dr. med. dent. Reinhard Hickel

Tag der mündlichen Prüfung: 29.06.2016

TABLE OF CONTENTS

INTRODUCTION	1
1 Epidemiology	1
2 Clinical presentation, diagnosis	1
3 Histology	1
4 Staging systems.....	2
4.1 SIOPEL.....	2
4.2 COG.....	3
5 Molecular alterations in hepatoblastoma	3
5.1 The canonical Wnt signaling pathway	4
5.1.1 Description of the pathway	4
5.1.2 Role in cell adhesion	5
5.1.3 Role in the liver	6
5.1.4 Alterations of canonical Wnt signaling in cancer.....	6
5.1.5 Deregulation of canonical Wnt signaling in hepatoblastoma.....	7
5.2 PI3K/AKT/mTOR axis.....	8
5.2.1 Receptor Tyrosine Kinase (RTK).....	8
5.2.2 PI3K kinases	9
5.2.3 AKT.....	10
5.2.4 The mTORC1 complex	10
5.2.5 The mTORC2 complex	13
5.2.6 Deregulation of PI3K/AKT/mTOR axis in cancer	13
5.2.7 Alteration of PI3K/AKT/mTOR pathway in hepatoblastoma	14
5.2.8 Other molecular alterations described in hepatoblastoma	15
6 Treatment strategies	16
7 SP/NK1R complex	17
7.1 Description	17
7.2 The NK1R, truncated and full length forms.....	17
7.3 NK1R antagonists	19
8 Goal of the study	19
MATERIALS	20
1. Eukaryotic cell culture.....	20
1.1 Cell lines.....	20
1.2 Cell culture reagents.....	20

1.3	Cell culture material	20
1.4	Spheres culture	21
2.	Plasmids	21
3.	Antibodies	22
4.	Chemicals / Reagents	22
5.	Primers	24
6.	Buffer and Solutions	24
7.	Enzymes	25
8.	Kits	25
9.	Consumables	25
10.	Equipment	26
11.	Sofwares	27
METHODS		28
1.	Cell culture	28
2.	RNA isolation and RT-PCR	28
3.	Proliferation assays	28
4.	<i>In vitro</i> analysis of apoptosis	28
5.	Western blot analysis	29
6.	Reverse-phase protein array (RPPA)	29
7.	<i>In vitro</i> analysis of cell cycle	30
8.	Immunofluorescence	30
9.	Super TOP/FOP (STF) luciferase reporter assay	30
10.	Sphere formation culture	31
11.	Patients and Tumor Tissues	31
12.	Statistical analysis	32
RESULTS		33
1.	Hepatoblastoma cells express NK1R and can be growth inhibited by aprepitant <i>in vitro</i>	33
1.1	NK1R is expressed in human hepatoblastoma cell lines	33
1.2	Aprepitant inhibits tumor growth in human hepatoblastoma cell lines	34
1.3	SP reverses the anti-proliferative effect of NK1R antagonists	36
1.4	Aprepitant and cytostatics synergistically induce cell death of hepatoblastoma cells	37
1.5	NK1R antagonists induce apoptosis in hepatoblastoma cells	38
2.	Targeting the NK1R compromises canonical Wnt signaling in hepatoblastoma	41

2.1	NK1R inhibition leads to downregulation of the PI3K/AKT/mTOR and Wnt signaling pathways.....	41
2.2	NK1R antagonism leads to differential expression of the PI3K/AKT/mTOR pathway	43
2.3	NK1R inhibition compromises FOXM1 expression and subsequently diminishes canonical Wnt signaling.....	46
2.4	Wnt pathway inhibition by aprepitant is effective downstream of β -catenin and disrupts the FOXM1- β -catenin interaction.....	50
2.5	NK1R antagonism inhibits growth of hepatoblastoma cancer stem-like cells	52
3.	Targeting the NK1R inhibits growth of human colon cancer cells.....	59
3.1	NK1R blocking leads to the regulation of specific proteins involved in PI3K/AKT/mTOR and canonical Wnt signaling.....	59
3.2	NK1R antagonism induces apoptosis and a G2 arrest.....	62
3.3	NK1R antagonism inhibits canonical Wnt signaling.....	64
3.4	The inactivation of the Wnt pathway is independent from initial Wnt baseline activity	66
4.	The NK1R is an ubiquitous anti-tumor target in hepatoblastoma and its expression is independent from tumor biology and stage	69
4.1	<i>NK1R</i> is overexpressed in human hepatoblastoma	69
4.2	Expression of <i>NK1R</i> -tr correlates with <i>NK1R</i> -fl	70
4.3	<i>NK1R</i> expression does not correlate with biological features.....	70
4.4	Expression of <i>NK1R</i> does not correlate with clinical features.....	71
	DISCUSSION	77
1.	Hepatoblastoma cells express NK1R and can be growth inhibited by aprepitant <i>in vitro</i>	77
2.	Targeting the NK1R compromises PI3K/AKT/mTOR pathway in hepatoblastoma	79
3.	Targeting the NK1R compromises canonical Wnt signaling in hepatoblastoma	82
3.1	Aprepitant induces a downregulation of Wnt signaling	82
3.2	Aprepitant targets cancer stem-like cells.....	83
3.3	Crosslinks between PI3K/AKT/mTOR and canonical Wnt signaling	84
4.	Targeting the NK1R inhibits growth of human colon cancer cells.....	85
5.	The NK1R is an ubiquitous anti-tumor target in hepatoblastoma and independent from tumor biology and stage.....	87
	SUPPLEMENTAL FIGURE	90
	ABSTRACT	91
	ZUSAMMENFASSUNG	92
	ACKNOWLEDGMENT	93
	REFERENCES	94
	LIST OF ABBREVIATIONS	105

INTRODUCTION

1 Epidemiology

Although being a rare childhood cancer accounting for 1% of all pediatric neoplasms, hepatoblastoma represents 80% of hepatic-related cancers in children. This tumor affects approximately 1:1,000,000 children under the age of 15 and most predominantly between 6 months and 3 years^{1,2}.

It has been reported that the risk of developing hepatoblastoma is increased in subjects that are afflicted by several syndromes including Beckwith-Wiedemann syndrome (BWS)³, hemihypertrophy or familial adenomatous polyposis (FAP)⁴. Previous studies have also reported an increased incidence in subjects with low birth weight⁵.

2 Clinical presentation, diagnosis

This tumor is most frequently detected by palpation of an asymptomatic hepatomegaly. Other clinical presentations can include jaundice, weight loss, pain and/or fatigue depending on the tumor progression. Blood test and imaging such as computed tomography scan and magnetic resonance imaging are key for diagnosis. Blood tests often reveal high levels of Alpha-Feto-Protein (AFP), a robust marker of hepatoblastoma⁶. Less importantly, in some instances, it reveals a disruption of coagulation homeostasis as proteins of coagulation are synthesized in the liver.

At diagnosis, imaging reveals either an unifocal or multifocal tumor. Synchronous metastases are present in 20% of hepatoblastoma and are often localized in the lung. On the other hand, metachronous metastases are generally found in the lung as well as the brain and bones⁷.

3 Histology

The etiology of hepatoblastoma is still not known but the tumorigenesis is believed to occur through a derailed development of immature hepatocytes precursors, which normally differentiate into several cell types, including hepatocytes, epithelial, biliary and mesenchymal cells. This explains the cell heterogeneity of the tumor and the different

INTRODUCTION

histological subtypes. Hepatoblastoma can be classified in the epithelial (56%) or mixed form (epithelial and mesenchymal, 44%). The epithelial form further regroups the pure fetal (31%), embryonal (19%), macrotrabecular (3%) and the small-cell undifferentiated (3%) subtypes⁸, the latter being associated with poor prognosis⁹.

4 Staging systems

There are currently four leading childhood liver study groups in the world: the International Society of Pediatric Oncology group (SIOPEL) which is located in Europe, the Children's Oncology Group (COG) in North America and the national study groups from Germany (GPOH) and Japan (JPLT). As mentioned above, techniques such as magnetic resonance imaging, computed tomography and blood tests are used to evaluate the PRE-Treatment tumor EXTension (PRETEXT), POST-Treatment EXTent of Tumor (POSTTEXT), AFP level, tumor histology and metastatic diseases¹⁰⁻¹³. Each group has their own staging system and treatment strategies although recent efforts are made toward standardization¹⁴. Here, we will only describe the methodologies instigated by the SIOPEL and COG groups.

4.1 SIOPEL

The PRETEXT staging system, originally created by the SIOPEL group, is based on imaging prior to any treatment to characterize the localization of the tumor using Couinaud's system of segmentation of the liver.

It distinguishes four PRETEXT stages (Figure 1) but also uses other parameters to assess the spread of the tumor beyond the liver (lymph node metastases, portal vein involvement, involvement of the inferior vena cava and/or hepatic veins, extrahepatic abdominal disease, tumor rupture or intraperitoneal haemorrhage disease, distant metastases)¹⁵.

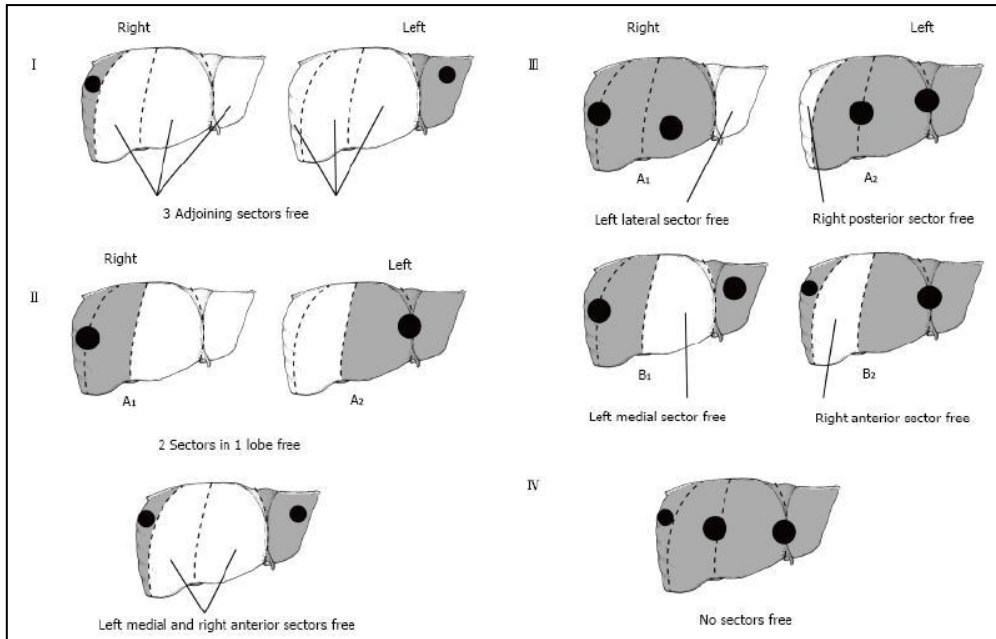


Figure 1: PRETEXT staging system

I: one section is involved and the 3 adjoining sectors are free. II: two sections are involved. III: two or three sections are involved and no two adjoining sections are free. IV: all sections are involved. Figure taken from Kadheri et al.¹⁶

4.2 COG

The POSTTEXT staging system was developed by the COG group. The staging methodology consists of an initial surgery attempt to completely resect the tumor followed by chemotherapy courses. Following the surgery, four groups are distinguished depending on the outcome: stage I, corresponds to complete resection; stage II to microscopic residual; stage III to macroscopic residual and stage IV to distant metastases.

5 Molecular alterations in hepatoblastoma

Different molecular alterations have been identified as being involved in the genesis of hepatoblastoma. More particularly, a deregulation of different signaling pathways has been described among which the canonical Wnt signaling, Sonic Hedgehog, Notch and phosphatidylinositol 3-kinase/protein kinase B/mammalian target of rapamycin (PI3K/AKT/mTOR)¹⁷.

5.1 The canonical Wnt signaling pathway

5.1.1 Description of the pathway

The canonical Wnt signaling pathway is known to play a vital role in the regulation of cell proliferation, survival and differentiation¹⁸. In 1982, the mouse mammary tumor virus caused tumor development in mice via increased expression of an unknown gene that became known as *Integration 1 (Int1)*¹⁹. Simultaneously, the previously discovered *Wingless (Wg)* gene, mutated in fruit flies lacking wings, was found to be a homologue of *Int1*²⁰. This led to the description of the Wnt pathway (Wnt is a fusion of Wg and Int1)²¹. The level of conservation also highlights the importance of this pathway in development.

Currently, we have a good understanding of the mechanisms involved in the Wnt pathway (Figure 2):

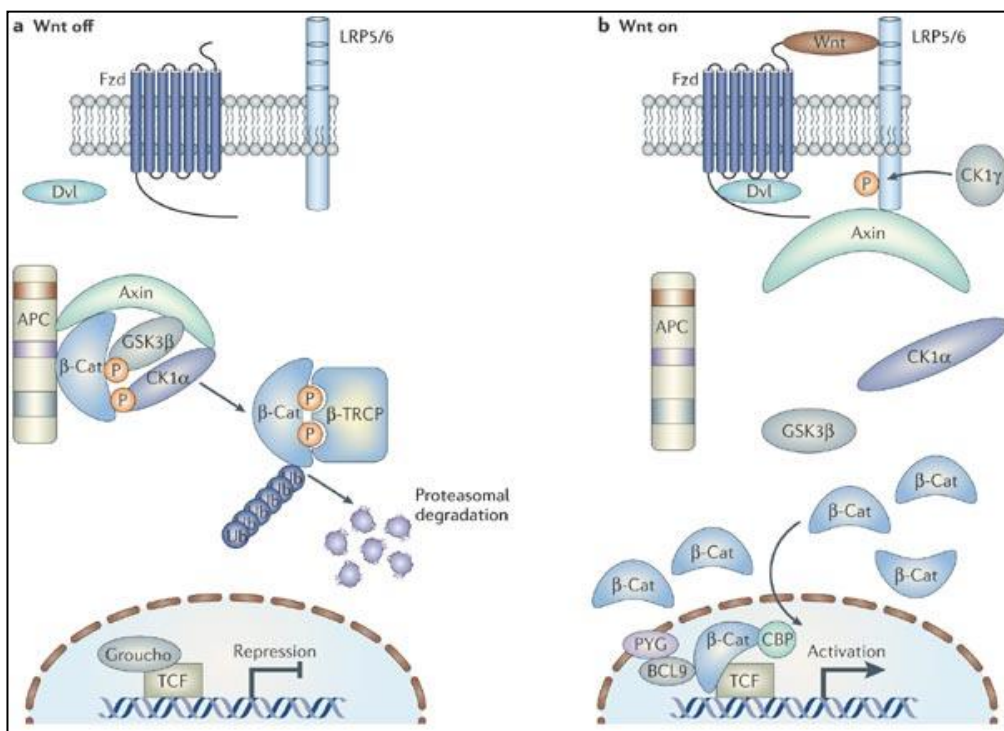


Figure 2: Representation of the canonical Wnt pathway

(a) Wnt off: ubiquitin-dependent degradation of β-catenin in the cytosol by the destruction complex (GSK3β, AXIN, CK1α, APC) through phosphorylation processes. TCF transcription factors are repressed by Groucho and Wnt target gene expression is inhibited. (b) The binding of the Wnt ligand to its receptor induces the sequestration of AXIN, which therefore inactivates the destruction complex. β-catenin subsequently accumulates in the cytoplasm and is free to translocate into the nucleus, where it binds to TCF to activate Wnt target gene expression. Figure taken from Barker et al.²²

In the absence of Wnt ligand, cytoplasmic β-catenin is taken up by a destruction complex, made up of APC, AXIN and two kinases, namely glycogen synthase kinase 3β (GSK3β)

INTRODUCTION

and casein kinase 1 α (CK1 α), which phosphorylates the N-terminus of β -catenin²³. It is then ubiquitinated by β -transducin repeat-containing protein and degraded in proteasomes, keeping cytoplasmic β -catenin at low levels²⁴. In this state, a molecule called Groucho interacts with and inhibits the transcription factors LEF/TCF of this pathway, suppressing the expression of the Wnt target genes²⁵.

However, in the presence of Wnt ligands (19 Wnt ligands have been discovered in humans²¹), they bind to Frizzled receptors and LRP5/6 co-receptors. This results in the phosphorylation of LRP5/6 by casein kinase 1 γ and the recruitment of the Dishevelled protein to the membrane, which causes AXIN translocation to the membrane²⁶. This inactivates the destruction complex, disrupting β -catenin phosphorylation, and hence stabilizing the β -catenin concentration in the cytosol. Therefore, β -catenin is free to translocate to the nucleus, where it displaces the repressive Groucho molecules, forming its own complex with LEF/TCF²⁷, resulting in the activation of Wnt target gene expression.

Many Wnt target genes have been discovered, most importantly the proto-oncogene *MYC* and *cyclin D1* involved in cell cycle regulation²⁸. Other target genes include the actual components of the Wnt pathway (*Frizzled*, *LRP5/6*, *AXIN*, *LEF/TCF*) providing a mechanism by which this pathway could auto-regulate itself²¹.

In the late 1990s, a number of Wnt pathway inhibitors were discovered: secreted Frizzled-related peptides, Wnt inhibitory factor 1 and Dickkopfs (DKKs)^{29, 30}. One study showed the inhibitory effect of one DKK receptor, Kremen, via LRP receptor internalization³¹. Another family of Wnt homologues, the R-spondins, have also been discovered to activate the canonical Wnt signaling pathway through interacting with the Frizzled/LRP complex³².

5.1.2 Role in cell adhesion

The presence of β -catenin is essential for cell adhesion. It creates a bridge between the cytoplasmic part of E-cadherin and the actin cytoskeleton to form adherens junctions, which promote lateral cell anchoring³³. Interestingly, previous work identified this complex as being involved in canonical Wnt signaling regulation. Indeed, the APC protein, β -catenin and E-cadherin never seem to associate simultaneously: the complexes APC/ β -catenin and E-cadherin/ β -catenin appear mutually exclusive³⁴. It has been reported that following the decrease of E-cadherin expression, the level of free β -catenin increases, which promotes its nuclear translocation and subsequently Wnt target gene expression³⁵.

INTRODUCTION

The mechanics by which β -catenin and E-cadherin interact is partially uncovered. In the endoplasmic reticulum, E-cadherin is specifically phosphorylated allowing its binding to β -catenin and at the same time, preventing its degradation³⁶. Once at the membrane, phosphorylation of β -catenin at distinct sites by several kinases, can regulate the complex association³⁷. For example, the hepatocyte growth factor triggers phosphorylation of β -catenin at tyrosine 654 and tyrosine 670 in hepatocytes, which induces the disruption of the complex and nuclear translocation of β -catenin³⁸.

5.1.3 Role in the liver

It is well established that canonical Wnt signaling plays an important role in liver homeostasis: from embryonic liver to its functional maturation, which reinforces its role in hepatoblastoma tumorigenesis³⁹⁻⁴¹. However, in the adult liver, canonical Wnt signaling is not activated except in the centrizonal region of the hepatic lobule as proved by positive nuclear and cytoplasmic β -catenin in this area⁴¹. This was associated with the regulation of genes involved in ammonia and xenobiotic metabolism.

Importantly, reactivation of this pathway also occurs during liver regeneration in adults⁴². It is a really unique process allowing for instance spontaneous regrowth of the liver after partial hepatectomy⁴³. This process is known to occur through the proliferation of mature cells, including hepatocytes, and doesn't cause any inflammation to the surrounding tissues⁴⁴. At the molecular level, Wnt signaling is quickly activated through inhibition of β -catenin degradation resulting in an increase of the protein by 2.5 fold and its nuclear translocation⁴². In the nucleus, β -catenin induces proliferation through positive regulation of genes implicated in cell cycle regulation such as *cyclin D1*⁴¹, and protein level returns back to normal 48 hours post resection⁴².

5.1.4 Alterations of canonical Wnt signaling in cancer

Mutations in the canonical Wnt signaling pathway have been shown to deregulate the cell cycle, resulting in the development of human cancers. For example, *CTNNB1* (the β -catenin gene) mutations are found in numerous cancers, including colorectal, hepatocellular, ovarian cancers and notably hepatoblastoma⁴⁵. The majority of these mutations result in the deletion/alteration of the N-terminal fragment of β -catenin, and hence

INTRODUCTION

its degradation in the cytosol⁴⁵. Therefore, excess β -catenin translocates to the nucleus and binds to LEF/TCF, resulting in the overexpression of Wnt target genes.

However, the most famous mutation of the Wnt pathway concerns *APC*, located at the 5q21-22 locus⁴⁶, which is mutated in FAP patients, an inherited disease associated with the development of thousands of benign polyps in the colon, of which a few inevitably become malignant⁴⁷, as well as in patients with sporadic colorectal cancers⁴⁷.

The APC protein contains a region of SAMP repeats (three repeats of a specific sequence of amino-acids) that are vital for its successful binding to both AXIN and β -catenin^{48, 49}. However, in colorectal cancer, numerous types of mutations (frameshift, nonsense and splice-site) build up prior to this region, leading to the truncation of 50% of the APC proteins⁴⁵. This disrupts the destruction complex, which allows an increase of cytoplasmic/nuclear β -catenin and thus an overexpression of Wnt target genes.

5.1.5 Deregulation of canonical Wnt signaling in hepatoblastoma

High frequency of point mutations and deletions in exon 3 of *CTNNB1* was first reported by Koch et al.⁵⁰ and confirmed by others (49%-89%)⁵¹ indicating a crucial role of this pathway in hepatoblastoma. Subsequent immunohistochemistry experiments confirmed an aberrant cytoplasmic/nuclear localization of β -catenin in the majority of hepatoblastomas⁵²⁻⁵⁴. Other members of the pathways have been screened for mutations in sporadic hepatoblastoma such as *AXIN1*, *AXIN2* or *APC*. Although some discrepancies exist between studies, *AXIN1* was found mutated in 1.6%⁵⁵ or 7.4%⁵⁶, whereas *AXIN2* was found mutated in 5.4%⁵⁷ of the cases investigated. Furthermore, germline mutations of *APC* were reported in 10%⁵⁸ and somatic mutations in 61.5%⁵⁹ of sporadic hepatoblastoma.

Apart from this, one study focusing on Wnt antagonists revealed a transcriptional up regulation of this particular class in hepatoblastoma cells. The fact that Wnt signaling is constitutively expressed in Wnt mutated cells despite the high level of antagonists, indicates the presence of a complex regulation mechanism of β -catenin within these cells⁶⁰.

Finally, previous studies have found no correlation between elevated Wnt activity and *MYC* expression in normal liver cells as well as hepatoblastoma cells, which implies that this gene is most likely not a Wnt target gene in this context^{53, 61, 62}.

5.2 PI3K/AKT/mTOR axis

The PI3K/AKT/mTOR signaling pathway is involved in the regulation of many cellular functions, such as metabolism, proliferation, survival and motility⁶³. This pathway is often deregulated in cancer cells, such as hepatoblastoma⁶⁴, as most of its proteins are tumor suppressor genes or proto-oncogenes whose mutation or anarchic expression can promote the development of a tumor^{65, 66}. Therefore, this pathway constitutes an interesting therapeutic target⁶⁷.

5.2.1 Receptor Tyrosine Kinase (RTK)

The PI3K/AKT/mTOR pathway is most often activated through a RTK, itself stimulated by multiple ligands (growth factors such as IGF, EGF or cytokines). It induces the activation of many intracellular proteins through cascades of phosphorylations⁶⁸. Numerous human RTK have been characterized today constituting 20 subfamilies illustrated in Figure 3. Of note, the epidermal growth factor receptor (EGFR) was the first RTK characterized and found mutated in cancer⁶⁹.

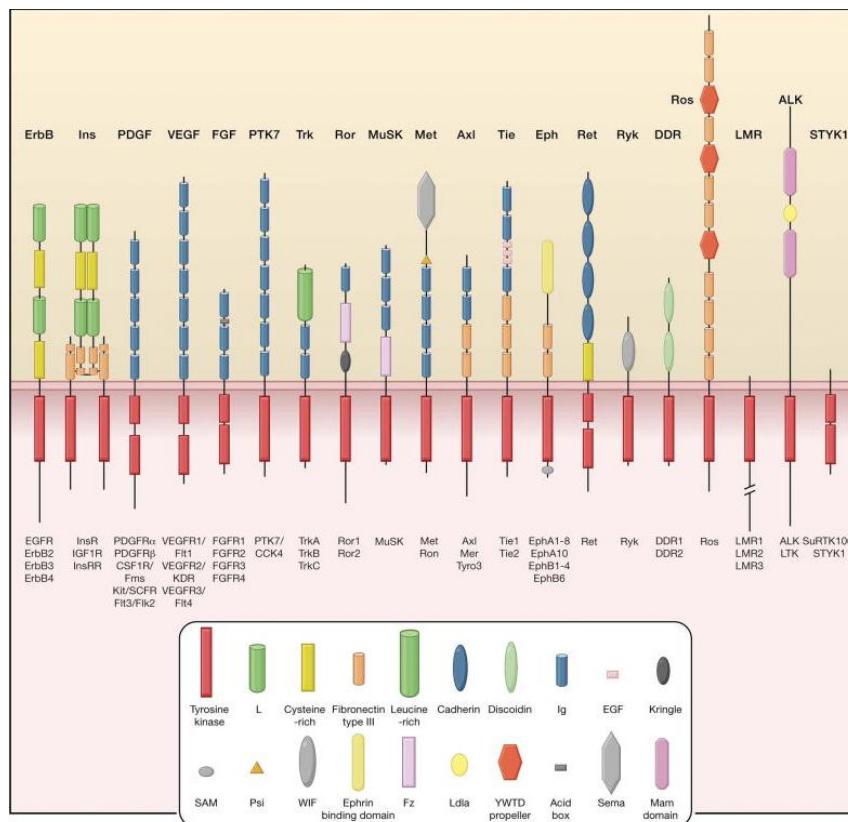


Figure 3: Illustration of the subfamilies of human RTK
 RTK are grouped into 20 subfamilies, all characterized by intracellular domains containing the tyrosine kinase (red rectangles). Members of each subfamilies are shown under each receptors. Figure taken from Lemmon et al.⁶⁸

INTRODUCTION

More precisely, following the binding of the ligand, the receptor is activated through dimerization and transphosphorylation of its intracellular portion mediated by conformational changes, corresponding to the activation of the tyrosine kinase domain⁷⁰. Several signaling pathways have been described to be activated following the activation of a RTK, the most described being the PI3K/AKT/mTOR, RAS/Raf/MAPK, JAK/STAT3 and Src/PLC γ pathways⁷⁰. Here, we will focus on the PI3K/AKT/mTOR pathway.

5.2.2 PI3K kinases

PI3K are lipid serine/threonine kinases constituted of 2 subunits: p85 (regulatory subunit) and p110 (catalytic subunit), the latter being activated by RTK. PI3K can be grouped in three different classes (I, II, III)⁷¹. PI3K from class I-A, a particular subgroup of class I, are the most commonly found in cancer. The regulatory subunit p85 contains a SH2 domain, recognizable by the phospho-tyrosine of the activated RTK as well as by adaptor proteins such as the insulin receptor substrate family of adaptors (IRS)⁷².

In any cases, upon activation, PI3K phosphorylates the phosphatidylinositol-4,5-bisphosphate (PIP₂) at the membrane through its catalytic subunit p110, to form the phosphatidylinositol-3,4,5-triphosphate (PIP₃)⁷³. At the membrane, PIP₃ can further recruit proteins with Pleckstrin Homology (PH) domain such as Phosphoinositide-Dependent Kinase-1 (PDK1) and AKT. PIP₃ is thus a phospholipid second messenger, which is mandatory for AKT activation⁷⁴. Phosphatase and tensin homologue (PTEN) catalyzes the dephosphorylation of PIP₃ into PIP₂, which abrogates the signal (Figure 4).

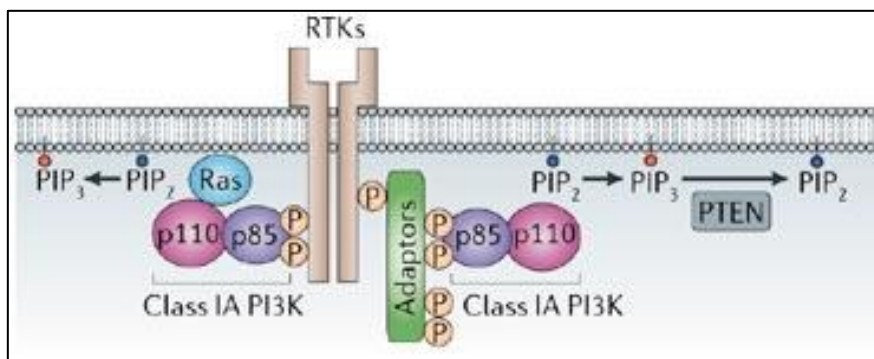


Figure 4: Mechanisms of activation of PI3K from class IA

PI3K from class IA can be activated by RTK or by adaptors through the SH2 domain of its regulatory subunit (p85), which recognizes and docks to phosphorylated tyrosines. Catalytic subunit of PI3K (p110) subsequently phosphorylates PIP₂ at the membrane to form PIP₃. Negative regulation of this pathway is mediated by the phosphatase PTEN, which dephosphorylates PIP₃ into PIP₂. Figure taken from Engelman et al.⁷⁵

5.2.3 **AKT**

AKT is a serine/threonine kinase whose activation is subsequent to its binding to PIP3 at the membrane through its PH domain⁷⁶. There are different isoforms of AKT kinases, which are encoded by the *AKT1*, *AKT2* and *AKT3* genes. AKT1 is found ubiquitously in human tissues and is characterized by two phosphorylation sites: threonine 308 (T308) and serine 473 (S473), which are essential for its activation. The association of AKT to PIP3 is followed by conformational changes leading to the exposure of AKT phosphorylation sites at T308 and S473. PDK1, another substrate of PI3K localized at the membrane, is responsible for the phosphorylation at threonine 308^{77, 78}, whereas the phosphorylation at S473 is performed by the complex mTORC2⁷⁹ (see 5.2.5).

AKT has several biologically relevant roles. For instance, it modulates the activity of Forkhead box O (FOXO) transcription factors (FOXO1, FOXO3a), which regulate the expression of genes implicated in stress, cell-cycle and metabolism⁸⁰. Furthermore, AKT can also inhibit GSK3 β by phosphorylation (serine 9), a member of the Wnt pathway⁸¹. Other important regulations concern the apoptosis process: AKT phosphorylates Bcl-2, a pro-apoptotic marker, which inactivates it and in turn promotes cell survival⁸².

5.2.4 **The mTORC1 complex**

mTOR is a 289 kDa serine threonine kinase, highly conserved between species, which belongs to the phosphatidylinositol 3-kinase-related kinase (PIKK) family. Its association with various proteins forms two distinct complexes: mTORC1 and mTORC2 implicated in fundamental biological processes, which monitor amino acid, glucose, oxygen, energy and growth factor levels (Figure 5).

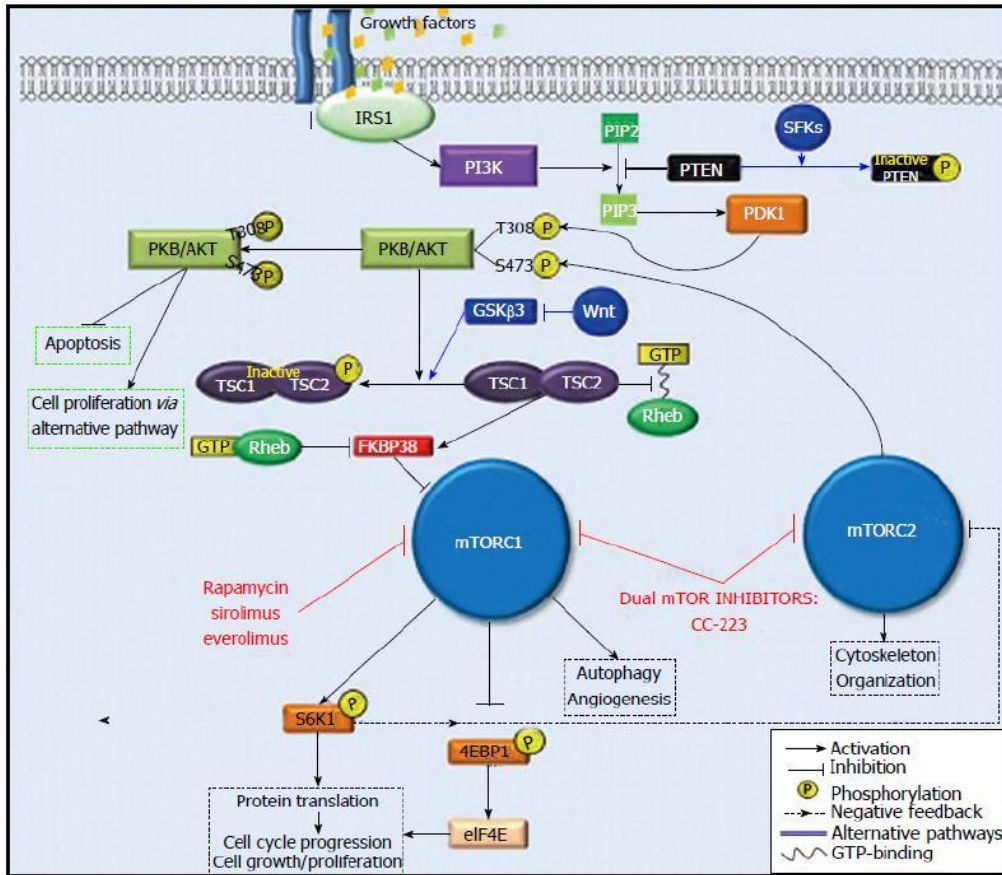


Figure 5: Schematic representation of PI3K/AKT/mTOR pathway

Upon activation, AKT phosphorylates TSC2, which inhibits its GAP (GTPase activating protein) activity and ultimately the TSC2/TSC1 complex. Therefore, Rheb remains in its active GTP conformation and mTORC1 complex is activated. mTORC1 regulates autophagy and angiogenesis as well as protein translation and cell proliferation through the modulation of p70S6K and 4EBP1. mTORC2 complex is involved in cytoskeleton organization and is negatively regulated by p70S6K. AKT also regulates fundamental processes via alternative pathways such as apoptosis and cell proliferation. Figure taken from Ashworth et al.⁸³

The mTORC1 complex, which is rapamycin sensitive, consists of 5 components, namely mTOR, mammalian Sec13 protein with lethal 8 (mLST8), Regulatory-Associated Protein to mTOR (RAPTOR), Proline-Rich AKT Substrate of 40kDa (PRAS40), DEP domain-containing mTOR-interacting protein (DEPTOR) and FKBP38. This complex is a global regulator of cell metabolism through modulation of anabolic and catabolic processes (such as autophagy), and of cell growth through control of protein synthesis. Its activity is thus related to the presence of growth factors and nutrient availability and is mediated by the regulation of its downstream proteins such as p70 ribosomal S6 kinase (p70S6K) and Eukaryotic Translation Initiation Factor 4E Binding Protein 1 (4E-BP1)^{84, 85}.

The mechanism by which this complex is regulated is partially elucidated. mTORC1 is negatively regulated by some of its constitutive components, namely PRAS40 and DEPTOR. These two proteins inhibit the complex by direct physical interaction^{85, 86}.

INTRODUCTION

Furthermore, mTORC1 can also be inhibited by GDP conformation of Ras homolog enriched in brain (Rheb) through the activation of the Tuberous Sclerosis complex 1/2 (TSC1/TSC2). Indeed, TSC2 is a GTPase-activating protein, which changes the state of Rheb from GTP (active) to GDP (inactive). On the contrary, when fully activated, AKT can inactivate TSC2 by phosphorylation, which results in Rheb-GTP conformation and promotes mTORC1 activity⁸⁷. The role of mLST8 remains unclear.

mTORC1 is an important regulator of protein synthesis as it is responsible for the phosphorylation of p70S6K, a kinase belonging to the AGC family. The activation of p70S6K triggers the phosphorylation of eIF4B, which promotes the cap-dependent translation and elongation by enhancing the RNA helicase activity of eIF4A⁸⁴. The regulation of p70S6K involves a complex interplay of phosphorylations⁸⁸.

The 14 kDa protein 4EBP1 is another key regulator of protein synthesis. Its phosphorylation by mTORC1 enables the activation of eIF4E, which permits the translation of mRNA by activation of eIF4F complex⁸⁹ (Figure 6).

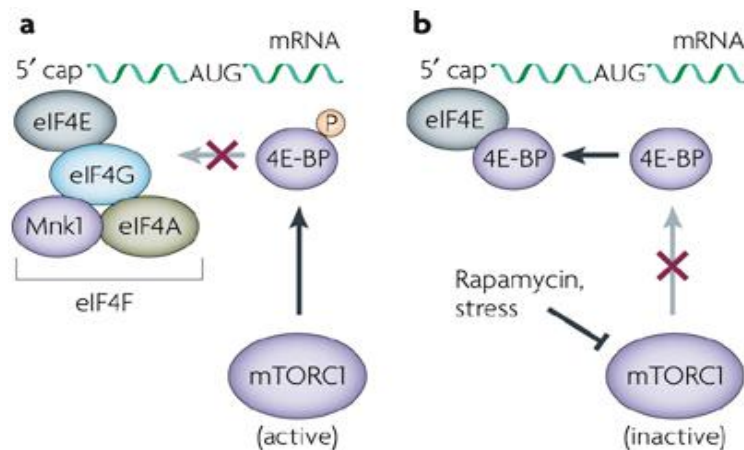


Figure 6: Regulation of cap-dependent translation by 4E-BP

eIF4F complex is composed of eIF4E subunits, which binds to the 5' cap, eIF4G a scaffold protein, MnK1 (Mitogen-activated protein kinase-interacting kinase 1) an EIF4E kinase and eIF4A an RNA helicase. a: Active mTORC1 phosphorylates and inactivates 4E-BP, therefore enabling the association of eIF4F complex and cap-dependant translation. b: In its dephosphorylated form, 4E-BP binds to and sequesters eIF4E inhibiting eIF4F formation. Figure taken from Buchkovich et al.⁹⁰

5.2.5 The mTORC2 complex

Comparatively to mTORC1, little is known about mTORC2. It is composed of different proteins, namely mTOR, Rictor (rapamycin-insensitive companion of TOR), SIN1 (stress-activated map kinase-interacting protein 1), mLST8 (also named GβL), DEPTOR and PPR5/PROTOR. Unlike mTORC1, it is relatively insensitive to rapamycin⁹¹. It is also involved in critical processes such as cytoskeleton organization, metabolism, cell survival and proliferation.

Previous studies have shown that Rictor and SIN1 were essential for mTORC2 activation and could have the same function as RAPTOR, that is complex stabilization and substrate recruitment⁹². Other studies have also linked TSC1/TSC2 to the activation of mTORC2⁹³. Moreover, experiments of mLST8 knockout have shown that this protein was mandatory for optimal mTORC2 activity⁹⁴. On the other hand, inhibition of mTORC2 activity was shown to be mediated partially by DEPTOR⁸⁵ and as far as is currently known, it is the only characterized endogenous direct inhibitor of this complex. The protein p70S6K was also shown to inhibit mTORC2 through inhibition of Rictor⁹⁵.

mTORC2 allows the activation of AKT as it is responsible for S473 phosphorylation. Other mTORC2 targets include members of the AGC kinase family such as protein kinase Cα (PKCα) and serum and glucocorticoid-induced protein kinase 1 (SGK1)⁹⁶. Of note, a negative feedback has been described between mTORC1 and mTORC2. Upon activation, mTORC1 inhibits mTORC2 activity via activation of p70S6K, which phosphorylates Rictor decreasing subsequently AKT phosphorylation at S473⁹⁷. Another negative feedback involves IRS proteins which abrogate PI3K dependent activation of AKT⁹⁸.

5.2.6 Deregulation of PI3K/AKT/mTOR axis in cancer

Several alterations of the pathway have been characterized such as in RTK, PI3K, PTEN or AKT inducing a constitutive activation of the pathway. These alterations can be due to chromosomal translocation, overexpression or gain of function mutation. In any cases, this leads to the breaking of the fragile balance between cell death and cell survival promoting the oncogenesis process.

PTEN is often found mutated in cancer and the result of these mutations is most often a truncated protein with loss of function. This leads to an accumulation of PIP3 and thus

INTRODUCTION

activation of the pathway. PTEN can also be altered due to epigenetic modifications as previously described in colorectal cancers. For instance, Goel et al. reported that hypermethylation of *PTEN* promoter correlated significantly with decrease or complete loss of PTEN protein expression in sporadic colorectal cancer with microsatellite-instability⁹⁹. Somatic mutations of the gene encoding the catalytic subunit of PI3K have also been identified in many solid tumors¹⁰⁰ as well as mutations of the kinase domain, which become constitutively active¹⁰⁰.

Finally, mutations in genes encoding AKT isoforms have been reported for instance in the PH domain, which confers a membranous localization independently of PIP3. Therefore, AKT become constitutively activated by phosphorylation mediated by PDK1 and mTORC2¹⁰¹.

5.2.7 Alteration of PI3K/AKT/mTOR pathway in hepatoblastoma

A study conducted by Hartmann et al.⁶⁴ revealed that point mutation of *PI3KCA* (p110 α subunit of PI3K) was present in 2% of the tumors investigated, resulting in a gain of kinase activity. Moreover, they found that PI3K/AKT/mTOR activation was actually central for hepatoblastoma survival as demonstrated by PI3K inhibition *in vitro* and subsequent reduction of AKT and GSK3 β phosphorylation⁶⁴. Further, the insulin like growth factor (IGF) axis was also shown to be implicated in hepatoblastoma growth¹⁰². This pathway was found to be over activated as a result of IGF2 ligand overexpression, conferring a constant anti-apoptotic signal to the cells mediated through the insulin-like growth factor 1 receptor (IGF1R)¹⁰³. An epigenetic mechanism was shown to be responsible for this alteration. Indeed, *IGF2* expression is normally restricted to the paternal allele as the maternal copy is epigenetically silenced (genomic imprinting). However, loss of imprinting was described for *IGF2* ultimately leading to a biallelic expression which is responsible for its overexpression¹⁰⁴. Finally, regulators of this axis have also been implicated in hepatoblastoma growth namely the insulin-like growth factor binding proteins (IGFBP). The function of these proteins is to repress ligands by physical interaction in order to prevent their binding to the receptor. In hepatoblastoma, altered expression of IGFBP-1 and IGFBP-2 has been described¹⁰⁵⁻¹⁰⁷.

5.2.8 Other molecular alterations described in hepatoblastoma

The two other embryonic pathways, Hedgehog and Notch, have been described to be altered in hepatoblastoma as well. A recent study has shown an overexpression of Hedgehog ligands, which contributes to the activation of the pathway and the expression of target genes mediated by the activation of the transcription factor *GLI*¹⁰⁸. These target genes, particularly implicated in cell cycle regulation, participate therefore in the tumorigenesis process and inhibiting this pathway with cyclopamine induces a striking growth inhibition of hepatoblastoma cells¹⁰⁸. On the other hand, activation of Notch signaling was more observed in fetal subtypes. Immunohistochemistry experiments revealed an overexpression of the receptor *NOTCH2* in 92% of the tumors compared to normal liver tissues¹⁰⁹, which was associated with an upregulation of its downstream target *HES1*¹¹⁰.

Other anomalies have been described at the epigenetic level. More particularly, several tumor suppressor genes have been shown to be altered through DNA methylation in their promoter sequence, which in turn inactivates them. For instance, secreted frizzled-related proteins (*SFRP*) are negative modulators of the Wnt pathway by competing with the actual ligands. Therefore, loss of expression results in enhanced Wnt activity. Similarly to *SFRP*, Hedgehog-interacting proteins (*HHIP*) which are negative modulators of the Hedgehog pathway, are also altered through hypermethylation¹⁰⁸. Finally, silencing of *APC* through hypermethylation has been described in about 30% of hepatoblastoma¹¹¹.

Genetic aberrations in several chromosomes have been identified such as gains of chromosomes 1q, 2q, 2p, 6q, 8q, 17q and 20, and losses on chromosomal region 4q¹¹². Interestingly, gains on chromosomes 8 and 2 were found to be associated with a so called C2 subclass of hepatoblastoma introduced by Cairo et al.⁵⁵.

Using gene expression profiling this group identified two subclasses of hepatoblastoma tumors namely C1 and C2, which exhibit similarity with distinct phases of liver development. The C2 subclass, which conforms to an embryonal histotype was found to proliferate faster than the fetal-like C1 subclass. In accordance, the C2 tumors highly expressed cell cycle related genes such as *CDC2* and *DLG7*, and displayed intense nuclear accumulation of β -catenin. Importantly, they described a 16-gene signature, which corresponds to the 16 most

INTRODUCTION

differentially expressed genes between C1 and C2, and therefore allows classification of the tumors between these two subclasses⁵⁵.

From a clinical perspective, the tumors with a C2 signature were shown to be associated with poor prognosis for the disease with a more advanced tumor stage (metastasis, vascular invasion). The 2 years overall survival was 44% for patients with C2 tumors against 92% for patients with C1 tumors⁵⁵.

6 Treatment strategies

During the last 30 years, several clinical trials have been conducted in order to increase the survival of children with hepatoblastoma. One of the major breakthroughs is the use of platinum based chemotherapeutic agents (such as cisplatin and carboplatin), which greatly improved the survival in children from 30% to 70%².

Cisplatin alone¹⁶ or in combination with other cytostatics (5-fluorouracil, vincristine, doxorubicin, carboplatin) remains the first choice for chemotherapy courses in all four liver study groups. The chemotherapy recommendations depend on the stage of the tumor and differ between the four liver study groups^{113, 114}, although all four groups adopted recently PRETEXT staging system¹¹⁵. For instance, SIOPEL recommends preoperative chemotherapy with the ultimate goal to shrink the tumor to allow tumor resection, which is the only way to achieve a definitive cure¹¹⁶. In some cases, such as in patients with a fetal histology tumor, chemotherapy is not advised and only surgery is advocated as being curative by itself¹¹⁷. However, in children with unresectable tumors, orthotopic liver transplantation is the main choice for treatment^{118, 119}.

Despite the progresses witnessed in hepatoblastoma treatment evoked above, there remains a large margin for progression, both in terms of the effectiveness of the treatments and of the severity of their side effects. For instance, high risk patients (SIOPEL PRETEXT IV or COG stage IV) have a 5-year overall survival rate in between 30.9% and 39.3% depending on the staging system¹²⁰. Furthermore, one limitation of chemotherapy treatment is multidrug resistance (MDR), which often occurs after four cycles of chemotherapy¹²⁰. It is associated with an increased expression of the *MDR* gene coding for P-glycoprotein¹²¹. This protein is a transmembrane receptor, which acts as an ATP-reliant pump allowing the evacuation of drugs or other molecules¹²². Another downside with the use of chemotherapeutic agents is the strong toxicity induced by these molecules. For instance,

INTRODUCTION

cisplatin is responsible for ototoxicity and nephrotoxicity after several courses¹²³, whereas doxorubicin is highly cardiotoxic¹²⁴.

New treatment strategies are needed that tackle the limitations and downsides of the aforementioned methods. A promising target for innovative approaches to hepatoblastoma treatment is the Substance P (SP)/Neurokinin-1 receptor (NK1R) complex.

7 SP/NK1R complex

7.1 Description

Currently, there are three main classes of neurokinin receptors characterized in human: neurokinin-1 receptor (NK1R), neurokinin-2 receptor (NK2R) and neurokinin-3 receptor (NK3R), which are encoded by *TACR1*, *TACR2* and *TACR3* genes, respectively. These three receptors, which are G-protein coupled receptors (GPCRs), have high sequence and structure homologies but are differentially expressed within human tissues. NK1R is expressed in the central nervous system as well as in the periphery, while NK2R is mainly expressed in peripheral tissues such as the gastrointestinal system, lungs, bladder and the uterus. NK3R is found in the central nervous system but its expression is also detected in some peripheral tissues such as the liver and lungs¹²⁵⁻¹²⁹.

The neurokinin receptors regulate a variety of fundamental biological processes: regulation of neuronal activity, cell proliferation, nociception, endocrine and exocrine secretions, vasodilatation, inflammation and regulation of the immune system^{125, 130-132}. The ligands of these receptors belong to the tachykinin family and each ligand has a specific affinity for the three receptors. For instance, neurokinin A binds preferentially to NK2R, neurokinin B to NK3R and SP to NK1R¹²⁵. We will now focus on NK1R.

7.2 The NK1R, truncated and full length forms

In humans, the *TACR1* gene is located on the chromosome 2 and is constituted of five exons. In its full length form, NK1R is a protein of 417 amino acids¹³³. It belongs to the class I of GPCRs and can be coupled to several groups of G proteins: the G α_q , G α_s and the G α_i ^{134, 135}. The receptor conformation and the types of ligands have been shown to determine the specificity of the response through the activation of a specific G protein^{136, 137}. Indeed, these proteins differ in their signaling pathway and effectors that they activate. For example, the coupling with the G α_q protein results in the activation of phospholipase C β

INTRODUCTION

(PLC β), which causes an increase of PIP3. The activation of PLC β also induces the release of diacylglycerol (DAG), which ultimately induces an increase of intracellular calcium¹³⁸.

The coupling with G α s activates the enzyme adenylyl cyclase (AC) and thus stimulates the production of cyclic adenosine monophosphate (cAMP). An increased concentration of cAMP activates the protein kinase A (PKA), which phosphorylates specific substrates¹³⁹. Finally, coupling with G α i inhibits AC decreasing thereafter the concentration of cAMP in the cell^{140, 141}. In any cases and most importantly, these cascades lead to a specific physiological response via the transcription of specific genes.

The NK1R, like other GPCRs, undergoes a rapid desensitization and internalization through phosphorylation processes, with a subsequent recycling at the membrane¹⁴². More precisely, this mechanism is relying on β -arrestin/clathrin proteins and endocytosis¹⁴³. Interestingly, Roosterman et al. showed that NK1R internalization is dependant on the SP concentration: at low concentrations (1 nM) the receptor is internalized and quickly recycled at the membrane, whereas at high concentrations (10 nM), the process takes more time with an endocytosis into perinuclear endosomes¹⁴⁴.

Recently, the description of a truncated form of the NK1R was reported (NK1R-tr) (Figure 7). This isoform is produced by alternative splicing: the intron between exons 4 and 5 is not removed and, therefore, a premature stop codon appears resulting in a protein lacking 96 amino acids at the C-terminus part^{145, 146}. Importantly, the loss of this specific part was associated with a loss of internalization¹⁴⁷.

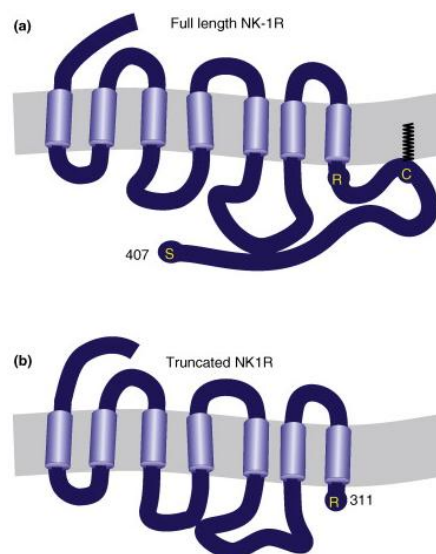


Figure 7: Representation of truncated and full length NK1R

(a) Full-length NK1R is a GPCR of 407 amino acids, whereas (b) the truncated isoform is lacking 96 amino acids at the C-terminus. Figure taken from Tuluc et al.¹⁴⁸

INTRODUCTION

NK1R-tr expression was detected in specific regions of the brain or the spinal cord and in the central nervous system. It is also abundant in peripheral tissues such as the prostate, adipose tissue, heart, lungs and spleen. Functional differences between the long (NK1R-fl) and the truncated form of NK1R have been described. Firstly, as mentioned above, NK1R-tr is resistant to desensitization. Secondly and contrary to NK1R-fl, the truncated form is able to induce a rapid but sustained calcium response¹⁴⁷. This difference could be explained by a lower affinity of SP for the truncated form and by the absence of a rapid desensitization, which therefore promotes a prolonged activity¹⁴⁵.

7.3 NK1R antagonists

The first generation of antagonists was developed from the modification of the SP sequence. However, these peptides were particularly unstable and toxic¹⁴⁹. A breakthrough in the development of NK1R antagonists, achieved by random screening of chemical libraries, was the discovery of non-peptide compounds such as L-733.138, L-733.060 and L-703.606, which showed a great affinity for the NK1R. By improving the pharmacokinetic properties of L-733.060, Merck Frosst developed the molecule MK860 or aprepitant¹⁵⁰. Aprepitant, or its commercial name Emend®, is the first NK1R antagonist approved by the Food and Drug Administration (FDA) and Health Canada in 2009 for its antiemetic properties. More precisely, it is used at low doses in triple therapy for the prevention of chemotherapy-induced nausea and vomiting in adults only¹⁵¹. Previous studies have unveiled other very interesting properties of these antagonists depending on the dose at which they are used. At medium doses, they can treat depression or pain, whereas at high doses, a potent anticancer effect has been shown^{152, 153}.

8 Goal of the study

In this study we investigated the SP/NK1R complex in hepatoblastoma as a therapeutic target. Previous work showed that targeting NK1R with the use of antagonist such as aprepitant can trigger a potent anti-cancer effect. However, very little is known about this complex in hepatoblastoma. The goal of this study was to:

- investigate the effect of NK1R antagonism on human hepatoblastoma cells,
- unravel the molecular mechanisms that lead to aprepitant-induced growth inhibition,
- study the SP/NK1R complex from a clinical perspective.

MATERIALS

MATERIALS

1. Eukaryotic cell culture

1.1 Cell lines

HuH6 <i>Homo sapiens</i> (human), liver, hepatoblastoma	JCRB, Osaka, Japan
HepT1 <i>Homo sapiens</i> (human), liver, hepatoblastoma	Pietsch et al. ¹⁵⁴
HepG2 <i>Homo sapiens</i> (human), liver, hepatoblastoma	ATCC, Manassas, USA
HuH7 <i>Homo sapiens</i> (human), liver, hepatocellular carcinoma	ATCC, Manassas, USA
DLD1 <i>Homo sapiens</i> (human), colon, colorectal cancer	ATCC, Manassas, USA
LiM6 <i>Homo sapiens</i> (human), colon, colorectal cancer	Bresalier et al. ¹⁵⁵
HEK293 <i>Homo sapiens</i> (humans), kidney	ATCC, Manassas, USA
L3.6pl <i>Homo sapiens</i> (humans), pancreas, pancreatic cancer	ATCC, Manassas, USA

1.2 Cell culture reagents

Dimethyl sulfoxide (DMSO), sterile	Merck, Darmstadt, Germany
Dulbecco's Phosphate-Buffered Saline (DPBS)	Invitrogen, Karlsruhe, Germany
Fetal Calf Serum (FCS), sterile	Invitrogen, Karlsruhe, Germany
Penicillin-Streptomycin (10,000 U/mL)	Invitrogen, Karlsruhe, Germany
Roswell Park Memorial Institute Medium (RPMI)	Invitrogen, Karlsruhe, Germany
Trypsin - EDTA 0.05 %	Invitrogen, Karlsruhe, Germany

1.3 Cell culture material

Biosphere® Filtertips 1-10 µL, sterile	Sarstedt AG & Co., Nümbrecht, Germany
Biosphere® Filtertips 1-100 µL, sterile	Sarstedt AG & Co., Nümbrecht
Biosphere® Filtertips 100-1000 µL, sterile	Sarstedt AG & Co., Nümbrecht
Cell scraper	Sarstedt AG & Co., Nümbrecht
Costar® Stripette® Serologic Pipettes 5 mL, sterile	Corning GmbH, Wiesbaden, Germany
Costar® Stripette® Serologic Pipettes 10mL, sterile	Corning GmbH, Wiesbaden
Costar® Stripette® Serologic Pipettes 25mL, sterile	Corning GmbH, Wiesbaden
EasyFlasks™, Cell culture flasks, 25 cm ² , non-pyrogenic	NUNC, Langenselbold, Germany
DNase und RNase free	NUNC, Langenselbold, Germany

MATERIALS

EasyFlasks TM , Cell culture flasks, 75 cm ² , non-pyrogenic DNase und RNase free	Greiner bio-one, Frickenhausen, Germany
Plastic tubes, 15 mL, sterile	Greiner bio-one, Frickenhausen, Germany
Plastic tubes, 50 mL, sterile	NUNC, Langenselbold, Germany
Petri dishes 100 x 20 mm, non-pyrogenic, sterile	NUNC, Langenselbold, Germany
6-Well Plates, non-pyrogenic, sterile BD	NUNC, Langenselbold, Germany
12-Well Plates, non-pyrogenic, sterile BD	NUNC, Langenselbold, Germany
24-Well Plates, non-pyrogenic, sterile BD	NUNC, Langenselbold, Germany
96-Well Plates, non-pyrogenic, sterile BD	NUNC, Langenselbold, Germany

1.4 Spheres culture

Human recombinant bFGF	Invitrogen, Karlsruhe, Germany
Human recombinant EGF	Invitrogen, Karlsruhe, Germany
L-Glutamine	Invitrogen, Karlsruhe, Germany
B27 serum free supplement 50X	Invitrogen, Karlsruhe, Germany
Methyl cellulose powder	Sigma, Steinheim, Germany
Minimum Essential Medium (MEM) Alpha Medium with Earle's salts without ribonucleosides, deoxyribonucleosides, and no L-glutamine	VWR, Darmstadt, Germany
Syringe Filter 0.45 µm SFCA	Santa Cruz Biotechnology, Heidelberg, Germany
96-well ultra-low attachment plates	Corning GmbH, Wiesbaden, Germany
100 mm x 20 mm ultra-low attachment dishes	Corning GmbH, Wiesbaden, Germany

2. Plasmids

pRL-CMV <i>Renilla</i> luciferase plasmid	Promega, Mannheim, Germany
TOPFlash <i>Firefly</i> luciferase reporter	Prof. Dr. Frank Kolligs (LMU Munich)
FOPFlash <i>Firefly</i> luciferase reporter	Prof. Dr. Frank Kolligs

MATERIALS

3. Antibodies

Rabbit anti-NK1R	Sigma, Steinheim, Germany
Rabbit anti-Substance P	Sigma, Steinheim, Germany
Mouse anti-human β -catenin	BD transduction laboratories, Heidelberg, Germany
Rabbit anti-human β -actin	Cell signaling technology, Danvers, USA
Rabbit anti-human β -catenin	Cell signaling technology, USA
Rabbit anti-human LRP5 (Low-density lipoprotein receptor-related protein 5)	Cell signaling technology, USA
Rabbit anti-human MYC	Cell signaling technology, USA
Rabbit anti-human PARP (Poly ADP Ribose Polymerase)	Cell signaling technology, USA
Rabbit anti-human caspase 3	Cell signaling technology, USA
Rabbit anti-human phospho-AKT (S473)	Cell signaling technology, USA
Rabbit anti-human phospho-AKT (T308)	Cell signaling technology, USA
Rabbit anti-human total AKT	Cell signaling technology, USA
Rabbit anti-human phospho-P70S6K (S371)	Cell signaling technology, USA
Rabbit anti-human total P70S6K	Cell signaling technology, USA
Rabbit anti-human phospho-4EBP1 (S65)	Cell signaling technology, USA
Rabbit anti-human total 4EBP1	Cell signaling technology, USA
Rabbit anti-human phospho-mTOR (S2448)	Cell signaling technology, USA
Rabbit anti-human total mTOR,	Cell signaling technology, USA
Rabbit anti-human FOXM1	Santa Cruz Biotechnology, Heidelberg, Germany

4. Chemicals / Reagents

6x DNA Loading Dye	Fermentas GmbH, St. Leon-Rot, Germany
Acetic Acid	Carl Roth, Karlsruhe, Germany
Agarose	PeQLab, Erlangen, Germany
Aprepitant	Selleck Chemicals, Munich, Germany
Albumin Fraction V (BSA)	Carl Roth, Karlsruhe, Germany
Bio Rad Protein Assay	Bio-Rad, Munich, Germany
Bromophenolblue	SERVA, Heidelberg, Germany
Chloroform	Carl Roth, Karlsruhe, Germany

MATERIALS

cOmplete Protease Inhibitor Cocktail Tablets	Roche, Mannheim, Germany
Dithiothreitol DTT (0.1 M), 500 µL	Invitrogen, Karlsruhe, Germany
Ethylenediaminetetraacetic acid (EDTA)	Carl Roth, Karlsruhe, Germany
Ethanol, absolut, PA, 2.5 L	Merck, Darmstadt, Germany
Ethidium bromide, 10 mg /mL	Sigma, Steinheim, Germany
Glycerol	Applichem, Darmstadt, Germany
Glycine, 1 kg	GERBU Biotechnik, Gaiberg, Germany
Isopropyl alcohol, 1 L	Sigma-Aldrich, Steinheim, Germany
Igepal CA-630	Sigma-Aldrich, Steinheim, Germany
Magnesium chloride	Carl Roth, Karlsruhe, Germany
β-Mercaptoethanol, 100 mL	Sigma-Aldrich, Steinheim, Germany
MOPS SDS Running Buffer (20X)	Invitrogen, Karlsruhe, Germany
MTT formazan powder	Sigma-Aldrich, Steinheim, Germany
Paraformaldehyde, 0.5 kg	Carl Roth, Karlsruhe, Germany
Phenol	Carl Roth, Karlsruhe, Germany
Potassium chloride, 1 kg	Merck, Darmstadt, Germany
Powdered milk	Carl Roth, Karlsruhe, Germany
Propidium iodide	Sigma-Aldrich, Steinheim, Germany
Random primer	Roche, Mannheim, Germany
Sodium acetat	Carl Roth, Karlsruhe, Germany
Sodium chloride, 1 kg	Carl Roth, Karlsruhe, Germany
Sodium dodecyl sulfat (SDS), 100 g	Carl Roth, Karlsruhe, Germany
Substance P	Sigma-Aldrich, Steinheim, Germany
TE-Buffer	Upstate, Billerica, USA
TRI Reagent® RNA Isolation Reagent	Sigma-Aldrich, Steinheim, Germany
Tris (hydroxymethyl)-aminomethane (TRIS)	Carl Roth, Karlsruhe, Germany
Triton X-100	Sigma-Aldrich, Steinheim, Germany
Tween	Sigma-Aldrich, Steinheim, Germany
Ultra Pure TM DNase/RNase-Free Distilled water	Invitrogen, Karlsruhe, Germany
Vectashield® with DAPI	Vector Laboratories Inc., Burlingame, USA

MATERIALS

5. Primers

The primers used in this study are listed in Table 1. They were synthesized by Eurofins (Hamburg, Germany).

gene name	Reference sequence number	forward	reverse
Full length <i>NK1R</i>	NM_001058.3	5'AACCCCATCATCTACTGCTGC3'	5'ATTCCAGCCCCTCATAGTCG3'
Truncated <i>NK1R</i>	NM_015727.2	5'GGGCCACAAGACCATCTACA3'	5'AAGTTAGCTGCAGTCCCAC3'
<i>AKT1</i>	NM_001014431	5'TGGACCACTGTCATCGAACG3'	5'TGCTTCTTGAGGCCGTCAG3'
<i>AKT2</i>	NM_001243027	5'GAAGGCTGGCTCCACAAGC3'	5'GGCCTCTCTTGTACCCAATG3'
<i>CD13</i>	NM_001150	5'CTACCGCAGCGAGTACATGG3'	5'GCTCATCGAAGCATGGGAAAG3'
<i>CD133</i>	NM_001145847	5'AAATGGGCCCTTCTGAGG3'	5'CCTGGTGATTTGCCACAAAAC3'
<i>AFP</i>	NM_001134	5'TGTGCTGGATTGTCTGCAGG3'	5'GCAGCATTCTGTTATTTGTTTGAC3'
<i>DLK1</i>	NM_001190703	5'GCAACCCCAAAATGGATTC3'	5'GAGGTCACGCACTGGTCACA3'
<i>EPCAM</i>	NM_002354	5'ATCGTCAATGCCAGTGTACTTCA3'	5'TGAGCCATTCAATTTCTGCCTT3'
<i>GEP</i>	NM_2087	5'CTGCCAGTGGGAAGTATGG3'	5'TGGATCAGGTCACACACAGTGC3'
<i>KRT19</i>	NM_002276	5'GCCACTACTACGACCATCCA3'	5'AGCCAGACGGGCATTGTC3'
<i>CTNNB1</i>	NM_001904.2	5'ACGTCCATGGGTGGGACA3'	5'CTAGGATGTGAAGGGCTCCG3'
<i>FOXM1</i>	NM_202002.2	5'CTCCCGCAGCATCAAGCAA3'	5'GCCAGGACGCTGATGGTCTC3'
<i>MYC</i>	NM_002467.3	5'CACCACCAGCAGCGACTCT3'	5'CAGACTCTGACCTTTTCCAGG3'
<i>AXIN2</i>	NM_004655.3	5'TATCCAGTGATGCGCTGACG3'	5'TGTTTCTTACTGCCACACGAT3'
<i>LGR5</i>	NM_003667.3	5'ACAGCAGTATGGACGACCTTCA3'	5'CAGGTCTTCTCAAAGTCAAGCA3'
<i>NANOG</i>	NM_024865	5'AGAACTCTCCAACATCTGAACCT3'	5'TCGGCCAGTTGTTTTTCTGC3'
<i>SOX2</i>	NM_003106.3	5'CCGTTTCATCGACGAGGCTAA3'	5'TTCTTCATGAGCGTCTTGGTTTT3'
<i>OCT4</i>	NM_002701.5	5'CACTGCAGCAGATCAGCCA3'	5'GCTTGATCGCTTGCCTTC3'
<i>KLF4</i>	NM_004235.4	5'ATCTCAAGGCACACCTGCG3'	5'CCTGGTCAGTTCATCTGAGCG3'
<i>TBP</i>	NM_003194.3	5'GCCCCGAAACGCCGAATAT3'	5'CCGTGGTTCGTGGCTCTCT3'

Table 1: Specific primers used in this study

6. Buffer and Solutions

TBE-Buffer:

- 89 mM Tris base, pH 8.0
- 2 mM EDTA
- 89 mM Boric acid

Transfer-Buffer 10X

- 25 mM Tris base
- 192 mM Glycine

Protein lysis buffer

- 0.5% Triton X-100
- 1 mM sodium orthovanadate
- 1 protease inhibitor cocktail tablet
- PBS

Blocking solution

- 5% BSA
- 0.1% Tween-20
- PBS

MATERIALS

RPPA Lysis buffer

- 1% Triton X-100
- 50 mM HEPES pH 7.4
- 150 mM NaCl
- 1.5 mM MgCl₂
- 1 mM EGTA
- 100 mM NaF
- 10 mM Na pyrophosphate
- 1 mM Na₃VO₄
- 10% glycerol
- protease and phosphatase inhibitors

Staining buffer for FACS

- PBS
- 0.1% Triton X-100
- 0.2 mg/mL RNase A
- 0.02 mg/mL propidium iodide

MTT solution

- 0.5 mg/mL
- PBS

Lysis buffer for proliferation assay

- 10% SDS
- 1M HCl

7. Enzymes

Super Script II Reverse Transcriptase

Invitrogen, Karlsruhe, Germany

SsoAdvanced Universal SYBR Green Supermix

Bio-Rad, Munich, Germany

8. Kits

Dual-Glo Luciferase Assay System

Promega, Mannheim, Germany

FITC Annexin V Apoptosis Detection Kit II

BD Biosciences, Heidelberg, Germany

9. Consumables

Biosphere® Filtertips

Sarstedt AG & Co., Nümbrecht, Germany

Coverglas

Menzel-Gläser, Braunschweig, Germany

Hybond-C extra Nitrocellulose membran

Amersham, Buckinghamshire, UK

MATERIALS

HyperfilmTMMP	Amersham, Buckinghamshire, UK
Microwell Plates	NUNC, Langenselbold, Germany
Multidishes NunclonTM	NUNC, Langenselbold, Germany
Nalgene® Cyrotube	Schubert&Weiss, Iphofen, Germany
Nunc™ F96 MicroWell™ White Polystyrene Plate	NUNC, Langenselbold, Germany
Object slide	Menzel-Gläser, Braunschweig, Germany
Pipette tips (10 µL, 100 µL, 1000 µL)	Sarstedt, Nümbrecht, Germany
8-Well PCR stripes	Eppendorf, Hamburg, Germany
PCR 96 Well Plates	PeQLab, Erlangen, Germany
Quarz cuvette QS 10.00 mm	Hellma, Müllheim, Germany
8 - 12% Tris-Glycin Gels	Invitrogen, Karlsruhe, Germany
Whatman paper	Whatman, Maidstone, UK
Safe-lock Eppendorf tube	Eppendorf, Hamburg, Germany

10. Equipment

Agarose gel electrophoreses apparatus	Bio-Rad, Munich, Germany
BD LSRFortessa cell analyzer	BD Biosciences, Heidelberg, Germany
Biofuge fresco, Heraeus	Kendro, Langenselbold, Germany
Biofuge pico, Heraeus	Kendro, Langenselbold, Germany
Bio Photometer	Eppendorf, Hamburg, Germany
Camera AxioCam MRm	Zeiss, Jena, Germany
Camera Power Shot G6	Canon, Krefeld, Germany
Cell screen Olympus IX50	Innovatis, Bielefeld, Germany
Centrifuge 5702	Eppendorf, Hamburg, Germany
Centrifuge J2-21	Beckman Coulter, Krefeld, Germany
Centrifuge LMC-3000	G. Kisker, Steinfurt, Germany
CO2-Incubator MCO-20AIC	Sanyo, Tokio, Japan
Excella E24 Incubator Shaker Series	New Brunswick Scientific
Heat block MR 3001	Heidolph, Kehlheim, Germany
Heatblock Thermomixer comfort	Eppendorf, Hamburg, Germany
GelJet Imager Version 2004	Intas, Göttingen, Germany

MATERIALS

GENios Microplatereader	Tecan, Crailsheim, Germany
Mastercycler ep gradient S	Eppendorf, Hamburg, Germany
Mastercycler personal	Eppendorf, Hamburg, Germany
Microlitercentrifuge MZ014	G. Kisker, Steinfurt, Germany
Microscope Axiovert 40 CFL	Zeiss, Jena, Germany
Microscope Axiovert 135	Zeiss, Jena, Germany
Micro scales Te1245	Sartorius, Göttingen, Germany
Microwave	Panasonic, Hamburg, Germany
NanoDrop 1000 instrument	Thermo Scientific, Wilmington, USA
FluoView™ FV1000 confocal microscope	Olympus, Hamburg, Germany
Incubator	Memmert, Schwabach, Germany
Shaker, Rock-N-Roller	G. Kisker, Steinfurt, Germany
Shaker, Unimax 1010	Heidolph, Schwabach, Germany
Thermomixer Compact	Eppendorf, Hamburg, Germany
Vortexer Genie2	Scientific Industries, NY, USA
Water bath GFL 1083	GFL, Wien, Austria
Western-Blot Detection system „CP1000“	AGFA, Köln, Germany
Work flow, Hera Safe	Kendro, Hanau, Germany
XCell IITM Blot Module	Invitrogen, Karlsruhe, Germany
XCell SureLock™ Electrophoresis Cell	Invitrogen, Karlsruhe, Germany

11. Sofwares

ImageJ software (NIH, Bethesda, MD, USA)

FlowJo 7.6.3 Software (Tree Star, Inc., Ashland, OR, USA)

GraphPad Prism (La Jolla, CA, USA)

METHODS

1. Cell culture

Three human hepatoblastoma cell lines (HuH6, HepT1 and HepG2), one human hepatocellular carcinoma cell line (HuH7), two colorectal cell lines (DLD1 and LiM6) as well as the pancreatic cell line L3.6pl were used in this study. All cell lines were grown in RPMI-1640 medium supplemented with 10% FCS and 1% Penicillin/Streptomycin at 37°C in a humidified incubator with 5% CO₂.

2. RNA isolation and RT-PCR

Total RNA was isolated from parental cells, spheres or tumor tissues using TRI-reagent. cDNA was synthesized from 2 µg of total RNA using random primers and SuperScript II Reverse Transcriptase according to the manufacturers instructions. For each PCR reaction we used 40 ng of cDNA, 500 nM of the primer pair and SsoAdvanced Universal SYBR Green Supermix for a total volume of 20 µL. Thermal cycling consisted of 40 cycles with denaturation at 95°C for 15 seconds, annealing at 55°C for 15 seconds, and elongation at 72°C for 30 seconds using the Mastercycler ep gradient S. Each experimental condition was assayed in duplicate.

3. Proliferation assays

Cell proliferation was assessed using 1-(4,5-dimethylthiazol-2-yl)-3,5-diphenylformazan (MTT) assay. 10,000 cells/well were seeded into 96-well plates. After 24 hours, cells were treated with increasing doses of aprepitant for 48 hours or with DMSO. To assess cell viability, MTT solution was first added to each well followed by 4 hours incubation at 37°C. Finally, a lysis solution was added overnight in each well. For the readout, a multi scanner microplate reader was used to measure the absorbance at 595 nm. Each experiment was realized three times and each condition was performed in triplicates.

4. *In vitro* analysis of apoptosis

After treatment with the respective NK1R antagonist, the cells were fixed in 4% paraformaldehyde. After three rinses with PBS, microscope slides were mounted with

METHODS

Vectashield containing 4,6-diamidino-2-phenylindole (DAPI). The pictures were taken using the Olympus FluoView™ FV1000 confocal microscope. Apoptotic cells were defined by chromatin condensation and nuclear fragmentation. We related the cell number of apoptotic cells to total cells of 10 randomly selected high power fields. Apoptosis was also assessed by flow cytometric analysis. After treatment, cells were stained for 15 minutes at room temperature with anti-Annexin V-FITC antibody and propidium iodide (PI). Then, 10,000 cells were analyzed on a BD Fortessa Flow Cytometer and the results processed with the FlowJo 7.6.3 software.

5. Western blot analysis

Cells were treated for 24 hours, washed with ice-cold PBS and lysed with a lysis buffer. The protein concentration was determined by using the BIO-RAD protein assay. For each condition, 20 µg of proteins were loaded on 8-12%, separated by electrophoresis and electroblotted onto nitrocellulose membranes. The membranes were then incubated for 2 hours in a blocking solution, followed by an overnight incubation with primary antibodies at a 1:1,000 dilution against β -catenin, LRP5 (low-density lipoprotein receptor-related protein 5), MYC, PARP (poly ADP ribose polymerase), caspase 3, phospho-AKT (serine 473, threonine 308), total AKT, phospho-p70S6K (threonine 389), total p70S6K, phospho-4EBP1 (serine 65), total 4EBP1, phospho-mTOR (serine 2448), total mTOR, β -actin and FOXM1. Finally, the blots were washed with TBS-0.1% Tween-20 and incubated for 1 hour at room temperature with a peroxidase-conjugated goat anti-rabbit IgG antibody at a dilution of 1:2,000. The detection was realized with an enhanced chemiluminescence reaction and β -actin served as a loading control.

Western blot band intensity was evaluated by ImageJ software and values of total proteins or ratios of phospho/total proteins were normalized to the housekeeping protein β -actin.

6. Reverse-phase protein array (RPPA)

Cells were treated for 24 hours with the indicated substrates. Samples were then washed in ice-cold PBS, denatured by a lysis buffer and stored at -80°C. Further processing of the samples was carried out by the functional proteomics RPPA core facility at MD Anderson cancer center as previously reported (14). Briefly, probes were spotted on nitrocellulose slides and a total of 172 different proteins were analyzed. Densitometry of these spots was

METHODS

quantified and normalized for protein loading and transformed to linear values, which was used for the following calculations. For quantization, we calculated the ratios with the linear protein intensity values of the treated probes and the linear protein intensity values of their respective control probes.

7. *In vitro* analysis of cell cycle

Cells were seeded onto 6-well plates at a density of 200,000 cells/well. After 24 hours, cells were treated for 24 hours with 30 μ M aprepitant or DMSO. Adherent cells were trypsinized and pooled together with non-adherent cells, rinsed with PBS and fixed with ice cold ethanol 70% for 2 hours minimum. Cells were washed with PBS and stained for 30 minutes with a staining buffer. Cells were analyzed by BD LSRFortessa cell analyzer.

8. Immunofluorescence

Cells were plated onto round cover slips with a diameter of 18 mm in 12-well plates at a density of 75,000 cells/well and treated as indicated in the results section. After 24 hours of treatment, cells were fixed in 4% paraformaldehyde for 15 minutes, permeabilized for 15 minutes with 0.15% TritonX-100 in PBS and blocked for 30 minutes with 1% BSA in PBS. The cells were then incubated overnight at 4°C with rabbit primary antibodies against β -catenin (monoclonal), phospho-AKT (polyclonal), phospho-mTOR or FOXM1 diluted in blocking solution at 1:80, 1:25, 1:80 and 1:25, respectively. After several washing steps, cells were then incubated for 1 hour in the dark with goat anti-rabbit antibody conjugated with Alexa Fluor 488 or goat anti-mouse antibody conjugated with Alexa Fluor 594 at a 1:200 dilution. After three rinses with PBS, microscope slides were mounted with Vectashield containing 4,6-diamidino-2-phenylindole (DAPI). The pictures were taken using the Olympus FluoView™ FV1000 confocal microscope.

9. Super TOP/FOP (STF) luciferase reporter assay

Luciferase assays for reporters were carried out using the dual-luciferase reporter assay system. Cells were plated in 24-well plates at a density of 50,000 cells per well, 24 hours before treatment and transfection. Fugene HD reagent and alphaMEM medium was used to mediate co-transfection with inducible *Firefly* luciferase expressing SuperTOP or SuperFOP vectors and constitutively *Renilla* luciferase expressing normalization vector pRL-CMV at a

METHODS

ratio of 50:1 as a control for transfection efficiency. The cells were simultaneously treated with different concentrations of aprepitant or DMSO. After 24 hours of incubation, total cell lysate was extracted using reporter lysis buffer and 5 µL of total extract was used to determine *Firefly* and *Renilla* luciferase activities using 25 µL of luciferase substrate LarII solution and 25 µL of Stop and glow 1X solution, respectively. The luminescence was measured with an integration time of 12 seconds. TCF-mediated transcriptional activity was determined by the ratio of SuperTOP/SuperFOP luciferase activities, each normalized to the respective luciferase activities of the pRL-TK reporter. Each experimental condition was assayed in triplicate.

10. Sphere formation culture

After trypsinization and rinses with PBS, 75,000 cells were seeded onto 100 mm * 20 mm ultra-low attachment dishes containing sphere formation medium composed of DMEM-F12, 1% Penicillin/Streptomycin, 10 ng/mL human recombinant bFGF, 20 ng/mL human recombinant EGF, 1% glutamine and B27 serum free supplement 1X. Spheres were cultivated for 6 - 14 days and treated with aprepitant, SP or DMSO for further analysis.

Sphere formation ability (SFA) was assessed in 96-well ultra-low attachment plates. Cells were seeded at a density of 500 cells per well in sphere formation medium supplemented with 1% methylcellulose that had been filtered with a 0.45 µm ultra cruz syringe filter. 100 µL of media was added every three days. Sphere numbers and sizes were determined under a microscope after 6-11 days depending on the cell type.

11. Patients and Tumor Tissues

Tumor tissue samples were analyzed from patients with hepatoblastoma who were all part of the German Cooperative Pediatric Liver Tumor Study HB99 and its subsequent Registry for Pediatric Liver Tumors. Both were multicentric and initiated by the German Society for Pediatric Oncology and Hematology (GPOH). They were open to registration for patients from Germany, Austria, and Switzerland up to the age of 20 years with untreated hepatoblastoma. The registry protocols were assigned by the institutional Ethical Committees and written consent from the parents for treatment, data collection and analysis was obtained.

METHODS

Clinical information including demographic, therapeutic, tumor and clinical outcome variables were retrieved in both clinical studies.

All tumor specimens were reviewed by the local Pathology as well as the Institute of Pediatric Pathology, University of Kiel, which served as a reference center. Liver tissue samples from the surgical specimens without macroscopic as well as microscopic tumor served as tumor free controls. Clinical and molecular data such as sex, age of diagnosis, PRETEXT stadium, vascular invasion, multifocality, metastatic disease, histology, *CTNNB1* mutation, 16-gene signature and overall survival were retrieved from the HB99 database.

12. Statistical analysis

Results are expressed as the mean \pm standard deviation (s.d.). All statistical comparisons were made with a standard t-test and Mann–Whitney-U-Test using the biostatistics software GraphPad Prism. The criterion for significance was $p < 0.05$ (*) and $p < 0.01$ (**) for all comparisons.

Kaplan-Meier estimates of specific survival time were compared using the log-rank Mantel-Cox test.

RESULTS

1. Hepatoblastoma cells express NK1R and can be growth inhibited by aprepitant *in vitro*

The results presented in this section are part of the publication: Hepatoblastoma cells express truncated neurokinin-1 receptor and can be growth inhibited by aprepitant *in vitro* and *in vivo*. Journal of Hepatology (2014, 60(5):985-94) Berger M, Neth O, Ilmer M, Garnier A, Salinas-Martín MV, de Agustín Asencio JC, von Schweinitz D, Kappler R, Muñoz M.

1.1 NK1R is expressed in human hepatoblastoma cell lines

In order to characterize the expression of the NK1R in human hepatoblastoma cell lines, distinct RT-PCR were carried out for the full-length (fl-) and truncated (tr-) NK1R transcripts. The expression levels of hepatoblastoma cell lines were compared to human fibroblasts, and the HEK293 cell lines which is known to express NK1R (Figure 8).

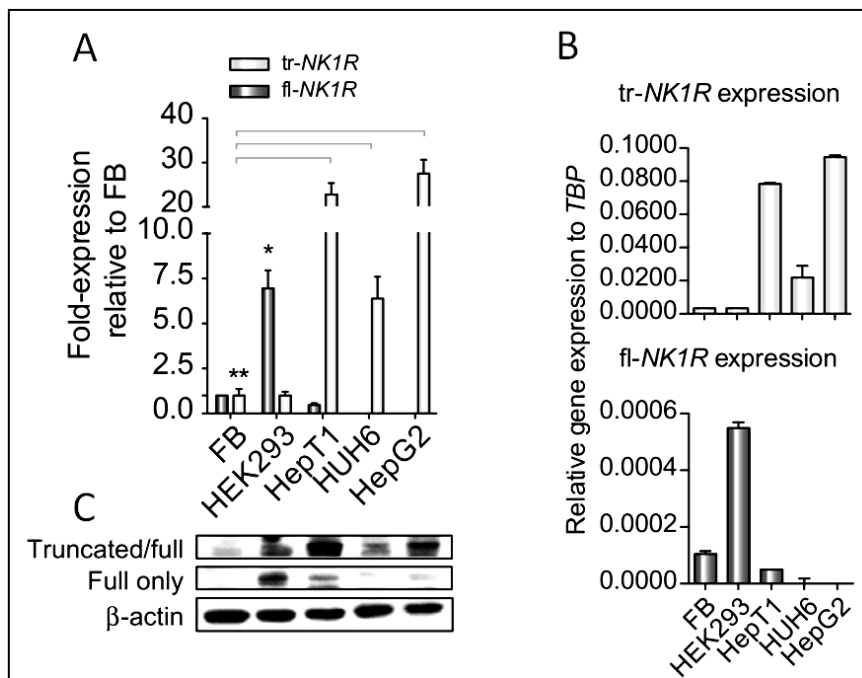


Figure 8: Expression pattern of NK1R in human hepatoblastoma cell lines

In (A), mRNA expression for *NK1R* is shown as fold expression relative to human fibroblasts (FB) or (B) as relative gene expression (fl, full length; tr, truncated). Expression levels obtained by RT-PCR were normalized to the housekeeping gene *TBP*. (C) Western blot is shown for specific antibodies binding to either the fl-NK1R or both tr- and fl-NK1R. Shown is the mean and error bars represent s.d.. Significance levels are as follows: n.s.: not significant, * $p < 0.05$ and ** $p < 0.01$. Figure taken from Berger et al.¹⁵⁶

The HEK293 cell line expressed the highest level of fl-NK1R. Surprisingly, the three hepatoblastoma cell lines HuH6, HepT1 and HepG2 expressed very little mRNA coding for fl-NK1R. They predominantly overexpressed the shorter truncated splice variant while

RESULTS

human fibroblasts and HEK293 expressed only slight amounts (Figure 8A and 8B). These findings were verified by Western blot (Figure 8C). As no specific antibody for the truncated version of NK1R is commercially available at this time, a pair of specific antibodies against the full version alone as well as against both versions were used for the study, following the technique introduced by Gillespie et al.¹⁵⁷.

1.2 Aprepitant inhibits tumor growth in human hepatoblastoma cell lines

In order to investigate cell survival after the antagonism of NK1R, the human hepatoblastoma cell lines as well as fibroblasts and HEK293 were treated with increasing concentrations of aprepitant for 48 hours, and an MTT assay was subsequently realized (Figure 9).

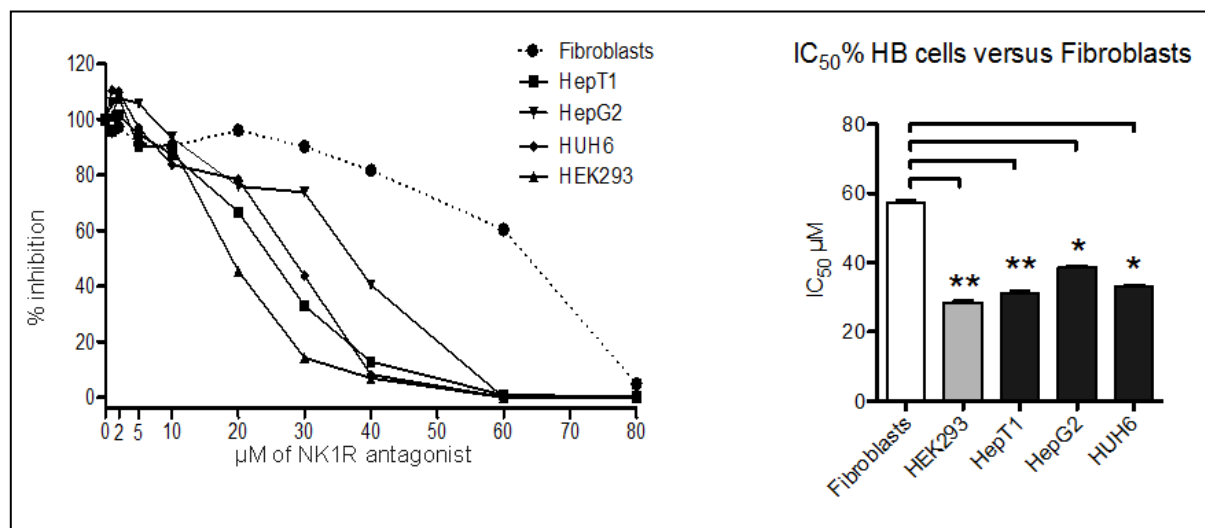


Figure 9: Aprepitant triggers growth inhibition in hepatoblastoma cell lines

MTT assays determining cell survival after treatment with aprepitant for 48 hours are shown for the cell lines HuH6, HepT1, HepG2, human fibroblasts, and HEK293 (left panel). Based on these data, IC₅₀ (μM) were calculated and compared to fibroblasts for statistical analysis (right panel). Shown is the mean and error bars represent s.d.. Significance levels are as follows: n.s.: not significant, * $p < 0.05$ and ** $p < 0.01$. Figure taken from Berger et al.¹⁵⁶

Aprepitant induced a concentration dependent growth inhibition in all cell lines examined. However, human fibroblasts, which did not express NK1R, were significantly more resistant to this treatment compared to hepatoblastoma cell lines. The concentrations required for a 50% growth reduction (IC₅₀) were 57.5 μM for fibroblasts and 28.5 μM, 31.1 μM, 33.18 μM and 36.61 μM for HEK293, HepT1, HuH6 and HepG2, respectively (Figure 9, right panel).

RESULTS

Taken together, these results indicate that benign human fibroblasts express significantly less NK1R compared to hepatoblastoma cell lines and that the NK1R expression predicts the response rate to aprepitant.

In order to complement the study, the inhibitory ability of aprepitant on proliferation of all hepatoblastoma cell lines was compared with that of other NK1R antagonists, namely L-733,060 and L-732,138 (Figure 10).

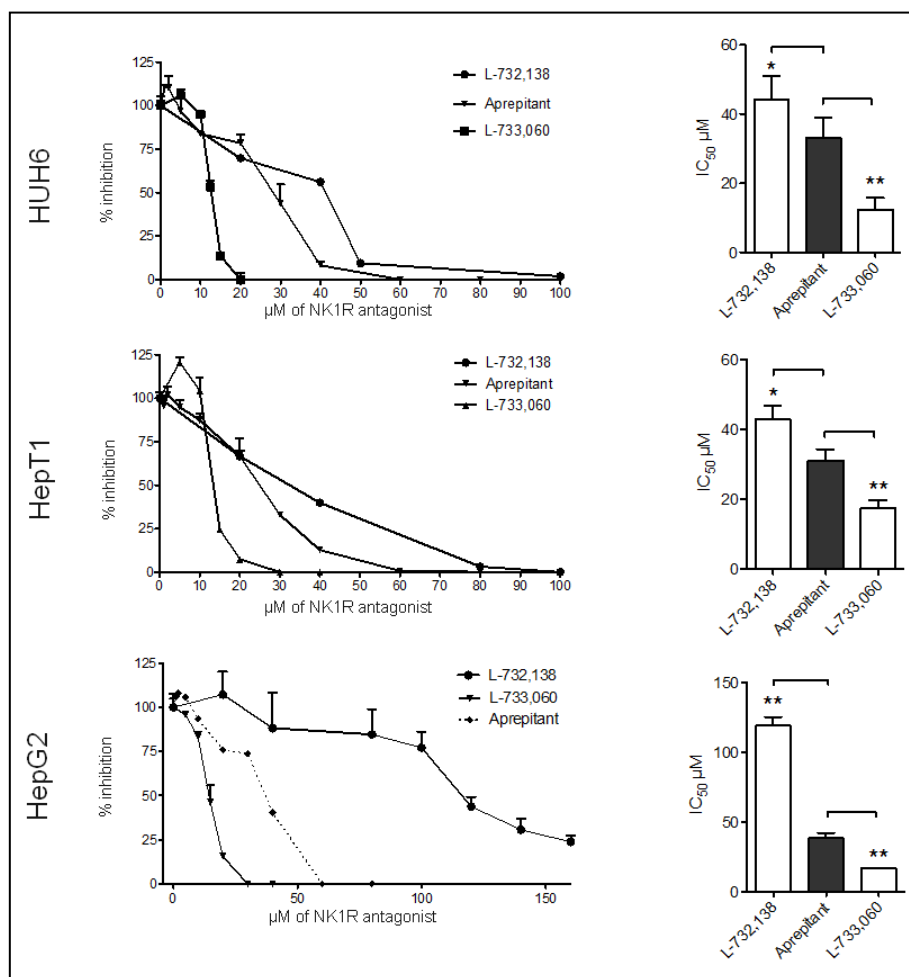


Figure 10: L-733,060 and L-732,138 induce growth inhibition in hepatoblastoma cell lines

Similarly to figure 9, cell survival is shown for the small molecules L-733,060 and L-732,138 in comparison to aprepitant in HuH6, HepT1 and HepG2 cells. Shown is the mean and error bars represent s.d.. Significance levels are as follows: n.s.: not significant, * $p < 0.05$ and ** $p < 0.01$. Figure taken from Berger et al.¹⁵⁶

L-733,060 was found to be significantly more potent and L-732,138 to be significantly less effective compared to aprepitant ($p < 0.01$).

RESULTS

1.3 SP reverses the anti-proliferative effect of NK1R antagonists

SP is the natural agonist of NK1R and a mitogenic effect has been observed in several cancer cells however very little is known in hepatoblastoma. By blocking SP or NK1R with anti-SP or anti-NK1R antibodies, a significant growth reduction was observed for all three cell lines (Figure 11). This suggests that hepatoblastoma cell growth could be influenced by autocrine secretion of SP.

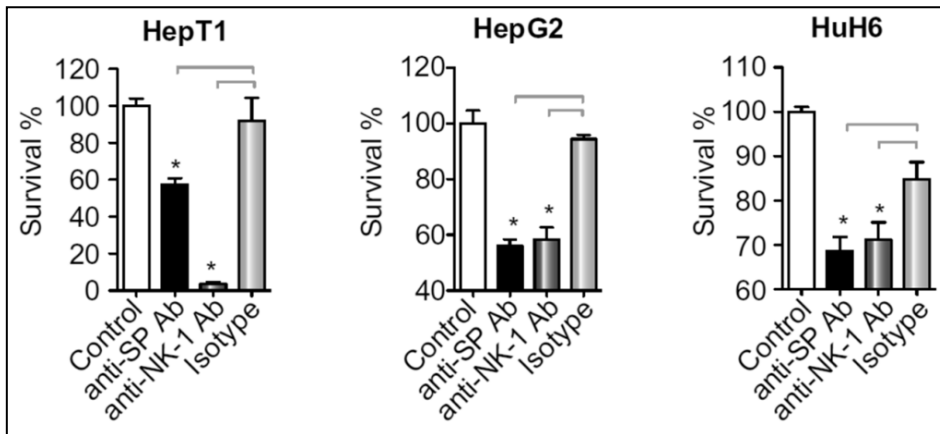


Figure 11: Blocking SP or NK1R with monoclonal antibodies decreases cell survival of hepatoblastoma cell lines

HepT1, HepG2, and HuH6 were treated with anti-SP, anti-NK1R and isotype antibodies at a final concentration of 1:100. Effects were analyzed with MTT proliferation assays. Shown is the mean and error bars represent s.d.. Significance levels are as follows: n.s.: not significant, * $p < 0.05$ and ** $p < 0.01$. Figure taken from Berger et al.¹⁵⁶

Further, when hepatoblastoma cells were treated with sub-lethal concentrations of either L-733,060 or aprepitant, the addition of SP reversed the anti-proliferative effect of NK1R blockage in a dose-dependent manner: in the case of HepT1, 10 nM of SP were sufficient for a significant reduction of the anti-proliferative effect of L-733,060 (10 μM) and aprepitant (25 μM) whereas higher concentrations of SP (50 nM) were needed for HuH6 and HepG2 cells (Figure 12).

These findings, together with the observation that human fibroblast express little NK1R and were more resistant to treatment with NK1R antagonists, clearly indicate that the described effect of NK1R antagonists in hepatoblastoma cells is not generally toxic but specifically triggered via the SP/NK1R complex.

RESULTS

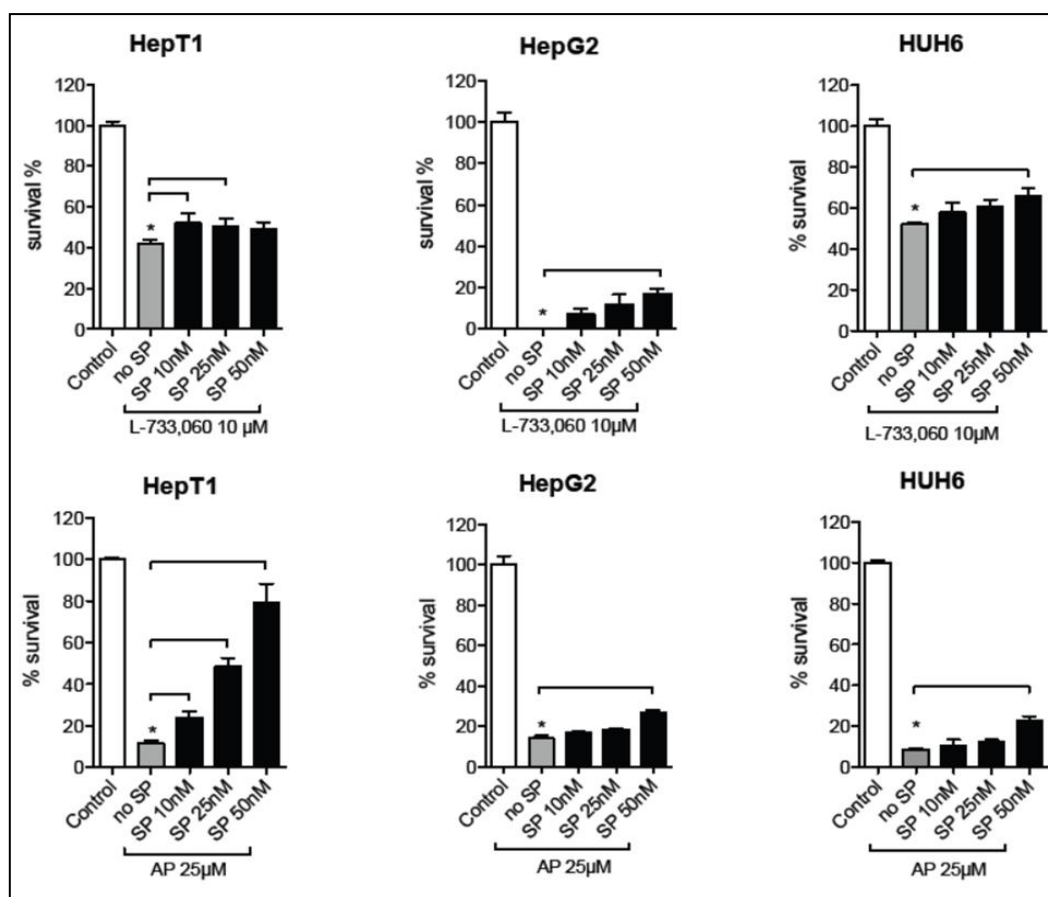


Figure 12: SP reverses the anti-proliferative effect of NK1R antagonism

MTT assays determining cell survival after treatment with aprepitant or L-733,060 with SP for 48 hours. Shown is the mean and error bars represent s.d.. Significance levels are as follows: n.s.: not significant, * p < 0.05 and ** p < 0.01. Figure taken from Berger et al.¹⁵⁶

1.4 Aprepitant and cytostatics synergistically induce cell death of hepatoblastoma cells

The robust anti-proliferative effect of NK1R antagonists that we observed prompted us to perform a comparative study with cytostatic drugs commonly used in the treatment of hepatoblastoma. HepT1, HuH6, and HepG2 cells were treated with their respective IC50 dose of aprepitant either separately or together with increasing doses of the cytostatics cisplatin and doxorubicin (Figure 13).

For HepT1 cells, a statistically significant synergistic effect was found for high-dose doxorubicin (10 μM) in combination with aprepitant (Figure 13, lower panel), whereas similar synergisms for cisplatin and aprepitant in the same cell line were not detected (Figure 13, upper panel). For HepG2, a marked synergistic effect was found for high-dose doxorubicin (10 μM) and cisplatin (10 μM) with aprepitant (Figure 13, lower panel).

RESULTS

Interestingly, even a low-dose doxorubicin (1 μM) showed an interesting synergistic effect with aprepitant. Similar results could be obtained for HuH6.

These results are consistent with the existence of a potent synergistic effect between the clinical drug aprepitant and cytostatics commonly used in hepatoblastoma therapy.

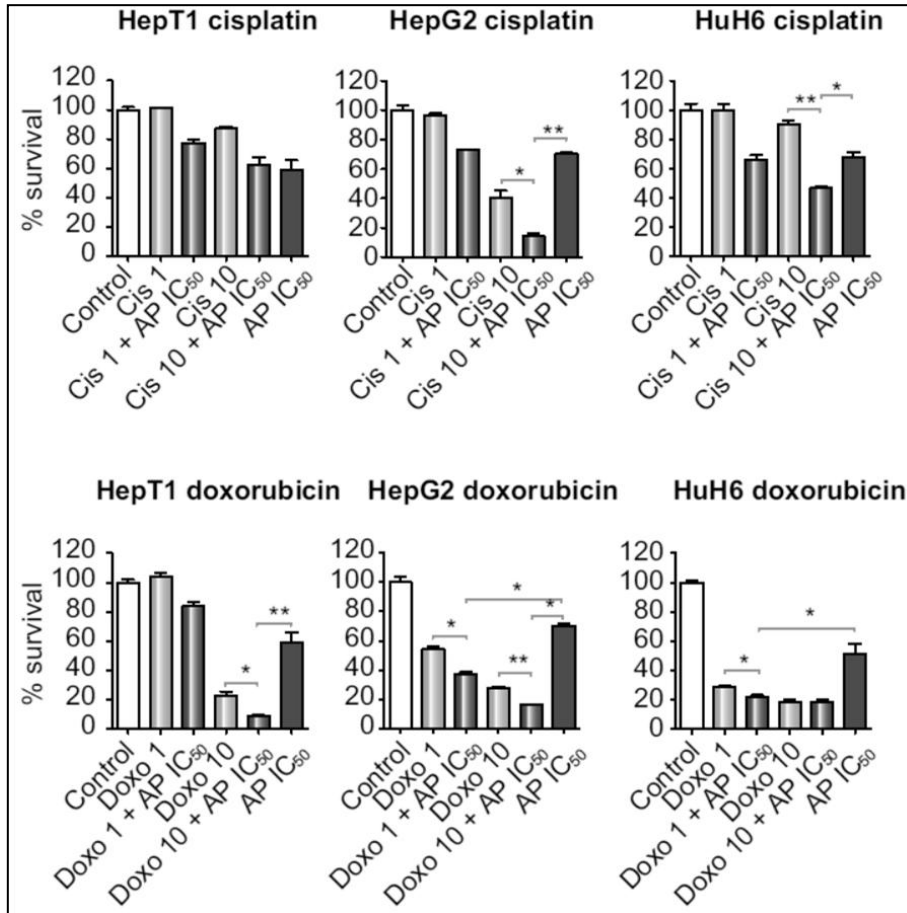


Figure 13: Synergistic inhibition of human hepatoblastoma cells with cytostatics and aprepitant

HepT1, HepG2, and HuH6 were treated either without or with IC₅₀ aprepitant combined with increasing doses of the cytostatics cisplatin or doxorubicin. Cell viability (% survival) was determined by MTT assay. All experiments were realized in duplicates (n=3). Shown is the mean and error bars represent s.d.. Significance levels are as follows: n.s.: not significant, * p < 0.05 and ** p < 0.01. Figure taken from Berger et al.¹⁵⁶

1.5 NK1R antagonists induce apoptosis in hepatoblastoma cells

In order to explain the observed decrease in survival of these cells, we performed experiments assessing whether these agents are apoptosis-inducing.

RESULTS

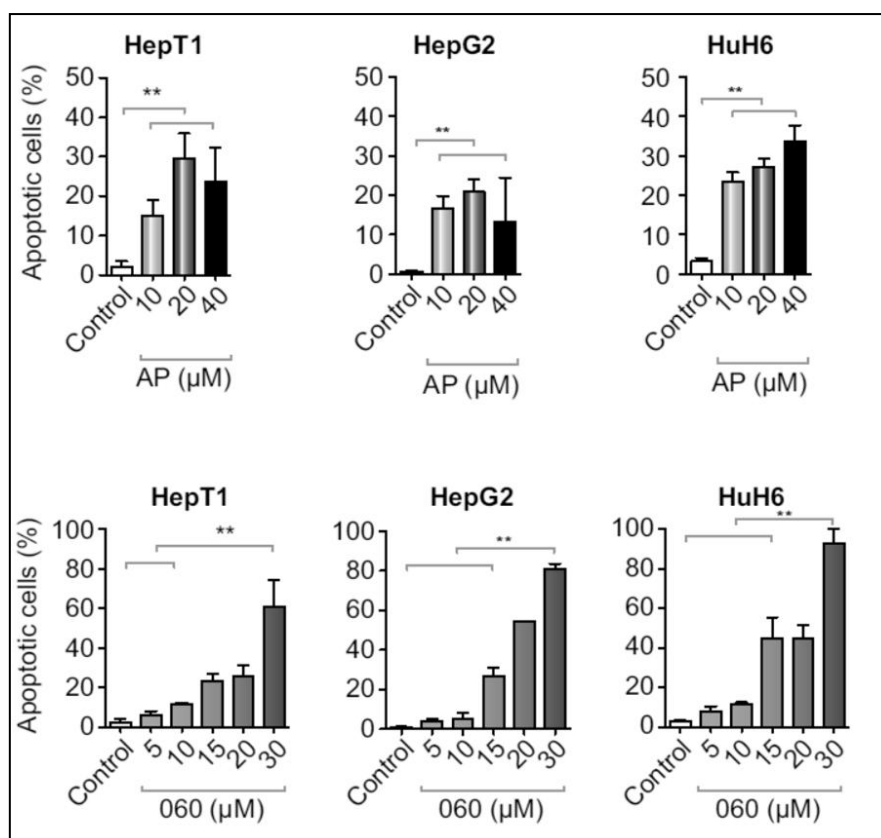


Figure 14: NK1R antagonism induces an increase of apoptotic cells in human hepatoblastoma cells

Cells were treated for 18 hours with increasing doses of L-733,060 or aprepitant and DAPI staining was carried out. Quantitative analysis was subsequently performed in duplicate, apoptotic cells were defined by chromatin condensation and fragmentation. Shown is the mean and error bars represent s.d.. Significance levels are as follows: n.s.: not significant, * $p < 0.05$ and ** $p < 0.01$. Figure taken from Berger et al.¹⁵⁶

In all cell lines, a dose-dependent increase of apoptotic cells after 18 hours was observed for both L-733,060 and aprepitant (Figure 14). To characterize apoptosis in detail, hepatoblastoma cell lines were treated with SP or increasing doses of aprepitant for 24 hours and Western Blot was carried against the apoptotic markers PARP and caspase-3 (Figure 15). A dose-dependent increased expression of cleaved PARP as well as cleaved caspase-3 was detected, indicating an activation of the late apoptotic machinery. However, treatment with 100 nM of SP had no effect on apoptosis.

RESULTS

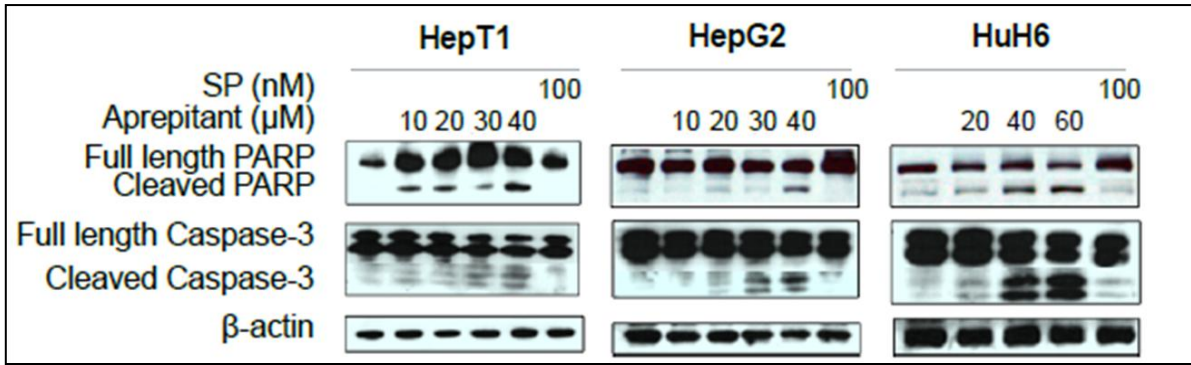


Figure 15: Dose-dependent increase of apoptosis markers after NK1R antagonism

HepT1, HepG2, and HuH6 cells were treated with increasing doses of aprepitant (10 μM, 20 μM, 30 μM and 40 μM), SP (100 nM) or DMSO (control) and Western blot analysis was performed for the apoptotic markers PARP and Caspase-3. β-actin served as a loading control. Figure taken from Berger et al.¹⁵⁶

Additionally, in order to better assess apoptosis, cells were treated with increasing doses of aprepitant and stained with anti Annexin V FITC antibody and propidium iodide (PI) (Figure 16) followed by FACS analysis.

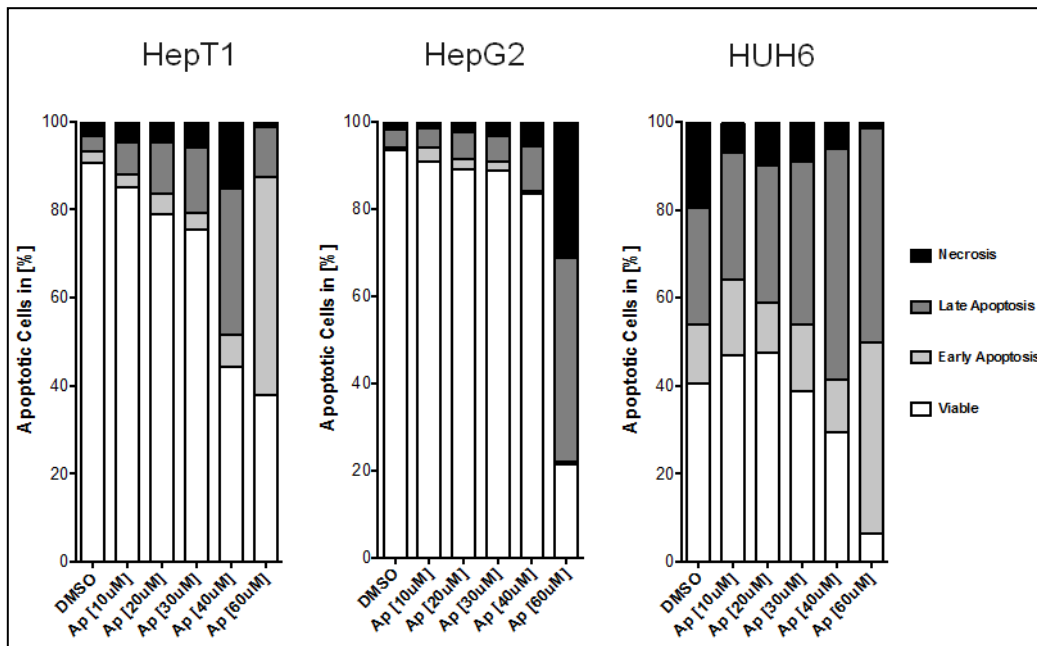


Figure 16: Aprepitant triggers a dose dependent increase of early and late apoptosis

HepT1 was treated with increasing doses of aprepitant (AP [10 μM], AP [20 μM], AP [30 μM], AP [40 μM] and AP [60 μM]) or with DMSO (control) and stained with Annexin V and propidium iodide (PI). Shown is the quantification of FACS analysis in the three hepatoblastoma cell lines HepT1, HepG2 and HuH6. Figure taken from Berger et al.¹⁵⁶

A dose-dependent increase of early and late apoptosis was observed in all cell lines as indicated by annexin V and the simultaneous staining of annexin V and PI, respectively (Figure 16). These results correlate with the overall action of NK1R antagonists on cell survival, indicating that the observed effects can be related to both apoptosis induction and growth inhibition in hepatoblastoma cells.

RESULTS

2. Targeting the NK1R compromises canonical Wnt signaling in hepatoblastoma

The results presented in this section are part of the publication: Targeting the neurokinin-1 receptor compromises canonical Wnt signaling in hepatoblastoma. *Molecular Cancer Therapeutics* (2015 Dec;14(12):2712-21) Ilmer M, Garnier A, Vykoukal J, Alt E, von Schweinitz D, Kappler R, Berger M.

2.1 NK1R inhibition leads to downregulation of the PI3K/AKT/mTOR and Wnt signaling pathways

In order to provide a mechanistic explanation for the effects of aprepitant on human hepatoblastoma cells, we next used reverse-phase protein array (RPPA) as a screening tool to identify proteins regulated by aprepitant treatment. The human hepatoblastoma cell lines HepT1, HepG2, and HuH6 (harboring β -catenin mutations) were treated with 20 μ M and 40 μ M aprepitant and subsequently screened for changes in expression level of 172 proteins and phosphoproteins associated with common cancer pathways. After averaging over all three cell lines, it was observed that most proteins did not change significantly compared to the untreated control (in black); few samples changed significantly with downregulation (in green) or upregulation (in red) (Figure 17).

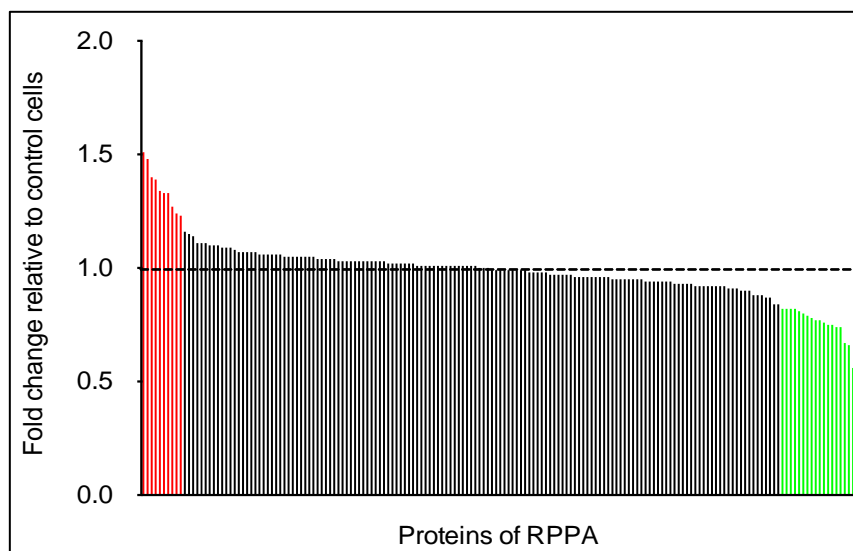


Figure 17: Pattern of regulation of 172 proteins analyzed by RPPA in the three hepatoblastoma cell lines

Hepatoblastoma cells (HepT1, HepG2, HuH6) were cultured in monolayer, treated with DMSO (control), aprepitant (20 μ M or 40 μ M) or substance P (SP) for 24 hours and protein lysates were analyzed by RPPA. The averaged changes after aprepitant treatment of all three hepatoblastoma cell lines for all the proteins investigated compared to untreated controls are shown. Ratios > 1.2 in red to the left, ratios < 0.8 in green to the right. In black, proteins with no significant changes in expression. The cut-offs were chosen according to the standard deviation of the values. Figure taken from Ilmer et al.¹⁵⁸

RESULTS

Significantly altered protein ratios after treatment are shown in Figure 18. By classifying proteins according to their pathway affiliation, we found several candidate proteins that belong to the PI3K/AKT/mTOR and Wnt group (Figure 18).

More particularly, in the PI3K/AKT/mTOR pathway, total AKT, 4E-BP1/2 (S65), p70S6K (T389), and S6 (S235/236 and S240/244) were downregulated. Additionally, 4E-BP1 (T37/T46) and PRAS40 (T246), a member of mTORC1, were upregulated upon aprepitant treatment. Furthermore, calculations of phospho/total protein ratios of the investigated proteins revealed that aprepitant treatment resulted in upregulation of AKT (S473 and T308) and mTOR (S2448) as well as downregulation of Rictor (T1135) (Supplemental Figure 1).

Concerning the Wnt associated proteins, FOXM1 in its total form was found downregulated. On the other hand, p-GSK3 α/β (pS21/S9), an important part of the β -catenin destruction complex, was found upregulated (Figure 18). Similar to the AKT pathway, phospho/total ratios for Wnt pathway associated proteins were calculated and confirmed the findings (Supplemental Figure 1). Overall, a dose-dependent effect with more drastic changes after treatment with 40 μ M (lower rows) than with 20 μ M was detected.

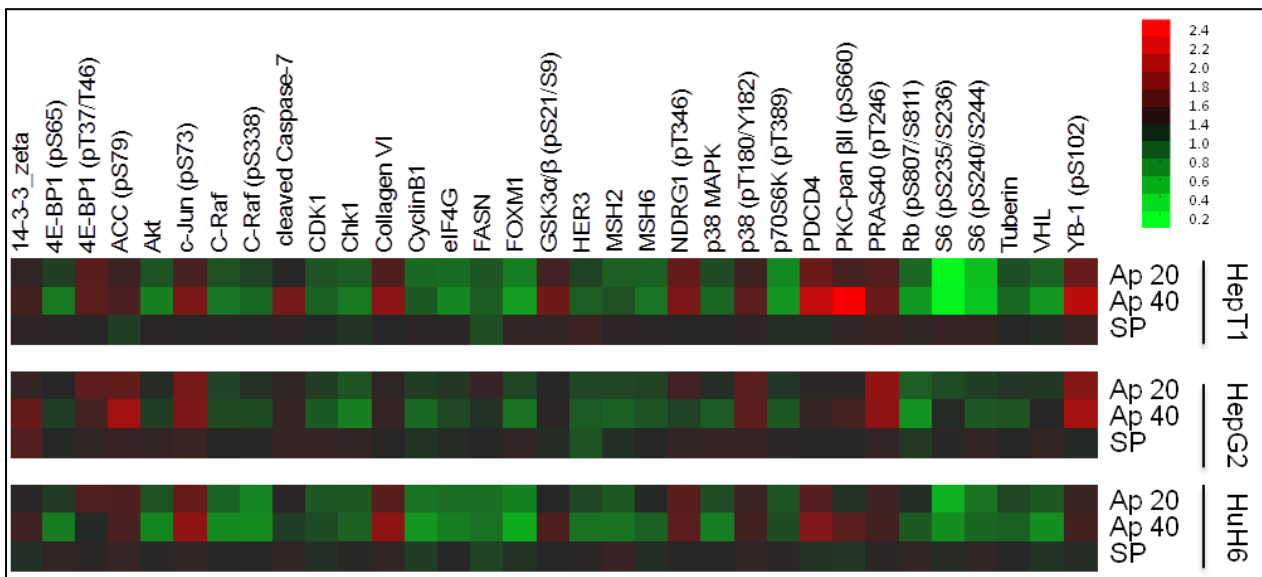


Figure 18: Heatmap of protein changes in the three hepatoblastoma cell lines compared to control
 Red indicates an increased signal and green a decreased signal in treated samples normalized against the control sample. Shown are all proteins with significant changes. Figure taken from Ilmer et al.¹⁵⁸

RESULTS

Taken together, these data indicate a strong downregulation of both the PI3K/AKT/mTOR and the canonical Wnt signaling pathways at the protein level upon NK1R inhibition with aprepitant.

2.2 NK1R antagonism leads to differential expression of the PI3K/AKT/mTOR pathway

To validate the findings of the RPPA analysis, the PI3K/AKT/mTOR pathway was first analyzed in greater detail (Figure 19).

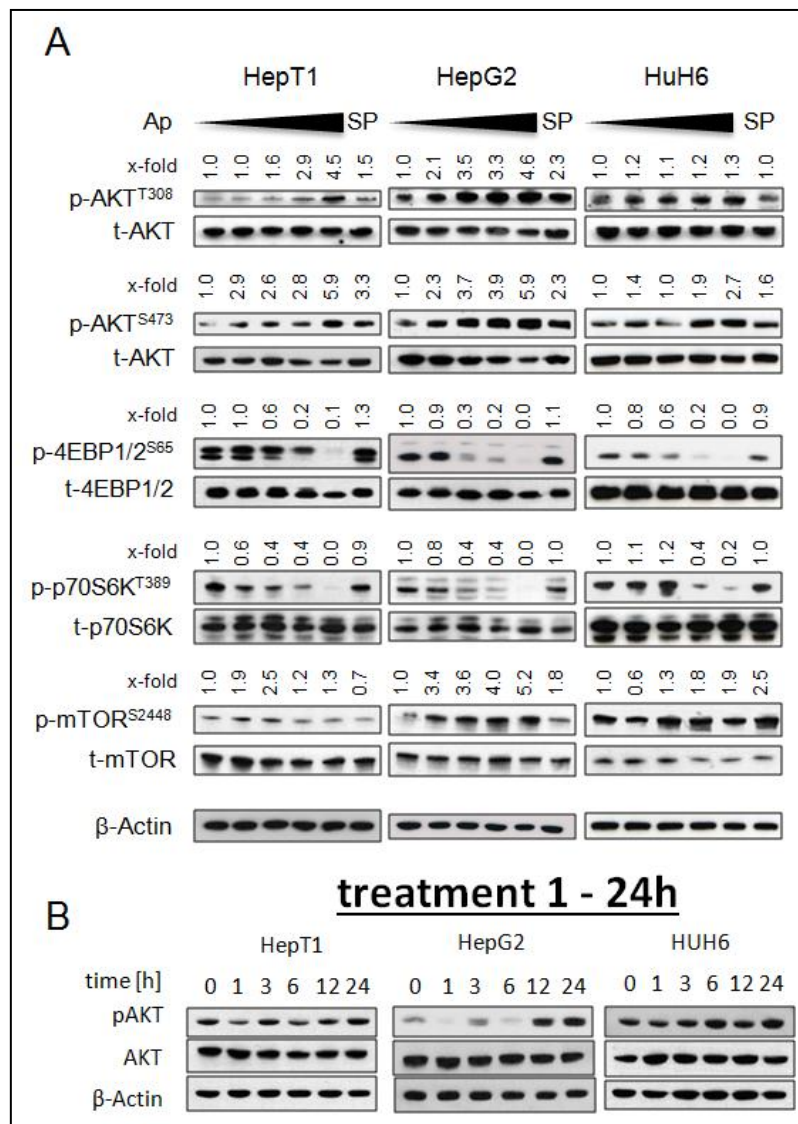


Figure 19: Analysis of the PI3K/AKT/mTOR pathway by Western blot

(A) Cells were treated with increasing doses of aprepitant for 24 hours and protein lysates probed for total and p-AKT (S473 and T308), total and p-4EBP1/2 (S56), total and p-p70S6 (T389), total and p-mTOR (S2448) and β -actin. (B) Cells were treated with IC₅₀ aprepitant, protein lysates harvested after 1, 3, 6, 12 and 24 hours and probed for p-AKT (ser473), total AKT and β -actin. Western blots were carried out at least twice and representative pictures are shown. Numbers on top of each band indicate the fold induction or decrease as determined by total and phospho-specific signals. Figure taken from Ilmer et al.¹⁵⁸

RESULTS

Hepatoblastoma cell lines (HepT1, HepG2 and HuH6) were treated with aprepitant for 24 hours and Western blot analysis was performed for AKT, 4E-BP1/2, p70S6K and mTOR in their phosphorylated and non-phosphorylated form (Figure 19A). Short time treatment were also realized in the three hepatoblastoma cell lines and phospho-AKT (ser473) and total AKT were analyzed (Figure 19B).

This experiment confirmed a robust decrease of p-4E-BP1 (S65) and p-p70S6K (T389) in all cell lines, but not in their total form. Interestingly, AKT activity was increased after aprepitant treatment as shown by increased p-AKT (S473, T308) to total AKT ratios as well as increased presence of p-mTOR (S2448) (Figure 19A and Supplemental Figure 1).

To analyze more in depth this pathway, mRNA expression levels of *AKT1* and *AKT2* were analyzed and immunofluorescence staining of p-AKT (S473) and p-mTOR (S2448) were realized in the three hepatoblastoma cell lines. With the exception of *AKT2* in HuH6, increasing doses of aprepitant led to decreasing mRNA levels of *AKT1* and *AKT2* in all the three hepatoblastoma cell lines analyzed so far (Figure 20).

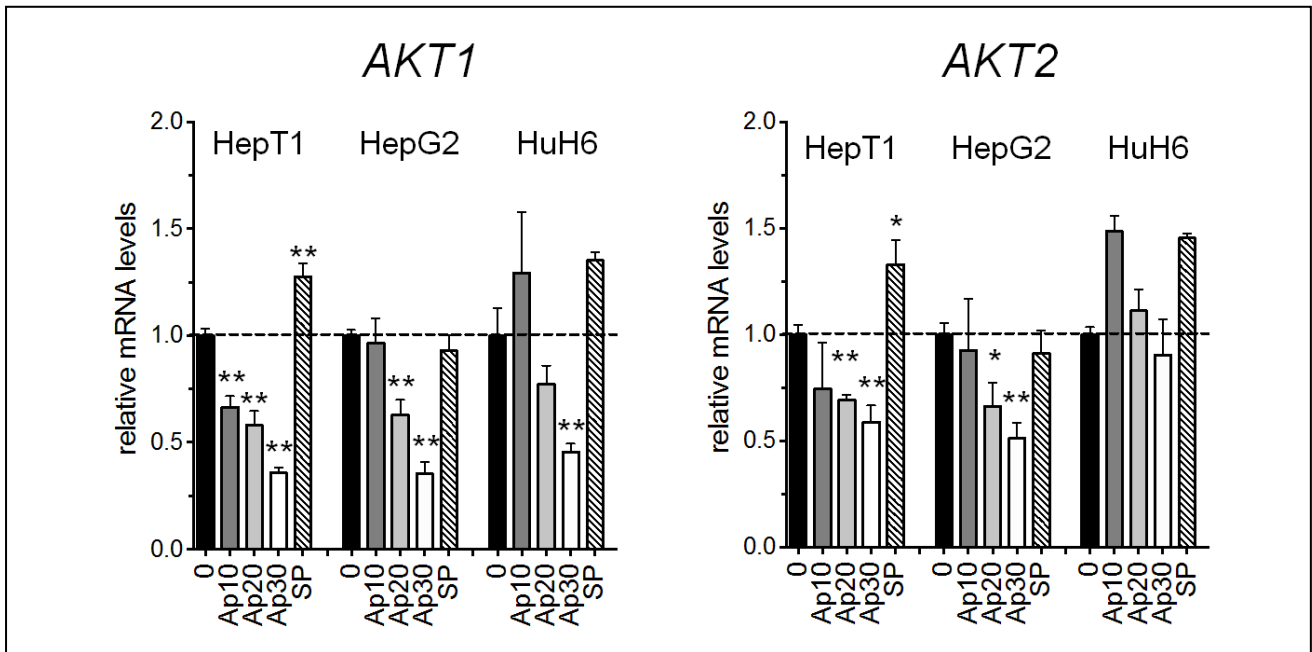


Figure 20: Analysis of *AKT1* and *AKT2* expression by qRT-PCR

Hepatoblastoma cell lines were subjected to mRNA analysis for *AKT1* and *AKT2* after aprepitant treatment (Ap 10 μM, Ap 20 μM and Ap 30 μM) or DMSO (0). All experiments were performed independently at least two times. Shown is the mean and error bars represent s.d.. Significance levels are as follows: * p < 0.05 and ** p < 0.01. Figure taken from Ilmer et al.¹⁵⁸

RESULTS

Immunofluorescence staining with p-AKT (S473) revealed that high doses of aprepitant led to an elevated number of cells with nuclear/paranuclear accumulation of p-AKT, which suggests an augmented activated AKT signaling in these cells (white arrow head in Figure 21, left panel). Even more impressive, we found that mTOR was activated, too, as evidenced by the translocation of p-mTOR (Ser2448) to the nucleus (white arrow head in Figure 21, right panel).

These results indicate that aprepitant treatment leads to an increased activity of AKT, a nuclear translocation of p-AKT (S473) and p-mTOR (S2448) after 24 hours, while downstream AKT targets, such as 4EBP1 or p70S6K, are significantly downregulated.

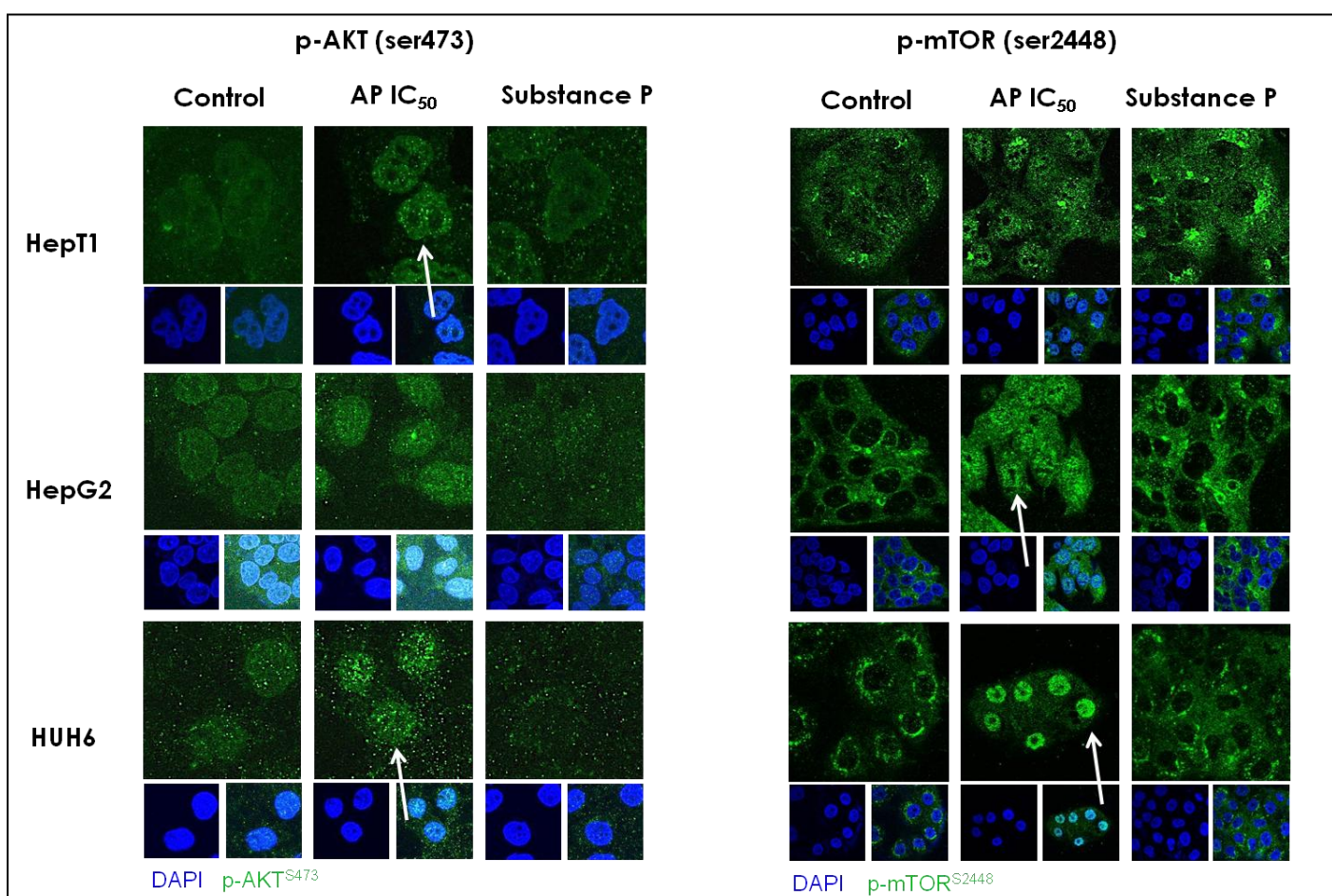


Figure 21: Nuclear translocation of p-AKT (S473) and p-mTOR (S2448) upon aprepitant treatment
Hepatoblastoma cells were treated for 24 hours with DMSO (Control), aprepitant (APIC50) or SP (70 nM). Subsequently, cells were fixed and stained for p-AKT (S473) or p-mTOR (S2448). Nuclei were stained with DAPI (blue). Shown are representative pictures of at least 4 randomly evaluated view fields. Figure taken from Illmer et al.¹⁵⁸

RESULTS

2.3 NK1R inhibition compromises FOXM1 expression and subsequently diminishes canonical Wnt signaling

FOXM1 has recently been shown to play an essential role in enhancing nuclear translocation of β -catenin as a shuttle protein, and in the subsequent increased activation of the canonical Wnt signaling cascade in glioma cells¹⁵⁹. Data from RPPA (Figure 18) suggested a decrease in FOXM1 expression upon Aprepitant treatment which was subsequently confirmed by Western blot (Figure 22A) and qPCR analysis (Figure 22B). In line with that, analysis of total β -catenin in the three hepatoblastoma cell lines revealed a decreased expression in HepT1 and HuH6 corroborating our data from RPPA analysis and indicating decreased activation of the Wnt pathway (Figure 22A).

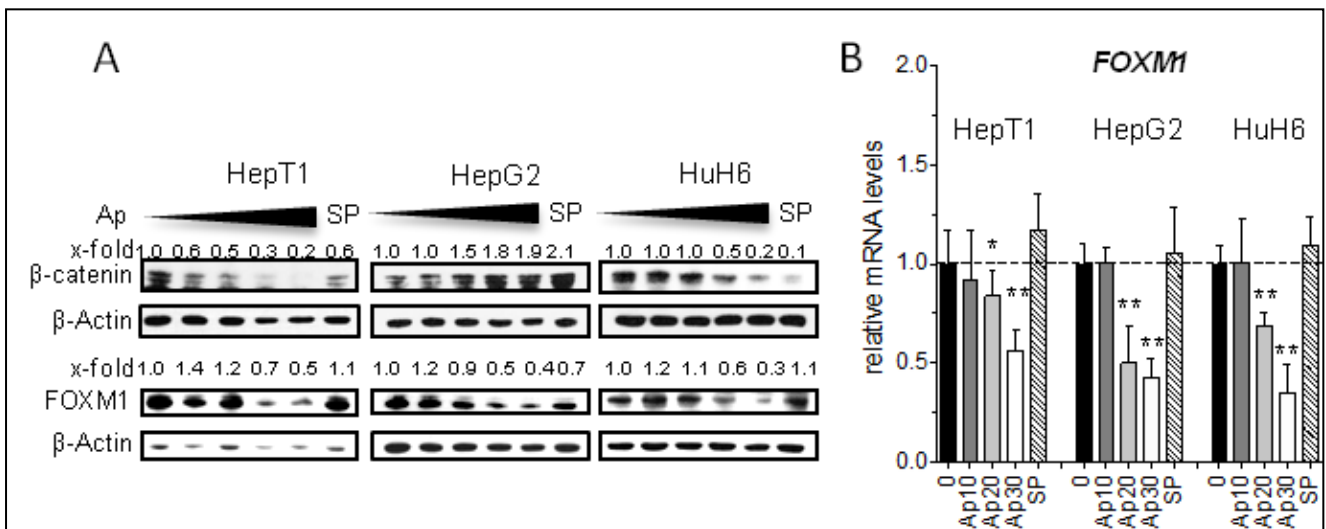


Figure 22: Aprepitant induces a downregulation of β -catenin and FOXM1 expression

(A) Western blot analysis of FOXM1 and β -catenin shows decreasing protein expression upon increasing doses of Aprepitant (0, 10, 20, 30, 40 μ M). Numbers on top of each band indicate the fold induction or decrease as determined by protein of interest to β -Actin signals. (B) qRT-PCR of FOXM1 shows dose-dependent decrease of gene expression after 24 hours of treatment with increasing doses of Aprepitant. Experiment was performed independently three times. Shown is the mean and error bars represent s.d.. Significance levels are as follows: * $p < 0.05$ and ** $p < 0.01$. Figure taken from Ilmer et al.¹⁵⁸

To further analyze the effects of Aprepitant on Wnt signaling, untreated cells were first stained for β -catenin and FOXM1 and subsequently analyzed by confocal microscopy. FOXM1 was found to colocalize in the cytoplasm and nucleus of HepG2 and HUH6 (Figure 23).

RESULTS

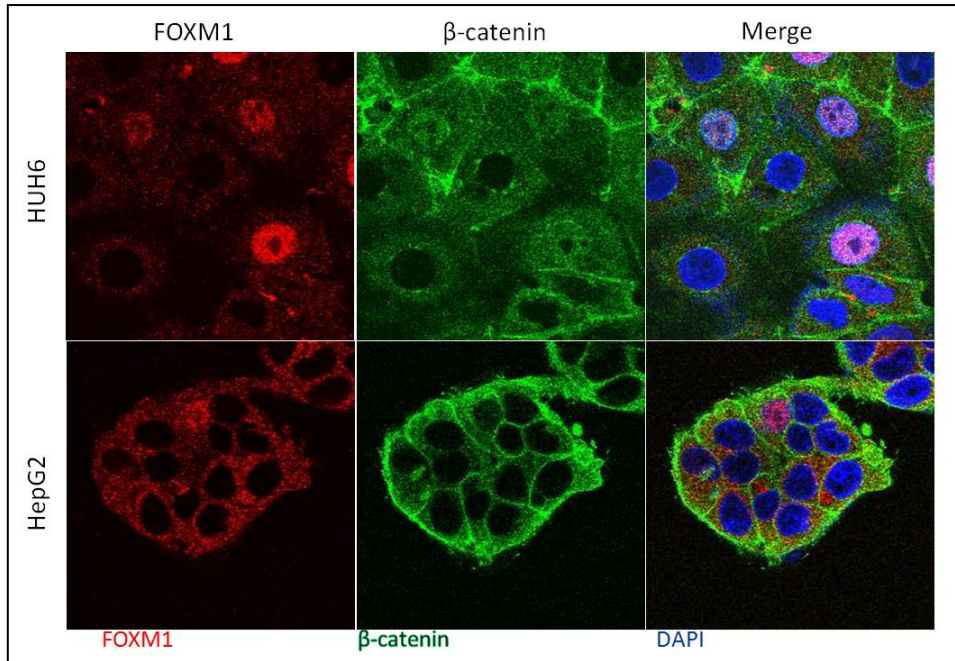


Figure 23: β -catenin and FOXM1 colocalize in hepatoblastoma cells

Untreated cells were stained for β -catenin (green) and FOXM1 (red), and analyzed by confocal microscopy. Nuclei were stained with DAPI (blue).

Cells were then treated with aprepitant (IC50) or SP (70 nM) for 24 hours, stained for β -catenin and analyzed by confocal microscopy. Interestingly, aprepitant induced a depletion of nuclear and cytosolic β -catenin as well as a strong accumulation of membrane-bound β -catenin (green) (Figure 24, left panel, white arrow), indicating an inactivation of canonical Wnt signaling. In contrast, stimulation with SP did not alter Wnt signaling significantly, presumably due to the high baseline Wnt activity in β -catenin mutated hepatoblastoma cell lines.

In order to investigate the role of FOXM1, the same treatments were repeated and cells were stained for FOXM1 (red). In contrast to β -catenin, FOXM1 increasingly translocated to the nucleus upon aprepitant treatment (Figure 24, right panel, white arrows), thereby moving in the opposite direction to β -catenin.

RESULTS

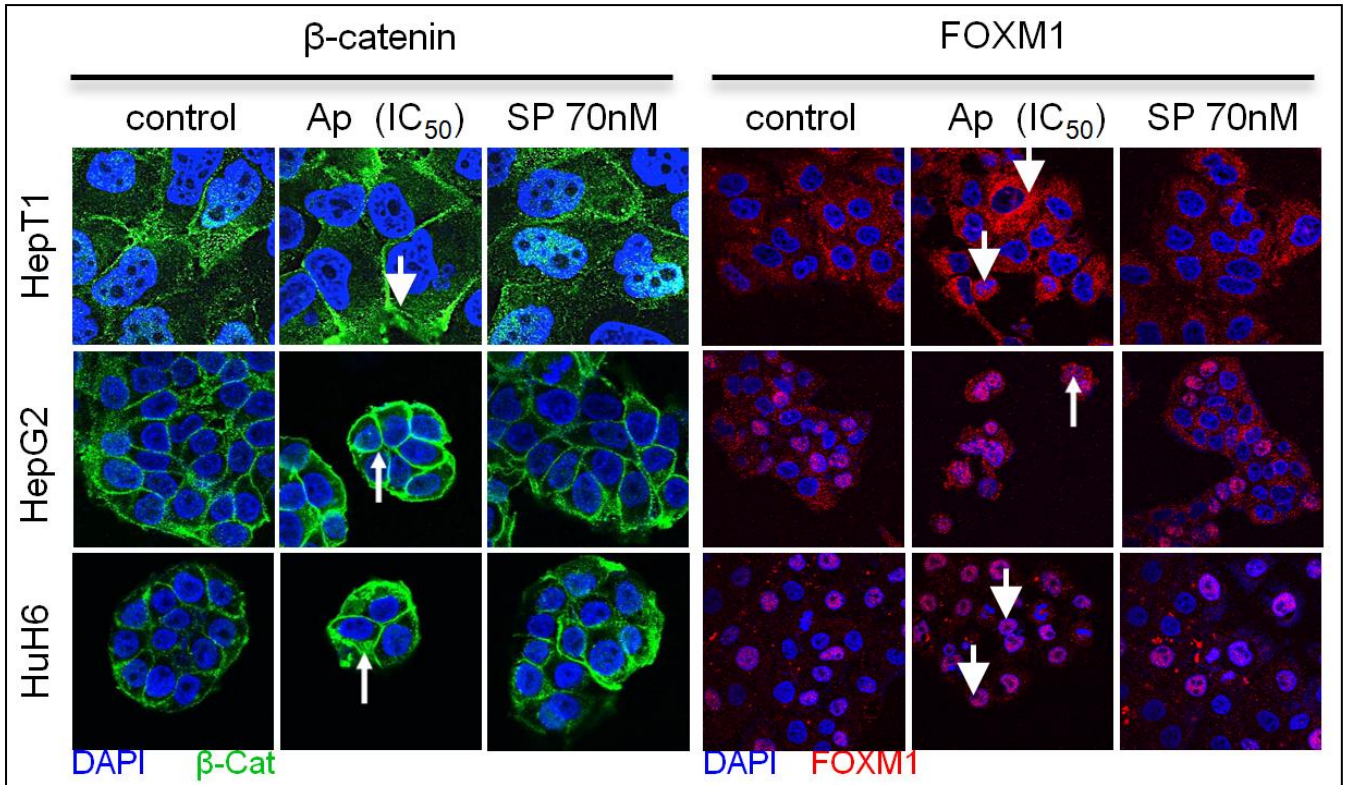


Figure 24: Immunofluorescence of β -catenin and FOXM1 in hepatoblastom cell lines
 Aprepitant (IC₅₀), SP (70 nM) and DMSO (control) treatments were carried out and immunofluorescent stainings for β -catenin (green) or FOXM1 (red) were performed. Nuclei were stained with DAPI (blue). Figure taken from Ilmer et al.¹⁵⁸

To support these important findings, quantification analysis of the immunofluorescence data was subsequently realized (Figure 25).

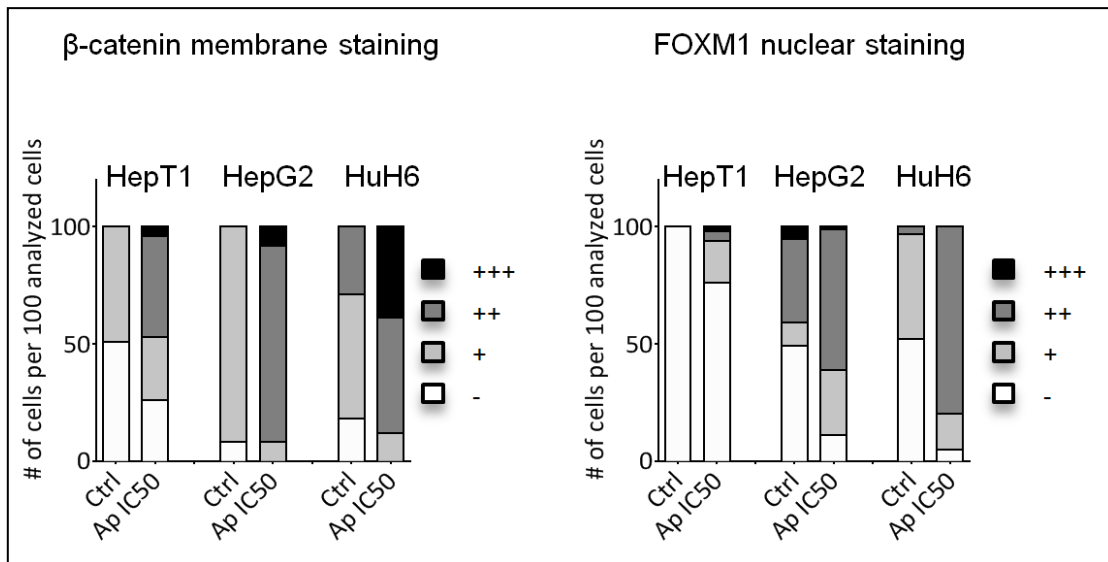


Figure 25: Aprepitant induces membrane-bound β -catenin and nuclear accumulation of FOXM1
 For each condition indicated in Figure 24, 100 cells from at least 9 random fields were analyzed regarding the localization (membranous and/or nuclear) and the signal intensity (from very high +++ to very low -) of β -catenin and FOXM1 staining. Aprepitant treatment increases membrane-bound β -catenin and depletes cytosolic/nuclear β -catenin accumulation (left panel). On the contrary, FOXM1 (red) is shifted into the nucleus (right panel). Figure taken from Ilmer et al.¹⁵⁸

RESULTS

To further investigate the action of Aprepitant on canonical Wnt signaling, we then included the hepatocellular carcinoma cell line HuH7 for subsequent experiments that doesn't carry mutations in the canonical Wnt signaling pathway, as opposed to the other hepatoblastoma cells that harbor β -catenin mutations. In accordance with this, a significant activation of Wnt signaling in HepT1, HepG2 and HuH6, but not in HuH7 was detected by Super TOP/FOP (STF) reporter luciferase assays (Figure 26A).

In a next step, STF assays were carried out after treatment with increasing doses of Aprepitant in the four cell lines. A robust inhibition of Wnt activity was detected in all β -catenin mutated hepatoblastoma cell lines, whereas Wnt activity in HuH7 remained unaffected (Figure 26B).

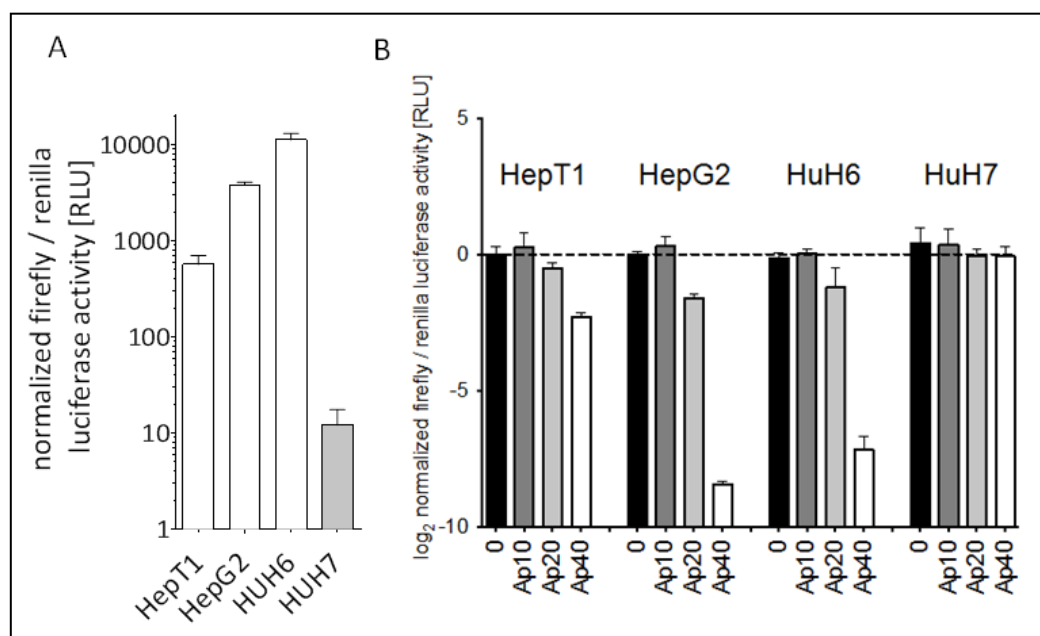


Figure 26: Aprepitant induces a decrease of Wnt activity in hepatoblastoma cell lines

Cells were treated with increasing doses of Aprepitant (Ap 10 μ M, Ap 20 μ M and Ap 40 μ M) or DMSO (0) and Super TOP/FOP (STF) assay was conducted. Measurements of Wnt activity were realized after 24 hours of treatment. Shown are the relative values to the untreated control sample (black column), the mean and error bars represent s.d.. Figure taken from Ilmer et al.¹⁵⁸

These results could be corroborated by findings with qRT-PCR in which the Wnt target genes *LGR5*, *CTNNB1* and *AXIN2* were dose dependently downregulated upon Aprepitant treatment in all hepatoblastoma cell lines. Interestingly, even HuH7 exhibited a downregulation of Wnt target genes (Figure 27).

RESULTS

Overall, these data indicate that antagonism to the SP/NK1R complex by aprepitant leads to reduced expression of the β -catenin shuttle protein FOXM1, which in turn potentially contributes to the observed decreased canonical Wnt signaling in hepatoblastoma cells harboring β -catenin mutations.

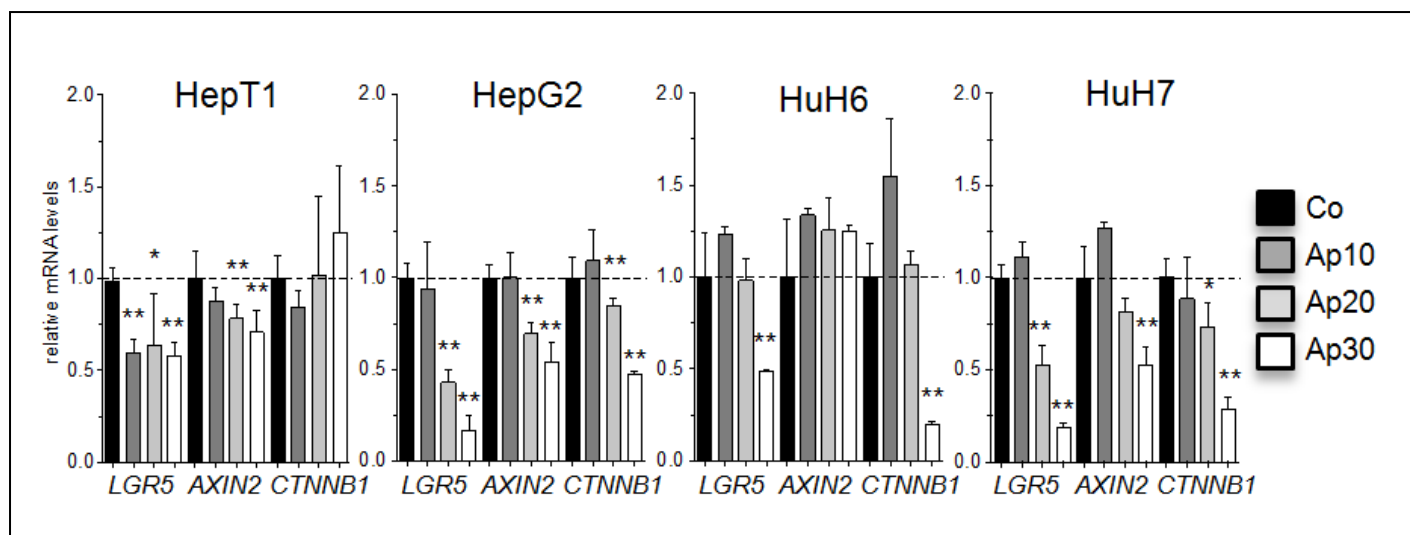


Figure 27: Aprepitant induces a decrease of Wnt target genes expression in hepatoblastoma
qRT-PCR on Wnt target genes (*LGR5*, *AXIN2*, *CTNNB1*) in HepT1, HepG2, HUH6 and HUH7. Shown are the relative values to the untreated control sample (black column) as fold changes after normalization to TATA-box binding protein (*TBP*). Cells were treated for 24 hours with 10 μ M (dark grey bars), 20 μ M (light grey bars) or 30 μ M aprepitant (white bars). Shown is the mean and error bars represent s.d.. Significance levels are shown as follows: * $p < 0.05$ and ** $p < 0.01$. Figure taken from Ilmer et al.¹⁵⁸

2.4 Wnt pathway inhibition by aprepitant is effective downstream of β -catenin and disrupts the FOXM1- β -catenin interaction

In order to investigate how aprepitant might block the Wnt signaling pathway, HEK293 cells were stimulated with lithium chloride (LiCl) which activates canonical Wnt signaling by inhibiting $GSK3\beta$ ¹⁶⁰. Wnt activity levels were subsequently analyzed by STF assays (Figure 28A). As expected, LiCl alone increased Wnt activity significantly, whereas additional aprepitant then lowered Wnt levels almost back to baseline, suggesting that the functional inhibition of Wnt occurs at the level of or downstream to the β -catenin disruption complex. Likewise, upon LiCl treatment, Wnt signaling increased in the β -catenin wild type cell line HuH7 as indicated by STF and β -catenin immunofluorescence staining (Figure 28A-B). In both cases, aprepitant treatment reduced the effects provoked by LiCl significantly.

RESULTS

FOXM1 reportedly builds an interaction with β -catenin that facilitates the translocation of the latter to the nucleus - hence, it is critical for enhanced Wnt signaling¹⁵⁹. To further analyze how aprepitant acts on this interaction in hepatoblastoma, HuH7 cells were treated with LiCl, aprepitant or a combination of both for 24 hours. Cells were subsequently co-stained for FOXM1 and β -catenin (Figure 28C). Similar to Figure 23, a co-localization of FOXM1 (red) and β -catenin (green) in the cytoplasm of unstimulated HuH7 was observed (DMSO). Upon LiCl treatment, a significantly increase of cytosolic β -catenin was noted, whereas aprepitant treatment or a combination of both induced a depletion of cytosolic β -catenin with an increase of free cytosolic FOXM1 (Figure 28C).

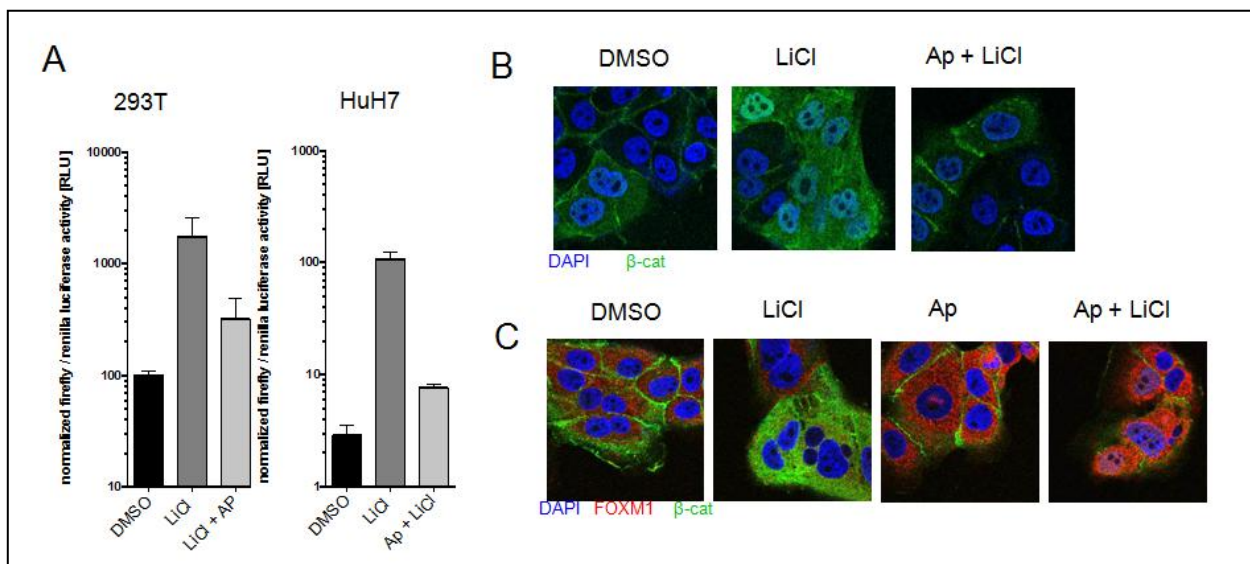


Figure 28: Aprepitant disrupts FOXM1/ β -catenin complex

(A) STF in HEK293 (293T) and HuH7: cells were treated with DMSO (black bar), 20 mM Lithium Chloride (LiCl) (dark grey bar) or a combination of 20 mM LiCl and 20 μ M aprepitant (Ap) (light grey bar) $n = 3$ (B) HEK293 cells were stained for β -catenin (green) and counterstained with DAPI (blue). (C) HuH7 cells were treated with DMSO, 20 mM LiCl, 20 μ M Ap or a combination (Ap + LiCl) and co-stained for FOXM1 (red) and β -catenin (green). Counterstaining was performed with DAPI (blue). Shown is the mean and error bars represent s.d.. Figure taken from Ilmer et al.¹⁵⁸

Taken together, these findings suggest that treatment with aprepitant inhibits canonical Wnt signaling downstream of GSK3 β most likely by disrupting proper FOXM1- β -catenin interaction in hepatoblastoma cells. However, co-immunoprecipitation experiments should be realized in order to validate this hypothesis.

RESULTS

2.5 NK1R antagonism inhibits growth of hepatoblastoma cancer stem-like cells

The Wnt pathway is known to be highly activated in cancer stem cells (CSCs)^{161, 162}. This is particularly interesting, because therapeutics that specifically target CSCs could potentially alter current treatment strategies. Therefore, in a next step, it was investigated whether such cells indeed show high activity of Wnt signaling and whether their growth could be inhibited by aprepitant. CSC-like cells were grown as non-adherent sphere cultures that were previously reported to enrich for CSCs¹⁶³. First, activity of Wnt signaling in sphere cultures was measured and compared to parental cell lines by measuring Wnt target gene expression. HepT1 spheres overexpressed *LGR5* and *AXIN2*, HepG2 spheres as well as their parental counterparts expressed similar levels for these markers, and the β -catenin wild type HuH7 spheres revealed a lower expression of *AXIN2* and *CTNNB1* (Figure 29).

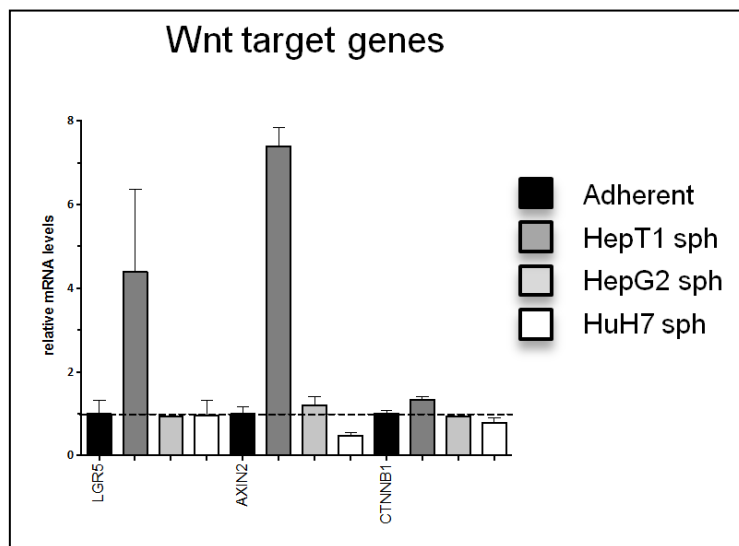


Figure 29: qRT-PCR of Wnt target genes in HepT1, HepG2, and HuH7 spheres

Shown are the relative values to adherent cells (black bars): HepT1 spheres in dark grey, HepG2 spheres in light grey, and HuH7 spheres in white. The error bars represent s.d.. Figure taken from Ilmer et al.¹⁵⁸

In order to assess their stemness, cells were analyzed for their expression of embryonic stem cell markers *SOX2*, *OCT4*, and *NANOG*¹⁶³. Expression of *NK1R-tr* and *NK1R-fl* was also analyzed. The results displayed an increased expression of *NANOG* in all spheres, an increased expression of *SOX2* in HepT1 and HepG2 spheres and an increased expression of *OCT4* in HepT1 and HuH7 spheres (Figure 30). A striking observation was that in HepT1 spheres, *SOX2* was overexpressed 7-fold while *OCT4* and *NANOG* were overexpressed 8-fold indicating increased stemness properties of these cells (Figure 30). Accordingly, HepT1

RESULTS

spheres also revealed the highest relative Wnt target gene overexpression (Figure 29). A noteworthy observation was that spheres overexpressed the truncated version of *NK1R* (*NK1R-tr*) compared to parental cells, whereas full length *NK1R* (*NK1R-fl*) was grossly unchanged (Figure 30).

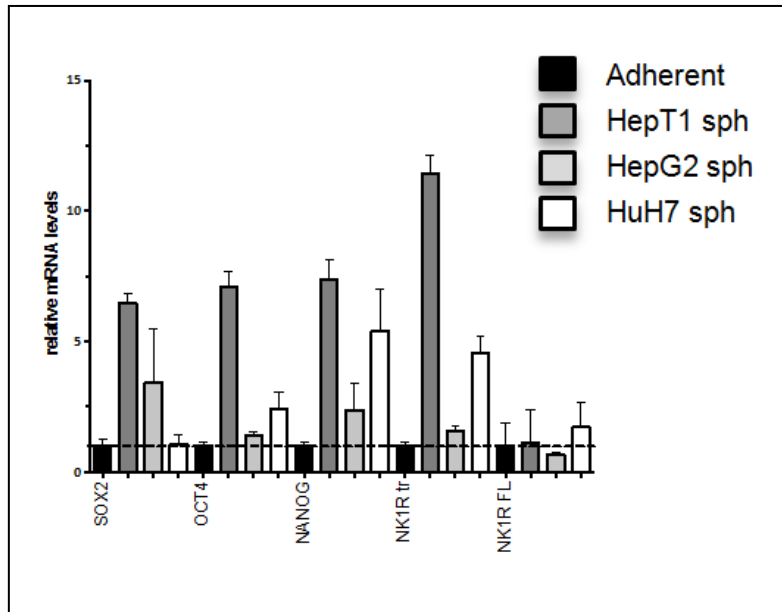


Figure 30: qRT-PCR on embryonic stemness markers in spheres compared to adherent cells

qRT-PCR of embryonic stem cell markers *SOX2*, *OCT4*, and *NANOG* as well as *NK1R* (*NK1R-tr* and *NK1R-fl*) in untreated adherent cells (black bars) and untreated spheres. Shown is the mean and error bars represent s.d.. Figure taken from Ilmer et al.¹⁵⁸

In order to investigate whether the expression pattern of stem cell markers may change following the inhibition of the *NK1R* receptor, CSC-like cells and their parental counterparts were treated with aprepitant and analyzed by qRT-PCR (Figure 31). First, a dose dependent downregulation of Wnt target genes *LGR5*, *AXIN2*, and *CTNNB1* was detected in spheres of all hepatoblastoma cell lines.

RESULTS

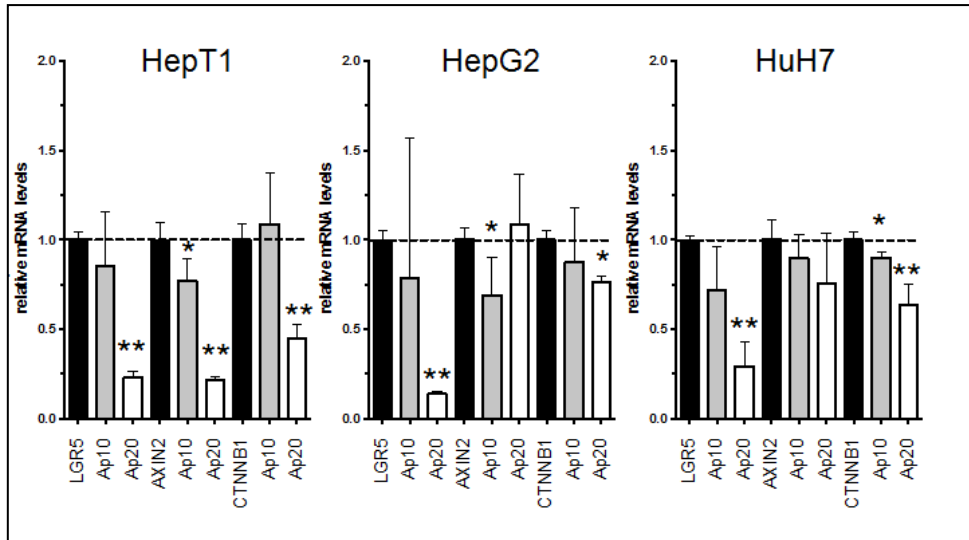


Figure 31: Aprepitant inhibits Wnt target genes expression in hepatoblastoma spheres
 (A) qRT-PCR of Wnt target genes in spheres. Spheres were treated for 24 hours with DMSO (black bars), 10 μM aprepitant (light grey bars) or 20 μM aprepitant (white bars). Data are normalized to *TBP* expression and presented as fold change in gene expression relative to DMSO treated controls. Shown is the mean and error bars represent s.d.. * p < 0.05 and ** p < 0.01 (n = 2). Figure taken from Ilmer et al.¹⁵⁸

Furthermore, mRNA expression of pluripotency markers as well as *NK1R* were analyzed in spheres upon aprepitant treatment. These markers were found downregulated in HepT1 and HepG2 parentals and spheres, whereas in HUH7 they tend to increase (Figure 32). In this regard, it seems the β-catenin mutated cell lines (HepT1 and HepG2) were more susceptible to aprepitant treatment than the β-catenin wild-type cell line HuH7.

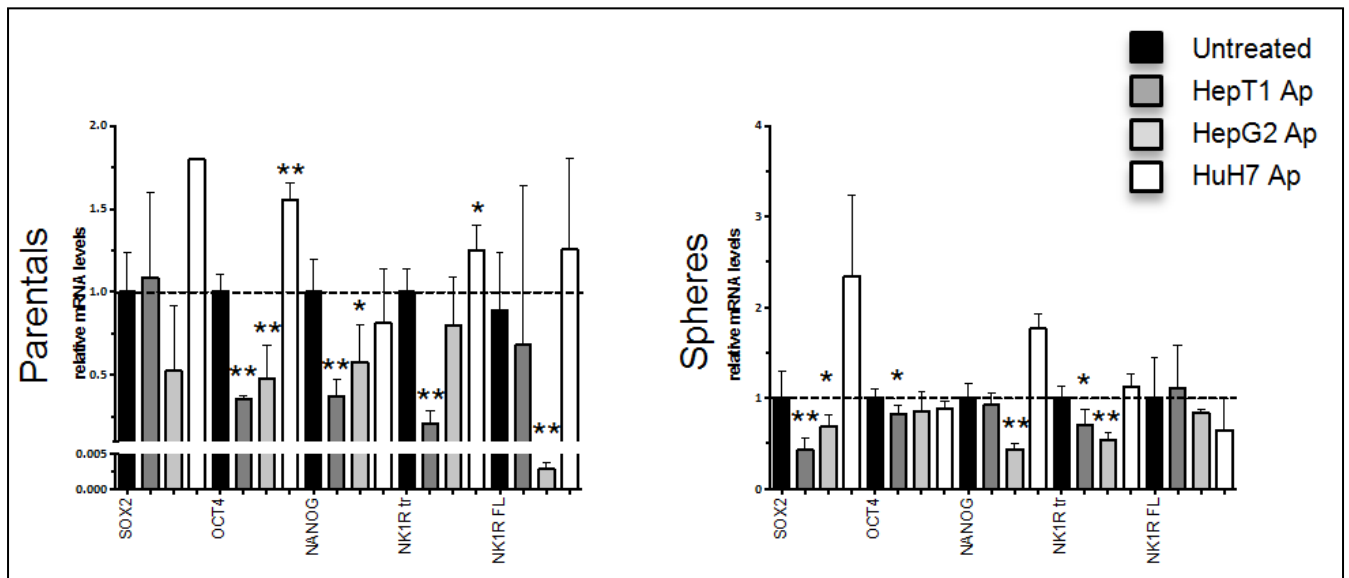


Figure 32: Inhibition of SP/NK1R compromises cancer stemness-associated traits in hepatoblastoma
 qRT-PCR of embryonic stem cell markers *SOX2*, *OXT4*, and *NANOG* as well as *NK1R* (*NK1R-tr* and *NK1R-fl*). Left panel: adherent cells were treated for 24 hours with DMSO (black bars) or 20 μM aprepitant. Data are normalized to *TBP* expression and presented as fold change in gene expression relative to DMSO-treated controls. HepT1 (dark gray bars), HepG2 (light gray bars), and HuH7 (white bars). Right panel: qRT-PCR analysis of stemness markers similar to the left panel in spheres. Shown is the mean and error bars represent s.d.. * p < 0.05 and ** p < 0.01 (n = 2). Figure taken from Ilmer et al.¹⁵⁸

RESULTS

Due to the modest changes in HuH7 cells, gene expression analysis of previously described liver-specific CSC markers ($CD13^{164}$, $CD133^{165}$, $CK19^{166}$, $EPCAM^{167}$, and GEP^{168}) as well as AFP , the serum marker of hepatoblastoma, were included in this study (Figure 33). AFP and $CD13$ were found downregulated in all hepatoblastoma spheres upon apreitant treatment as well as $CD133$, $CK19$, $EPCAM$, and GEP in either HepT1 or HepG2 spheres (Figure 33).

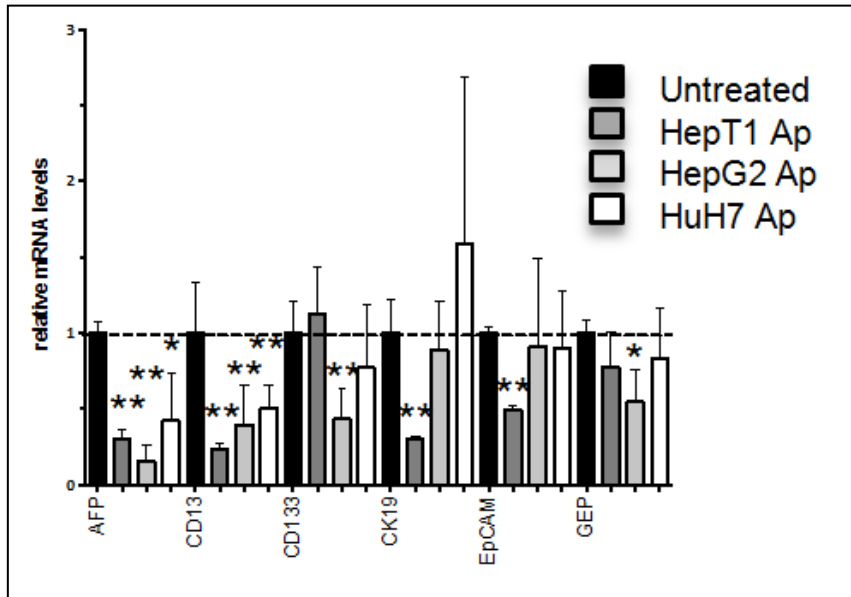


Figure 33: Apreitant targets liver specific cancer stem cell markers in hepatoblastoma

Spheres were treated as indicated in Figure 32. qRT-PCR of liver-specific CSC markers. Shown is the mean and error bars represent s.d.. Significance levels are as follows: * $p < 0.05$ and ** $p < 0.01$ ($n = 2$). Figure taken from Ilmer et al.¹⁵⁸

Finally, $FOXM1$ expression was also analyzed in spheres. Its expression decreased in a dose-dependent manner in all hepatoblastoma spheres (Figure 34) similar to the findings in the respective parental cell lines (Figure 22B).

RESULTS

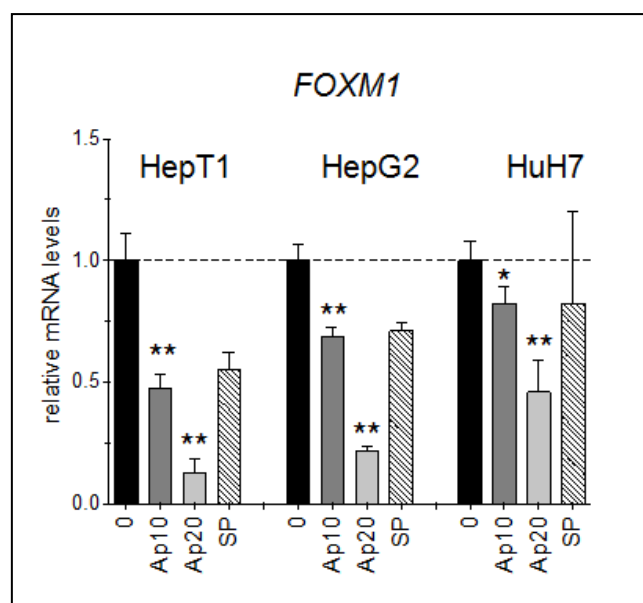


Figure 34: Aprepitant induces a downregulation of *FOXM1* expression in spheres

Spheres were treated with aprepitant for 24 hours (Ap 10 μ M or 20 μ M) or DMSO (0) and qRT-PCR analysis for *FOXM1* was performed. Shown are the relative values standardized to *TBP*. Shown is the mean and error bars represent s.d.. Significance levels are as follows: * $p < 0.05$ and ** $p < 0.01$ ($n = 2$). Figure taken from Ilmer et al.¹⁵⁸

Having seen a decreased activity of the Wnt pathway as well as a downregulation of defined liver stem cell markers upon inhibition of NK1R by aprepitant, the next step was to investigate whether self-renewal of CSC-like cells could be targeted with aprepitant. In order to do so, sphere formation ability (SFA) assays were performed, which assess functional anoikis-resistant self-renewal behavior of CSCs *in vitro*.

Aprepitant induced a robust inhibition of sphere formation with simultaneous treatment (Figure 35A) in HepT1, HepG2 and the β -catenin wild-type cell line HuH7. Because aprepitant induced apoptosis in parental hepatoblastoma cells, Western blot analysis for PARP were realized in the same cell lines after aprepitant treatment. Similarly, apoptosis induction was detected in spheres as evidenced by increased PARP cleavage upon aprepitant treatment (Figure 35C).

To rule out that inhibition of sphere formation is only executed by apoptosis induction, cells were pretreated in adherent conditions and only seeded viable cells were seeded for SFA assays. Intriguingly, a single pretreatment with aprepitant was sufficient to significantly diminish their sphere formation capacity (Figure 35B) indicating that aprepitant might not only exert its effect by reducing three-dimensional cell growth or inducing cell death in CSC-

RESULTS

like cells, but moreover sustainably influences CSC properties in cancer cells, which support the data obtained by qRT-PCR (Figure 31 and 32).

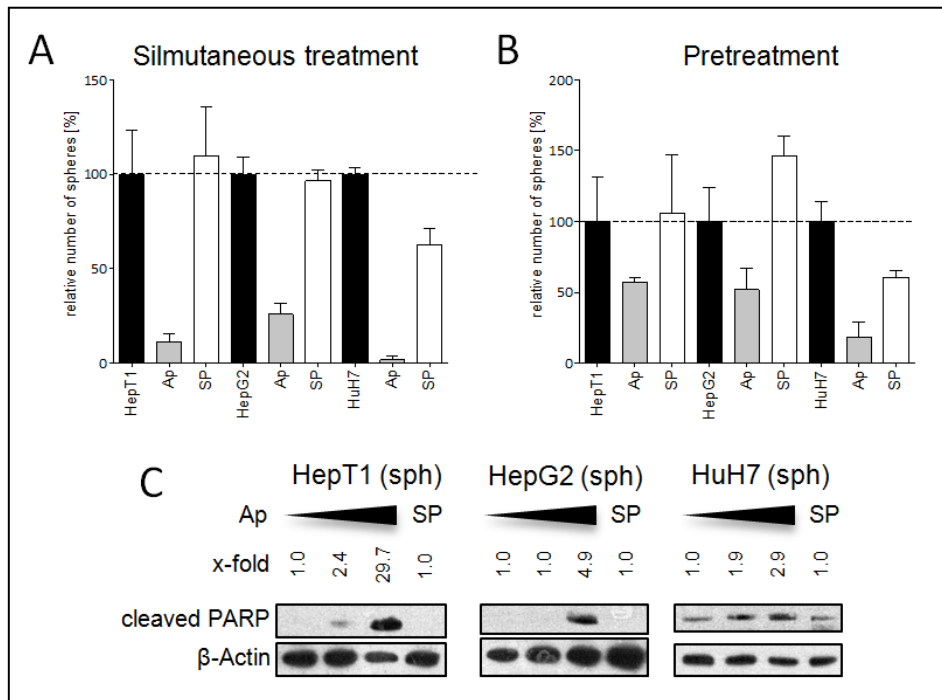


Figure 35: Aprepitant impairs sphere formation ability and triggers apoptosis in spheres

(A) Simultaneous treatment: sphere formation ability (SFA) assays in hepatoblastoma cell lines HepT1 and HepG2 as well as in the hepatocellular carcinoma cell line HuH7. Spheres were cultures for several days in 1% methylcellulose media. Treatment was realized every three days with the addition of 100 μL of 1% methyl cellulose media supplemented with 20 μM aprepitant (grey bars), 70 nM SP (white bars) or DMSO (black bars). Shown is the relative number of spheres per 500 seeded cells in an ultra low-attachment 96-well plate. (n = 2) (B) Pretreatment: Adherent cells were pretreated with 20 μM aprepitant or 70 nM SP for 24 hours, then viable cells seeded into SFA assays, and grown without any further treatment for 10 days. Shown is the relative number of spheres per 500 seeded cells. (n = 2) (C) Western blot analysis of PARP in HepT1, HepG2 and HuH7 spheres after treatment with 10 μM or 20 μM aprepitant, or 70 nM SP. Fold changes of protein expression compared to control and standardized to β-actin is shown on top of each band. Shown is the mean and error bars represent s.d.. (n = 1). Figure taken from Ilmer et al.¹⁵⁸

Taken together, these findings illustrate that in addition to conventional human hepatoblastoma, hepatoblastoma cells with stem cell-like properties (CSC-like cells) can be growth inhibited by targeting the NK1R.

Altogether, our study uncovered the effect of aprepitant on hepatoblastoma cells at a molecular level identifying a downregulation of PI3K/AKT/mTOR pathway and inhibition of Wnt activity possibly through the downregulation of FOXM1 as the major components of this inhibition (Figure 36).

RESULTS

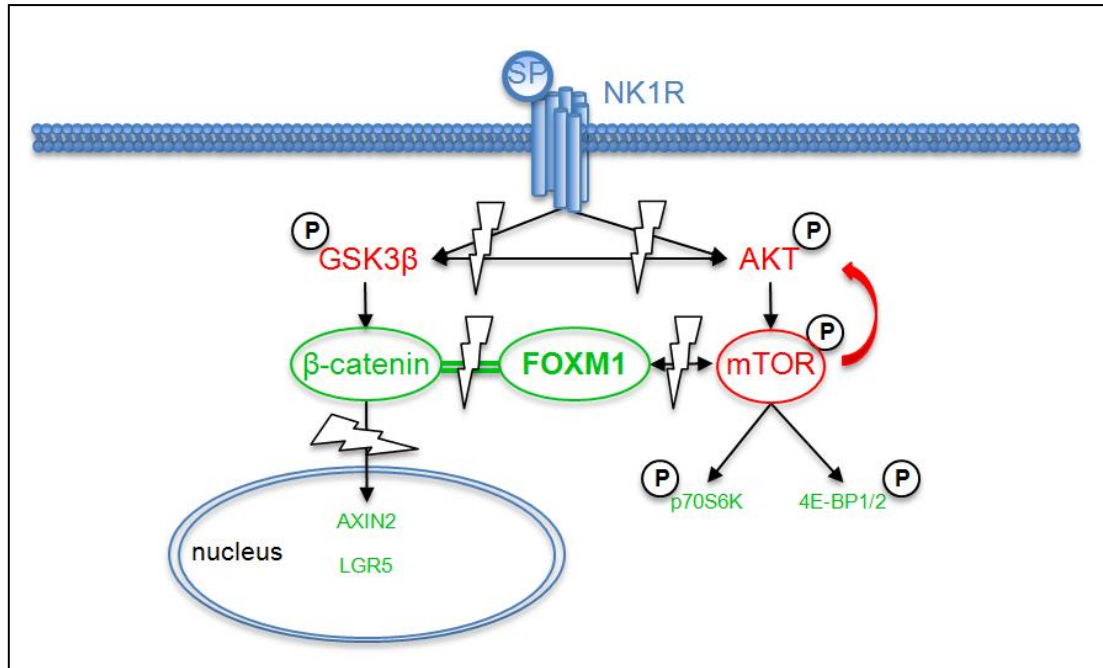


Figure 36: Graphical illustration of crosstalk between NK1R, PI3K/AKT/mTOR pathway, and canonical Wnt signaling.

According to our data, the SP/NK1R system seems to positively influence downstream PI3K/AKT/mTOR (right side of the illustration) and Wnt signaling (left side of the illustration). Upon blockage of NK1R with aprepitant, both phosphorylation sites of AKT (S473 and T308) as well as mTOR (S2448) (in red) become increasingly phosphorylated after 24 hours indicating an activation of upstream PI3K/AKT/mTOR signaling, whereas downstream actors of PI3K/AKT/mTOR (p70S6K and 4E-BP1/2) appear to be down-regulated (in green). On the other hand, aprepitant treatment increases GSK3β phosphorylation (in red), but robustly inhibits canonical Wnt signaling as evidenced by decreased β-catenin as well as downregulated Wnt target genes *AXIN2* and *LGR5* (all in green). The key mechanism for the latter seems to be disruption of the FOXM1-β-catenin interaction. Figure taken from Ilmer et al.¹⁵⁸

RESULTS

3. Targeting the NK1R inhibits growth of human colon cancer cells

The results presented in this section are part of the publication: Targeting the neurokinin-1 receptor inhibits growth of human colon cancer cells. *International Journal of Oncology* (2015 Jul;47(1):151-60) [Garnier A](#), Vykoukal J, Hubertus J, Alt E, von Schweinitz D, Kappler R, Berger M, Imer M.

In the previous sections, we studied the consequences of blocking the NK1R using aprepitant in hepatoblastoma cell lines. Globally, we observed both growth reduction and apoptosis of the treated cells. At the intracellular level, we discovered that aprepitant disrupts the Wnt and PI3K/AKT/mTOR pathways, which possibly explains some of its effects. In this section, we investigated the effects of aprepitant on human colon cancer cell lines in order to extrapolate our results in another model harboring a deregulation of Wnt signaling as well.

3.1 NK1R blocking leads to the regulation of specific proteins involved in PI3K/AKT/mTOR and canonical Wnt signaling

First, human colorectal cancer (CRC) cell lines LiM6 (*CTNNB1* mutation¹⁶⁹) and DLD1 (*APC* mutation¹⁷⁰) were treated with increasing doses of aprepitant for 48 hours and standard MTT assays were subsequently realized. As observed with the hepatoblastoma cell lines, aprepitant induced a dose-dependent reduction of cell growth in both cell lines (Figure 37).

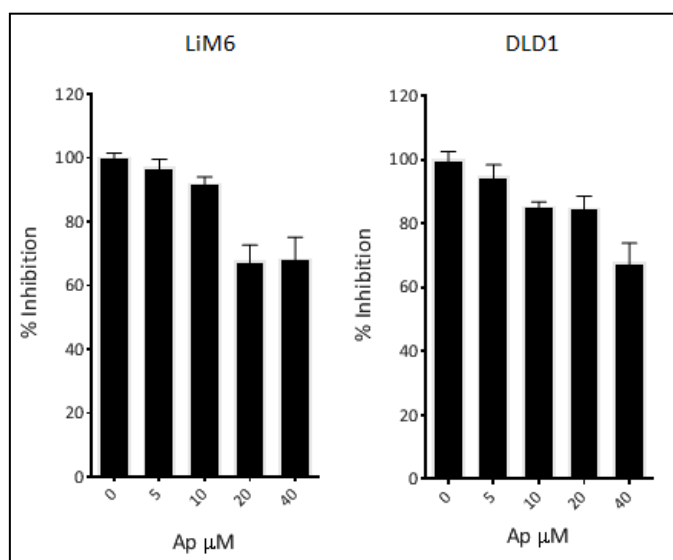


Figure 37: Aprepitant triggers growth inhibition in colorectal cancer cells

(A) MTT assay in DLD1 and LiM6. Cells were treated with increasing concentration of aprepitant or with DMSO (control) for 48 hours to assess cell survival. Shown is the mean and error bars represent s.d.. Figure taken from Garnier et al.¹⁷¹

RESULTS

In order to have a better understanding of the downstream molecular mechanisms responsible for these observed effects, RPPA was also realized in these cells. Similarly to hepatoblastoma cells, CRC cell lines LiM6 and DLD1 were treated with 20 μM or 40 μM aprepitant for 24 hours and 172 proteins were screened for changes in protein expression. To better scrutinize the regulation pattern in the two cell lines, we again averaged the changes after aprepitant treatment over the two cell lines conditions and for each protein (Figure 38). According to the cut off values, only a small number of proteins exhibited an upregulation (red) or downregulation (green) common in the two cell lines. However, compared to hepatoblastoma cells, aprepitant seemed to have a more potent effect on changes in expression in CRC cells (Figure 38).

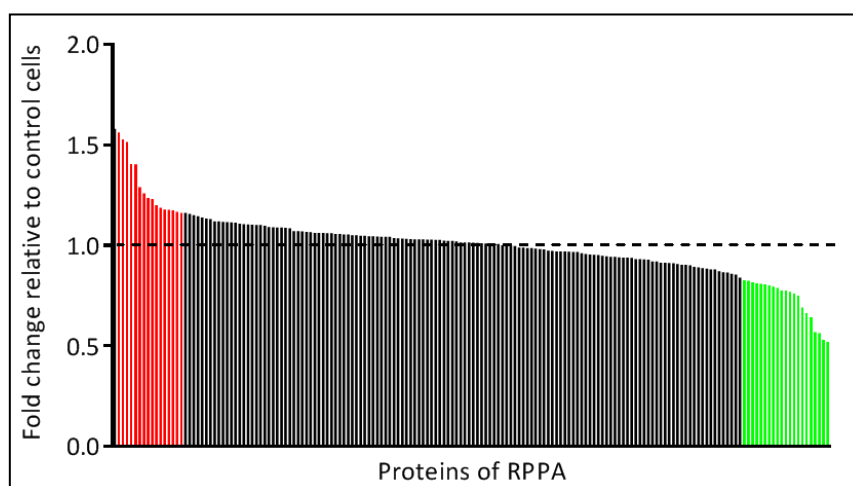


Figure 38: Pattern of regulation of 172 proteins analyzed by RPPA in two CRC cell lines

CRC cells (LiM6 and DLD1) were cultured in monolayer, treated with DMSO (control), aprepitant (20 μM or 40 μM) or substance P (SP) for 24 hours and protein lysates were analyzed by RPPA. The averaged changes after aprepitant treatment of all two CRC cell lines for all the proteins investigated compared to untreated controls are shown. The cut-offs were chosen according to the standard deviation of the values. In red, the selected proteins with a relative fold-change ≥ 1.163 and in green, the selected proteins with a relative fold-change ≤ 0.836 are shown. In black, proteins with no significant changes in expression. Figure taken from Garnier et al.¹⁷¹

A key outcome of this experiment is the finding of a similar intracellular pattern of regulation after aprepitant treatment between human hepatoblastoma and CRC cells. Indeed, some of the proteins which were significantly regulated could be associated to the PI3K/AKT/mTOR pathway and the Wnt signaling. Among the latter, the target gene MYC and the β -catenin interacting factor FOXM1 were found downregulated. Interestingly, β -catenin was not found significantly altered (Figure 39).

RESULTS

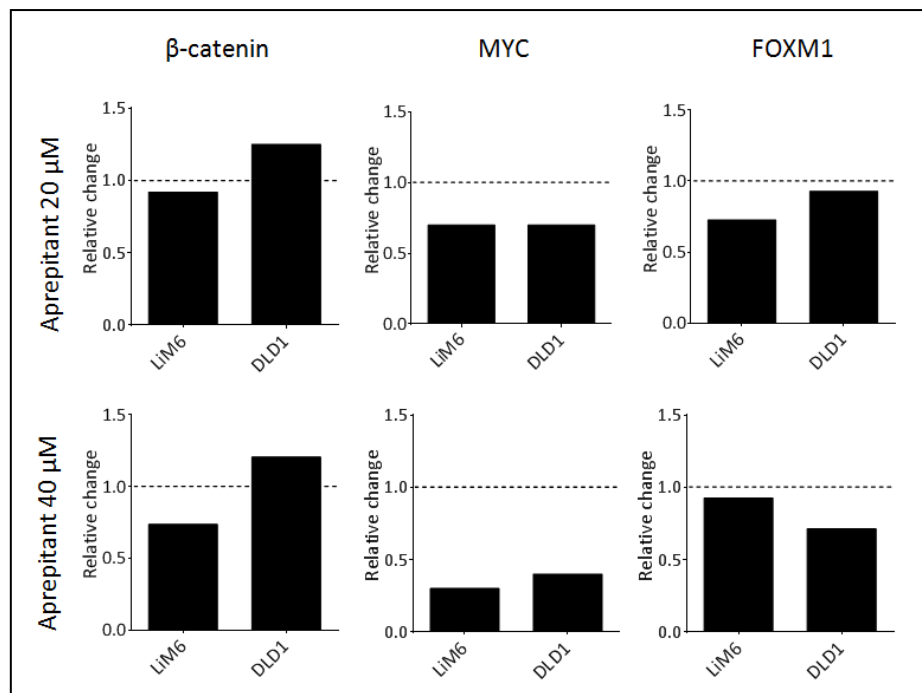


Figure 39: Aprepitant alters expression of Wnt associated proteins in CRC cells

Graphical representation of relative fold-changes of proteins associated with Wnt pathway (β -catenin, MYC, FOXM1) after aprepitant treatment (20 μ M or 40 μ M). Cells were treated with 20 μ M or 40 μ M aprepitant, values were put into relation with the control (DMSO) and normalized to 1. Figure taken from Garnier et al.¹⁷¹

Concerning the PI3K/AKT/mTOR pathway, its downstream proteins 4E-BP1/2 (S65), p70S6K (T389) (grey bars) were also found downregulated compared to their total forms (black bars). Total AKT was also dose-dependently downregulated upon aprepitant treatment in the two cell lines, whereas no clear trend could be extracted from its phosphorylated form at T308. In contrast, phosphorylation of AKT at S473 was upregulated along with its substrate PRAS40 at T246 (Figure 40).

RESULTS

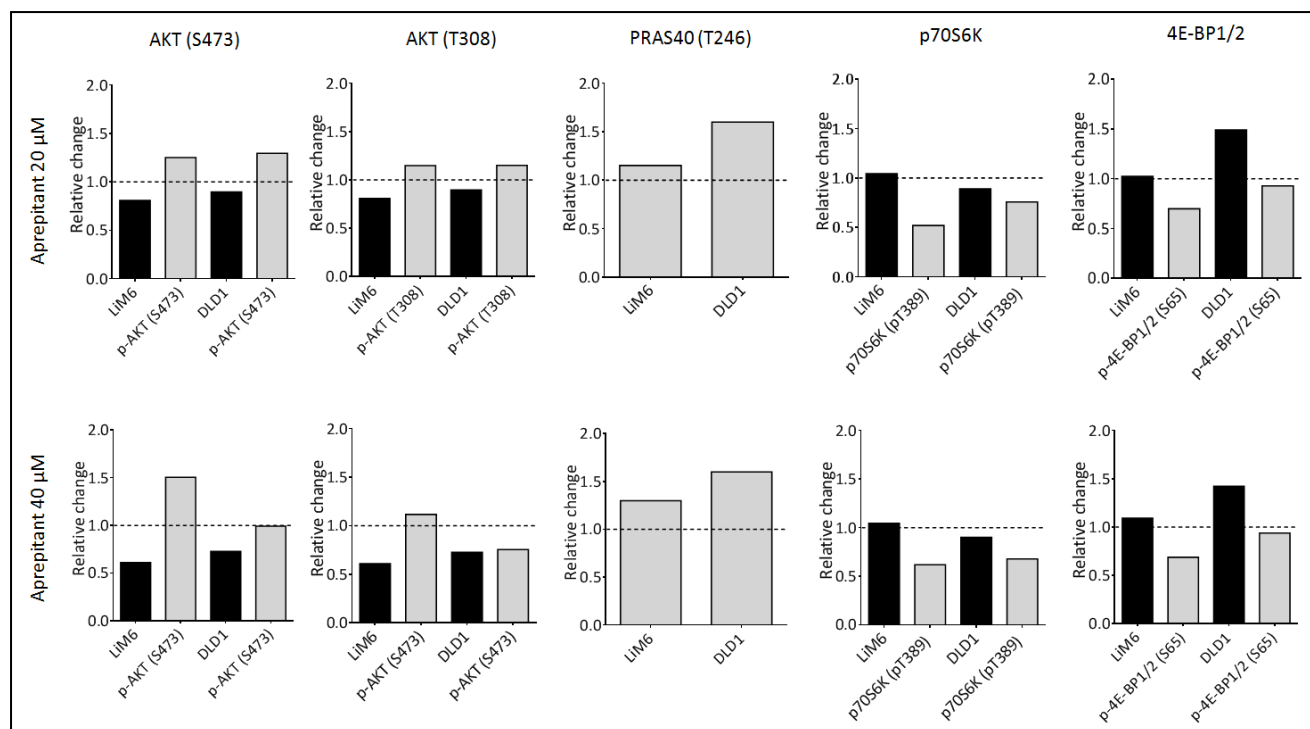


Figure 40: RPPA reveals an inhibition of PI3K/AKT/mTOR pathway in CRC cells

Relative fold-changes of proteins involved in PI3K/AKT/mTOR pathway. Cells were treated with 20 μM or 40 μM Aprepitant, values were put into relation with the control (DMSO) and normalized to 1. For AKT (S473), AKT (T308), PRAS (T246), p70S6K (T389) and 4E-BP1/2 (S65) the phosphorylated proteins are shown in grey bars and the total proteins in black bars. Figure taken from Garnier et al.¹⁷¹

3.2 NK1R antagonism induces apoptosis and a G2 arrest

In the earlier sections, it was shown that Aprepitant induced apoptosis in human hepatoblastoma cells. Therefore, as a next step it was investigated whether this held true in CRC cells. First, data obtained by RPPA were screened for alterations in apoptosis markers. For instances, cleaved caspase 7 and phospho-c-Jun (S73), two well known mediators of apoptosis^{172, 173} were upregulated upon Aprepitant treatment (Figure 41A). In order to confirm the RPPA data, DLD1 cells were treated for 24 hours with increasing concentration of Aprepitant and Western blot analysis for PARP was performed. As expected, Aprepitant induced a dose-dependent increase of cleaved PARP indicating an activation of apoptosis, whereas SP had no effect (Figure 41B). Moreover, HER3 was found to be downregulated and targeting this receptor in CRC cells has been described to induce a G2 arrest as well as apoptosis¹⁷⁴ (Figure 41A).

RESULTS

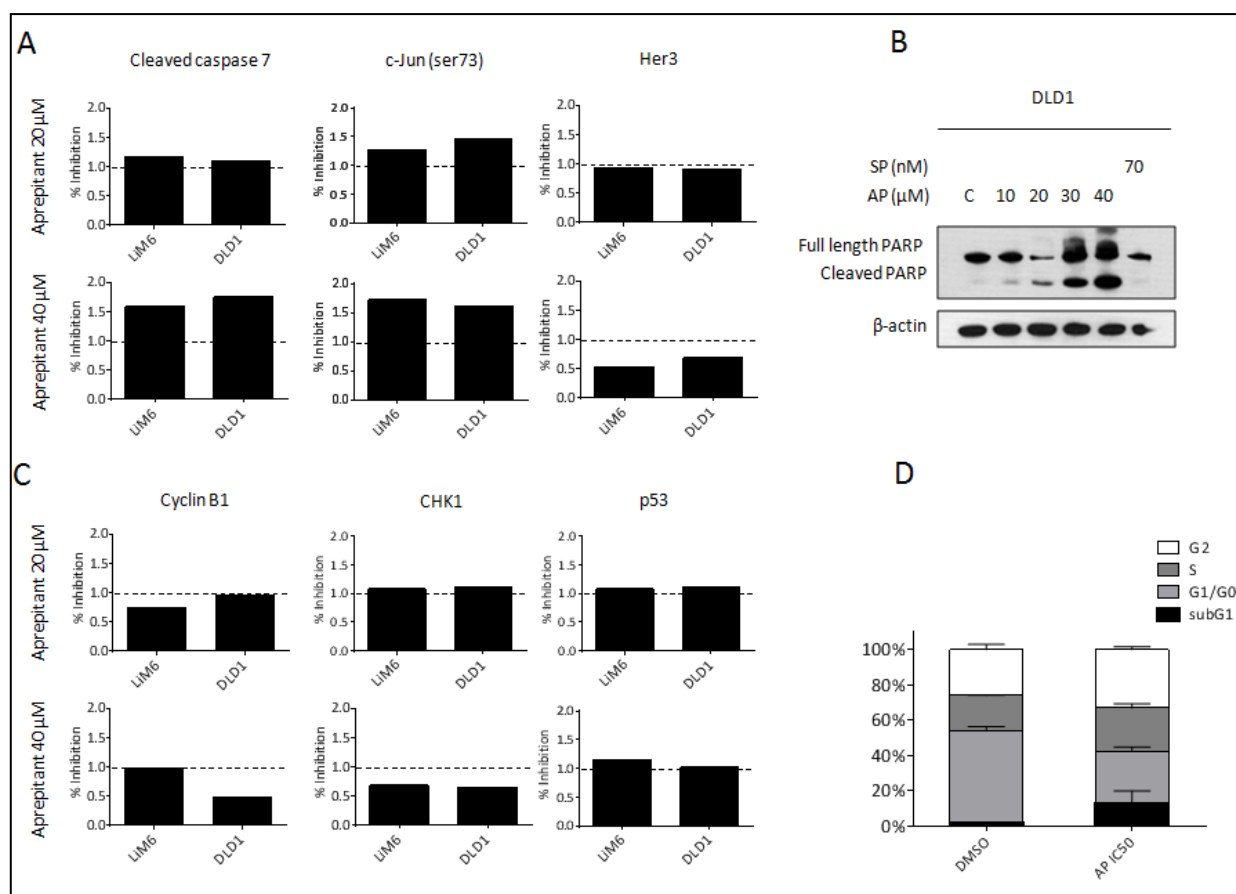


Figure 41: Aprepitant induces a G2 arrest and apoptosis in colorectal cancer cells

(A) Relative fold-change of selected up and downregulated proteins involved in apoptosis or (C) in cell cycle regulation are shown. (B) Western blot analysis of total and cleaved PARP after treatment with increasing doses of aprepitant for 24 hours. (D) Analysis of the cell cycle by flow cytometry in DLD1. Cells were treated with 30 μM aprepitant or DMSO for 24 hours and stained with propidium iodide. The data are represented as the percentage of cells at different stages: subG1 (black), G1/G0 (black and grey), S (grey) or G2 (white). Values are shown in percent and n=2. Figure taken from Garnier et al.¹⁷¹

In order to scrutinize the molecular basis of aprepitant-induced growth inhibition, cell cycle analysis was realized. The RPPA data revealed a downregulation of cyclin B1 and Checkpoint kinase 1 (CHK1), whereas p53 was slightly upregulated (Figure 41C). These proteins are known to regulate the G2-M transition¹⁷⁵. To take a step further, DLD1 cells were treated with aprepitant for 24 hours with 30 μM aprepitant and cell cycle profile by propidium iodide staining and FACS analysis was performed. As shown in Figure 41D, aprepitant induced a G2 arrest (33% compared with 26% for DMSO-treated cells, white bar) and an increase of cells in the subG1 phase (12.7% compared with 1.63% for DMSO-treated cells, black bar) indicating either late apoptosis or necrosis.

RESULTS

3.3 NK1R antagonism inhibits canonical Wnt signaling

RPPA data in CRC cells suggested that aprepitant might induce a reduction of Wnt activity as observed in hepatoblastoma cell lines. In order to confirm this hypothesis, STF assays were performed first in non-treated cells to assess the baseline Wnt activity in DLD1 and LiM6, and in the pancreatic cancer cell line L3.6pl, a cell line known to express little Wnt¹⁷⁶. As expected, both colon cancer cell lines displayed high levels of Wnt activity with approximately a 500-fold increased activity compared to L3.6pl (Figure 42A). However, upon aprepitant treatment, a robust inhibition of Wnt activity in both colorectal cell lines was observed (Figure 42B).

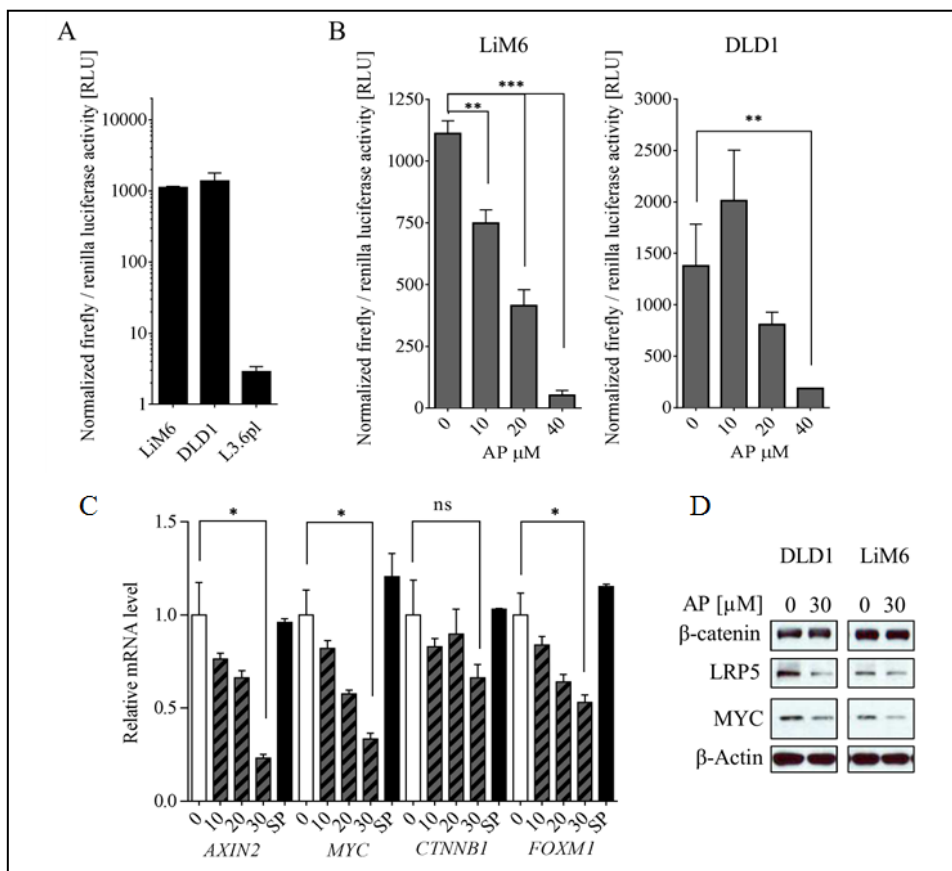


Figure 42: Aprepitant induces a robust inhibition of Wnt activity in CRC cells.

(A) Baseline Wnt activity was assessed using the TOP/FOP flash reporter system. Cells were transfected with TOPflash (non mutated TCF/LEF binding sites) or FOPflash (mutated TCF/LEF binding sites) for 24 hours. Results are represented by the ratio of TOP on FOP *Firefly* luciferase and normalized to *Renilla* luciferase. (B) Ratio of TOP to FOP after 24 hours of treatment with different concentrations of aprepitant (10, 20 or 40 μM) or DMSO (0) in LiM6 and DLD1. (C) qRT-PCR of Wnt target genes (*AXIN2*, *MYC*, *CTNNB1*) and Wnt-associated gene (*FOXM1*). Cells were treated with increasing doses of aprepitant (10 μM, 20 μM or 30 μM, gray and black columns), SP (black columns) or DMSO (white columns) for 24 hours. (D) Selected proteins of the Wnt pathway were validated by Western blot analysis (β-catenin, LRP5, MYC). Cells were treated with 30 μM aprepitant or DMSO (0) for 24 hours followed by extraction of total cell lysates. Figure taken from Garnier et al.¹⁷¹

RESULTS

These results were corroborated by qRT-PCR data in DLD1. The Wnt target gene *MYC* was dose-dependently downregulated upon aprepitant treatment along with *AXIN2* and *FOXM1* (Figure 42C). Intriguingly, in contrast to the RPPA data, *CTNNB1* was downregulated, too, although the trend was not as convincing as observed in the other genes. Finally, cells were treated with 30 μ M aprepitant and Western blot analysis was performed. The Wnt co-receptor LRP5 as well as the Wnt target *MYC* were expressed at markedly lower levels upon aprepitant treatment compared to the respective control. In the same experiment, the expression of β -catenin following aprepitant treatment was analyzed. Similar to the RPPA data, no changes of total β -catenin could be noted in whole cell lysates of LiM6 or DLD1 (Figure 42D).

In order to investigate this hypothesis as well as the downregulation of the β -catenin/Wnt signaling pathway following aprepitant treatment, cells were cultured with 30 μ M aprepitant or 70 nM SP for 24 hours, stained for β -catenin and analyzed by confocal microscopy. Similarly to hepatoblastoma cells, aprepitant induced a strong accumulation of membrane-bound β -catenin whereas SP did not affect β -catenin/Wnt signaling when compared to the control (Figure 43).

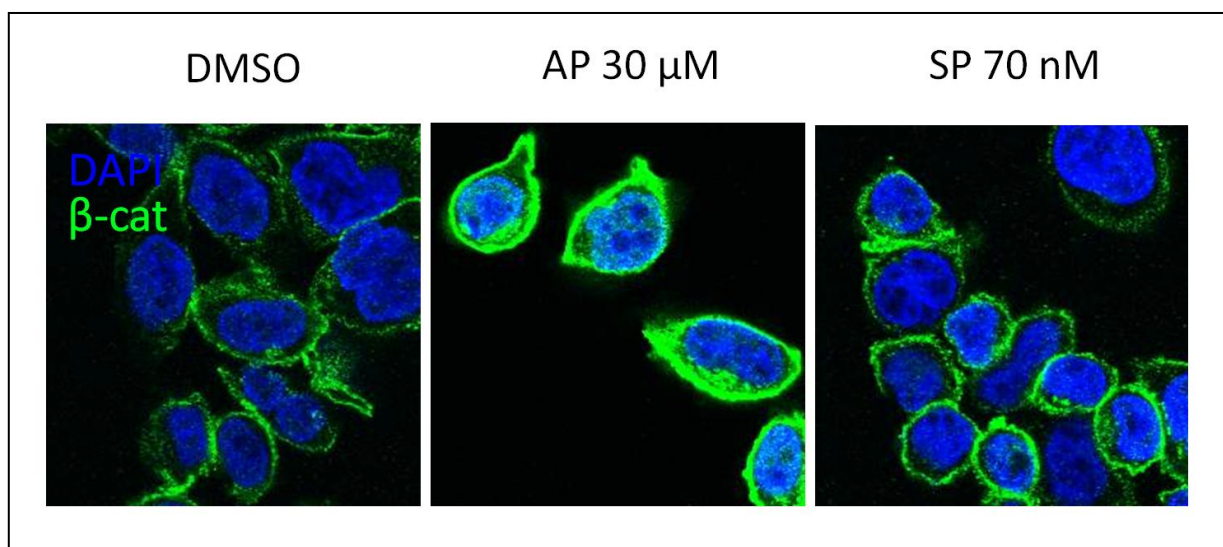


Figure 43: Aprepitant promotes membrane-bound β -catenin in colorectal cancer cells

Immunofluorescent staining of β -catenin (green) in DLD1 and nuclear staining with DAPI (blue). Cells were treated with 30 μ M aprepitant (AP 30 μ M), 70 nM SP or DMSO for 24 hours. The staining was examined by confocal microscopy. Figure taken from Garnier et al.¹⁷¹

In a next step, SFA assays were performed with both DLD1 and LiM6 in order to confirm the potential of aprepitant to reduce three-dimensional cell growth of CSC-like spheres.

RESULTS

Aprepitant induced a striking decrease in sphere number and size. A noteworthy fact is that activation of the SP/NK1R system with recombinant SP significantly increased the SFA of DLD1 CSCs in number and size, whereas in LiM6, such effects could not be detected (Figure 44).

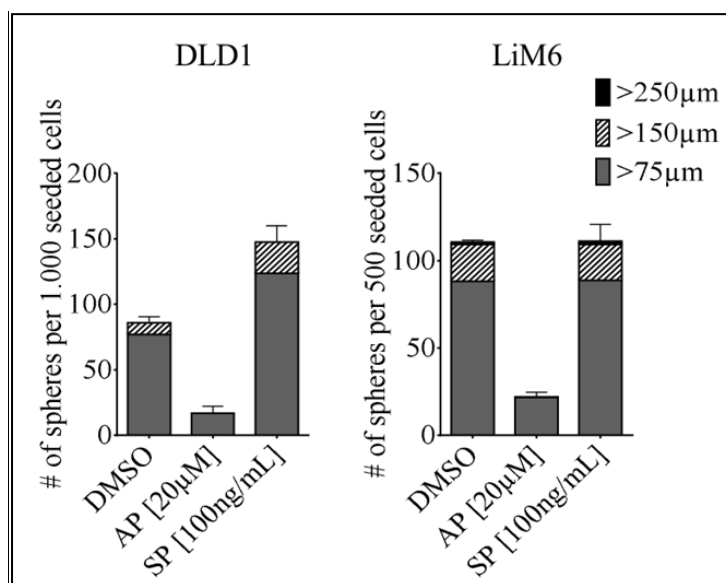


Figure 44: Aprepitant induces a robust inhibition of Wnt activity and promotes membrane-bound β -catenin in colorectal cancer cells

Sphere formation ability (SFA) assays in DLD1 and LiM6 with simultaneous treatment with aprepitant (AP) or SP. Shown are the number of spheres per 500 seeded cells in an ultra-low attachment 96-well plate after 10 days. Sphere sizes were evaluated and categorized as follows: >250 μ m (black) >150 μ m (black and grey) and >75 μ m (grey) n=3. Figure taken from Garnier et al.¹⁷¹

In conclusion, the inhibition of the SP/NK1R system with aprepitant induced a decrease of canonical Wnt signaling in colorectal cancer cells, likely by arresting β -catenin in its membrane-bound localization, and affected negatively the growth of CSC-like colorectal spheres.

3.4 The inactivation of the Wnt pathway is independent from initial Wnt baseline activity

In order to better understand the inhibitory effect of aprepitant on Wnt signaling, it was investigated whether differences exist regarding the response rate to aprepitant treatment within cell populations that are constitutively active with respect to the Wnt pathway. Such cells with high constitutive Wnt activation have been described to have higher stemness

RESULTS

properties¹⁷⁷. In order to have comparable findings to those from Vermeulen et al.¹⁷⁷, the colorectal cell lines LiM6 and DLD1 were transduced with a 7xTCF-eGFP/SV40-mCherry (7TGC) lentiviral construct¹⁷⁸ allowing cell separation regarding their Wnt activities by single cell sorting via FACS (Figure 45A). Wnt activity in cells with the same level of mCherry intensity then correlates with their GFP intensity. After separation, Wnt^{high} and Wnt^{low} expressing cells were independently cultured and subsequently treated with increasing doses of aprepitant for 48 hours (Figure 45B). Interestingly, no differences in cell survival were observed for any of the doses tested between cells with high or low Wnt activity.

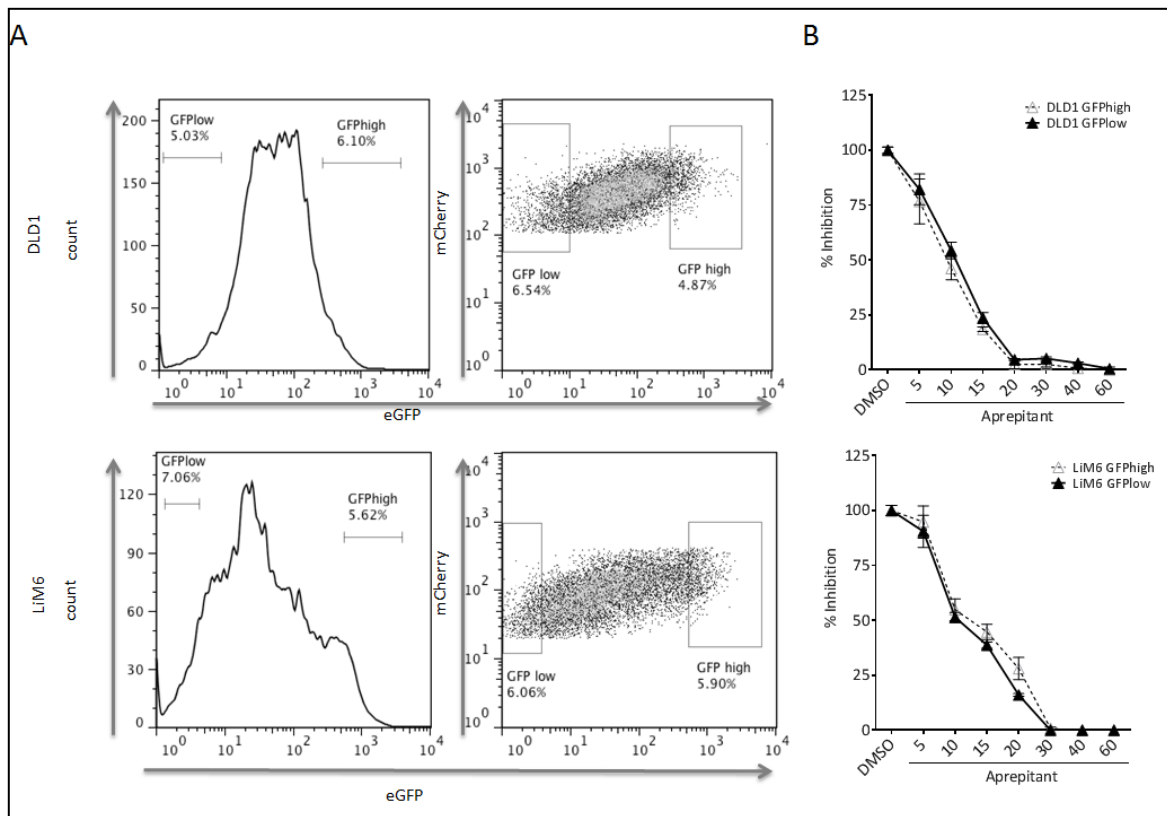


Figure 45: Aprepitant affects the cell viability of GFP/Wnt^{high} and GFP/Wnt^{low} cells to the same degree (A) CRC cells were transduced with the lentiviral construct 7xTCF-eGFP/SV40-mCherry (7TGC). The 5% GFP^{high} and 5% GFP^{low} cells were sorted via FACS and used for further evaluation. Shown are representative FACS plots with DLD1 in the upper panel and LiM6 in the lower panel. The left panels show cell counts on the y-axis and eGFP intensities on the x-axis; the right panels show mCherry intensities on the y-axis and eGFP intensities on the x-axis. (B) GFP^{high} or GFP^{low} cells from (A) were treated for 24 hours with increasing doses of aprepitant or with DMSO. Subsequently, MTT cell viability assays were carried out and relative cell viability compared to DMSO treated cells is shown (n = 3). Figure taken from Garnier et al.¹⁷¹

These findings suggest that the apoptosis-inducing property of NK1R targeting is maintained even in cells with supposedly increased cancer stemness potential (Wnt^{high}). Furthermore, these data indicate that in a particular cell line or population, the observed inhibitory effects caused by NK1R antagonism are independent of the initial Wnt baseline activation.

RESULTS

Taken together, these data clearly demonstrate that the anti-cancer effect of aprepitant is not limited to hepatoblastoma but concern also CRC cell lines. Interestingly, aprepitant seems to triggers identical molecular responses by targeting PI3K/AKT/mTOR and canonical Wnt pathways, which implies that this molecule could be used in a broad variety of cancers harboring these two types of deregulations.

RESULTS

4. The NK1R is an ubiquitous anti-tumor target in hepatoblastoma and its expression is independent from tumor biology and stage

The results presented in this section are part of the publication: The neurokinin-1 receptor is an ubiquitous anti-tumor target in hepatoblastoma and its expression is independent from tumor biology and stage. *Oncology Letters* (2015, 11:870-878) [Garnier A](#), Ilmer M, Becker K, Häberle B, von Schweinitz D, Kappler R, Berger M.

4.1 *NK1R* is overexpressed in human hepatoblastoma

The final step of this study in the assessment of NK1R as an interesting anti-tumor target was to evaluate its expression in tumor samples, and determine whether its expression correlate with clinical, histological and biological parameters. In order to address this question, the gene expression pattern of *NK1R-fl* as well as *NK1R-tr* was first analyzed in tumor tissue samples of hepatoblastoma and non-tumorous liver tissue. *NK1R-tr* was significantly overexpressed in hepatoblastoma compared to the control specimens (Figure 46A). Although not statistically significant, the expression of *NK1R-fl* also tended to be higher in tumor specimens (Figure 46B). These results correlated with the previous findings *in vitro* (Figure 8) in which *NK1R-tr* is overexpressed in malignant hepatoblastoma cells, which in turn correlates with the responsiveness to treatment with NK1R antagonists such as aprepitant.

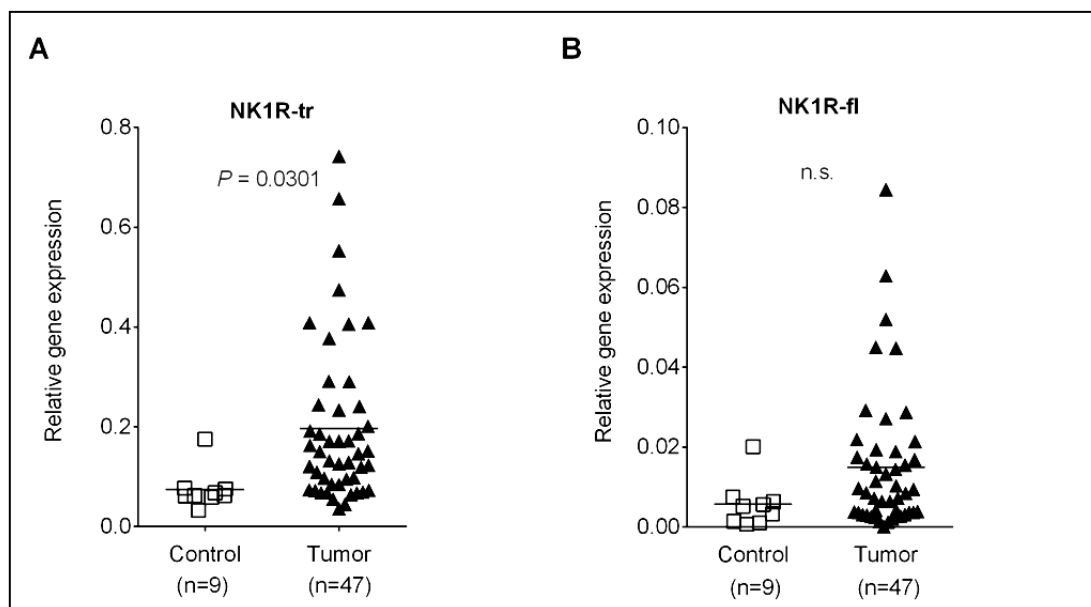


Figure 46: Hepatoblastoma tumors overexpress *NK1R* compared to normal liver tissue

(A) Statistically significant different relative gene expression ($p=0.0301$) of *NK1R-tr* in hepatoblastoma ($n=47$, black triangles) compared to normal liver tissue ($n=9$, white squares). (B) Gene expression of *NK1R-fl* in the same samples as in (A); no significant difference could be detected. Figure taken from Garnier et al.¹⁷⁹

RESULTS

4.2 Expression of *NK1R-tr* correlates with *NK1R-fl*

Because of the wide range of gene expressions, the results were displayed as ratio of *NK1R-tr* vs. *NK1R-fl*. The ratios were found to be comparable between the tumor and the control specimens (Figure 47A), suggesting a positive correlation of the two splice variants. When analyzed in depth, a statistically significant weak correlation ($r=0.3542$) between *NK1R-tr* and *NK1R-fl* was found, potentially indicating a mutual dependency (Figure 47B).

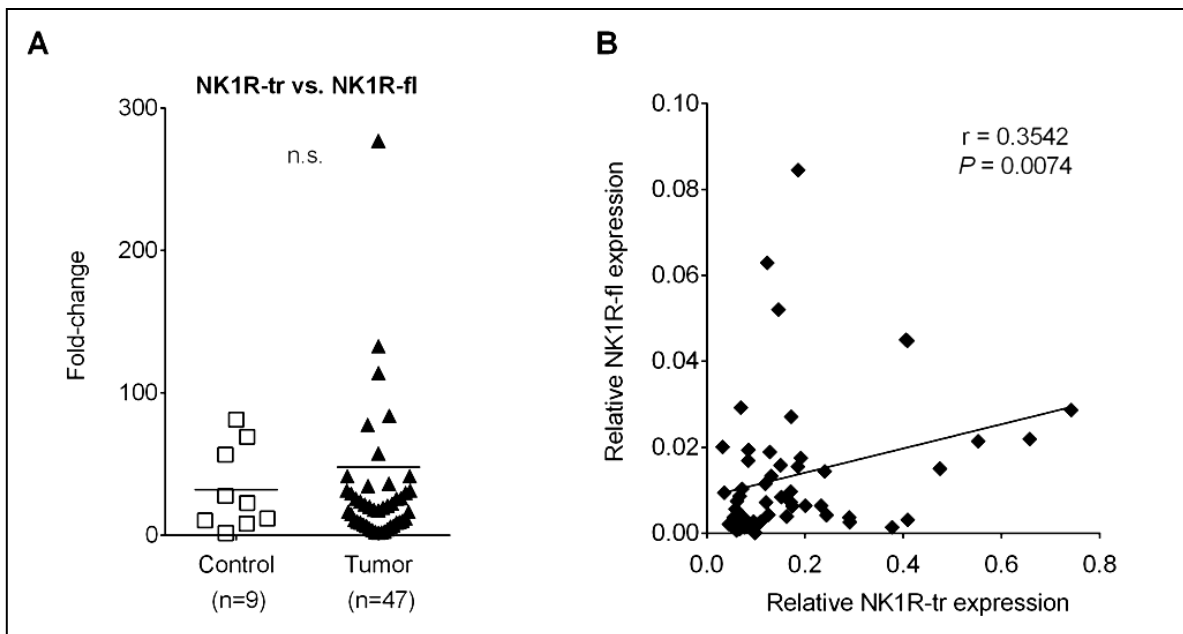


Figure 47: Expression of *NK1R-tr* correlates with *NK1R-fl*

(A) The ratio of the gene expression values of *NK1R-tr* (Figure 46A) vs. *NK1R-fl* (Figure 46B) was calculated for hepatoblastoma tumors and liver tissue. (B) The correlation of the gene expression values of *NK1R-tr* (Figure 46A) vs. *NK1R-fl* (Figure 46B) was calculated and graphically illustrated (black squares). $P=0.0074$, $r=0.3542$. Figure taken from Garnier et al¹⁷⁹

4.3 *NK1R* expression does not correlate with biological features

For a better understanding of whether the expression level of either splice variant or their ratio correlates with the biological features of the tumor, *NK1R* expression was analyzed accordingly.

The first analysis focused on the truncated variant due to its significance in hepatoblastoma as a potential therapeutic target as demonstrated in this work. The presence of a correlation was investigated between the relative expression of *NK1R-tr* with a recently described 16-gene molecular signature known to associate with prognosis⁵⁵. Similarly to the original

RESULTS

description of this signature, the cohort of this study could be separated into 29 hepatoblastoma belonging to the C1 signature (61.7%) and 18 hepatoblastoma grouped into the adverse C2 signature (38.2%) (Table 2).

Relative gene expression of *NK1R*-tr revealed no significant difference between C1 and C2 (Figure 48, upper left panel). Next, the same features were analyzed in correlation to the gene expression of *NK1R*-fl (Figure 49, upper left panel). Here, a significant correlation was found of low *NK1R*-fl with the C2 population of the 16-gene signature ($p = 0.0222$). Of note, 55.6% of the specimen grouped into the C2 population displayed very low levels of *NK1R*-fl. Next, the ratio of both variants – truncated vs. full length – was used to see whether it could be correlated with the 16-gene signature. Intriguingly, very low ratios were found in the favorable C1 population and very high ratios were found within the C2 population, but this effect was not statistically significant (Figure 50, upper left panel).

Characteristic	Groups	Numbers [%]
16-gene signature	C1	29 [61.7]
	C2	18 [38.2]
Metastasis	Yes	17 [36.2]
	No	30 [63.8]
PRETEXT	I-II	17 [36.2]
	III	19 [40.4]
	IV	11 [23.4]
Vascular invasion (VI)	Yes	8 [17.1]
	No	39 [82.9]
VI and C2		6 / 8 [75]
VI and metastasis		7 / 8 [87.5] (24)
Histology	Fetal	35 [74.5]
	Embryonal	12 [25.5]
Onset	1 – 24 months	32 [68.1]
	> 24 months	15 [31.9]
Multifocality	Yes	13 [27.7]
	No	34 [72.3]
<i>CTNNB1</i> status	wild-type	14 [29.8]
	mutated	33 [70.2]
Sex	Female	24 [51.1]
	Male	23 [48.9]

Table 2: Classification of the cohort

4.4 Expression of *NK1R* does not correlate with clinical features

In a next step, the expression patterns of both *NK1R*-fl and *NK1R*-tr was correlated with clinical, biological and histological features such as metastasis, vascular invasion, histology, multifocality, *CTNNB1* mutations, sex and the preoperative classification PRETEXT

RESULTS

(Figures 48 and 49). Over the entire cohort, 63.8% had no metastasis at the time of diagnosis, 82.9% had no vascular invasion, while only 27.7% were multifocal. Sex was equally distributed (female 51.1% vs. male 48.9%) and most tumors had a fetal histology (74.5% vs. 25.5% embryonal). As expected, 70.2% of tumors possessed a β -catenin mutation (*CTNNB1* mutation). The age of diagnosis was mainly within the first 24 months of life (68.1%) and the specimen were distributed among PRETEXT 1-2 (36.2%), PRETEXT 3 (40.4%), and PRETEXT 4 (23.4%) (Table 2).

After analyzing *NK1R*-tr expression, no statistically relevant differences could be detected with respect to the above-mentioned clinical features. An interesting observation was that high expressions of *NK1R*-tr correlated with a better overall survival (Figure 48, lower left panel), although this was only a trend and did not reach statistically significant levels.

Similarly, when analyzing the pattern of *NK1R*-fl expression with metastasis, PRETEXT, vascular invasion, histology, age of diagnosis, multifocality, *CTNNB1* mutations or sex, no significant correlation was found (Figure 49). When clustered into groups according to high versus low expression of *NK1R*-fl, overall survival curves did not deviate from each other contrary to the finding for *NK1R*-tr (Figure 48 and 49, lower left panels).

When considering the ratio of both variants – truncated vs. full length – again, no statically significant differences could be found with regards to most of the characteristics, with the only exception that higher truncated to full-length ratio was found predominantly in PRETEXT 1-2 compared to PRETEXT 3 (Figure 50, upper right panel). Similarly to the analysis considering *NK1R*-tr alone, overall survival was worse with a low ratio of *NK1R*-tr/*NK1R*-fl (Figure 50).

Because the original description of the 16-gene signature by Cairo et al.⁵⁵ suggested a worse prognosis for the C2 signature, it was interesting to investigate whether either factor (*NK1R*-tr, *NK1R*-fl or the ratio thereof) could refine the predictive value in the set of tumors of this study. Therefore, the overall survival was reanalyzed within the C2 hepatoblastoma tumors and their outcome was analyzed with respect to high vs. low expression of *NK1R* or its ratio. Low *NK1R*-tr predicted a bad prognosis for C2 tumors with a higher significance than *NK1R*-tr alone (Figure 48, lower right panel). Although not significant, high *NK1R*-fl suggested a worse outcome (Figure 49, lower right panel) and the ratio of both variants

RESULTS

showed the same trend as the truncated variant alone and as analyzed in the whole cohort, but with a clear tendency to a worse prognosis for low *NK1R-tr/NK1R-fl* in the C2 group (Figure 50, lower right panel).

To sum up, a strong correlation of either gene expression of *NK1R-tr*, *NK1R-fl* or the ratio thereof with clinical and histological data could not be found. However, and especially when added to the C2 signature, a low *NK1R-tr* expression level or a low truncated-vs-full ratio was associated to a worse prognosis, whereas no significance could be found in *NK1R-fl* with a slight trend to worse outcomes in the C2 and high *NK1R-fl* expression cases.

RESULTS

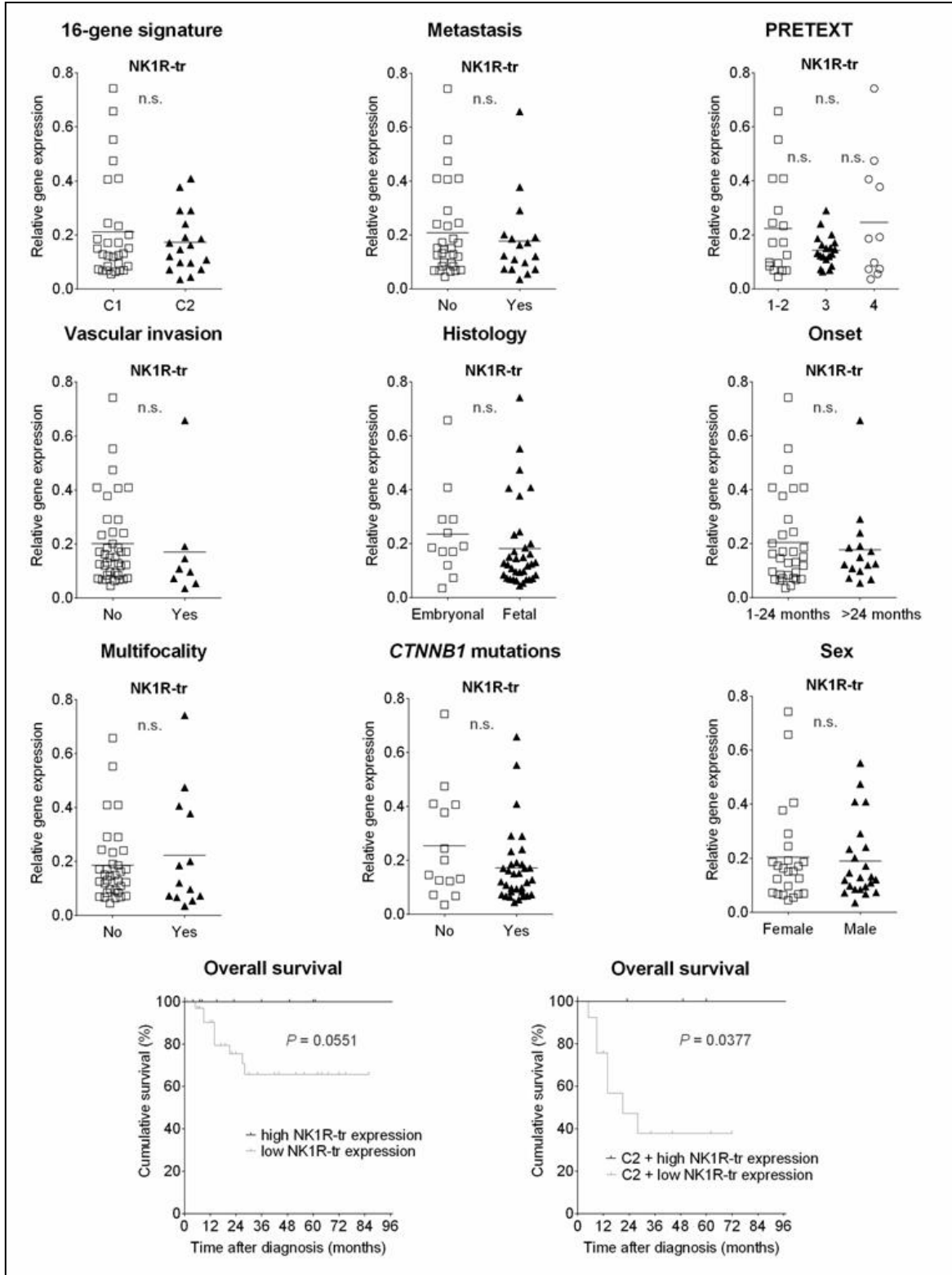


Figure 48: *NK1R-tr* expression is not associated with clinical parameters.

Relative gene expression of *NK1R-tr* was correlated to the 16-gene signature, metastasis, the preoperative staging system PRETEXT, vascular invasion, histology, age of diagnosis, multifocality, *CTNNB1* mutation status (no = wild type, yes = mutated β -Catenin), and sex (no significant differences). Overall survival is shown for high and low *NK1R-tr* expressers with a difference in survival ($p=0.0551$). High expression is defined as > 3-fold of the mean of 9 normal liver tissues. Low expression of *NK1R-tr* significantly lowers overall survival in hepatoblastoma tumors harboring the C2 signature ($p=0.0377$). n.s. = not significant. Figure taken from Garnier et al¹⁷⁹

RESULTS

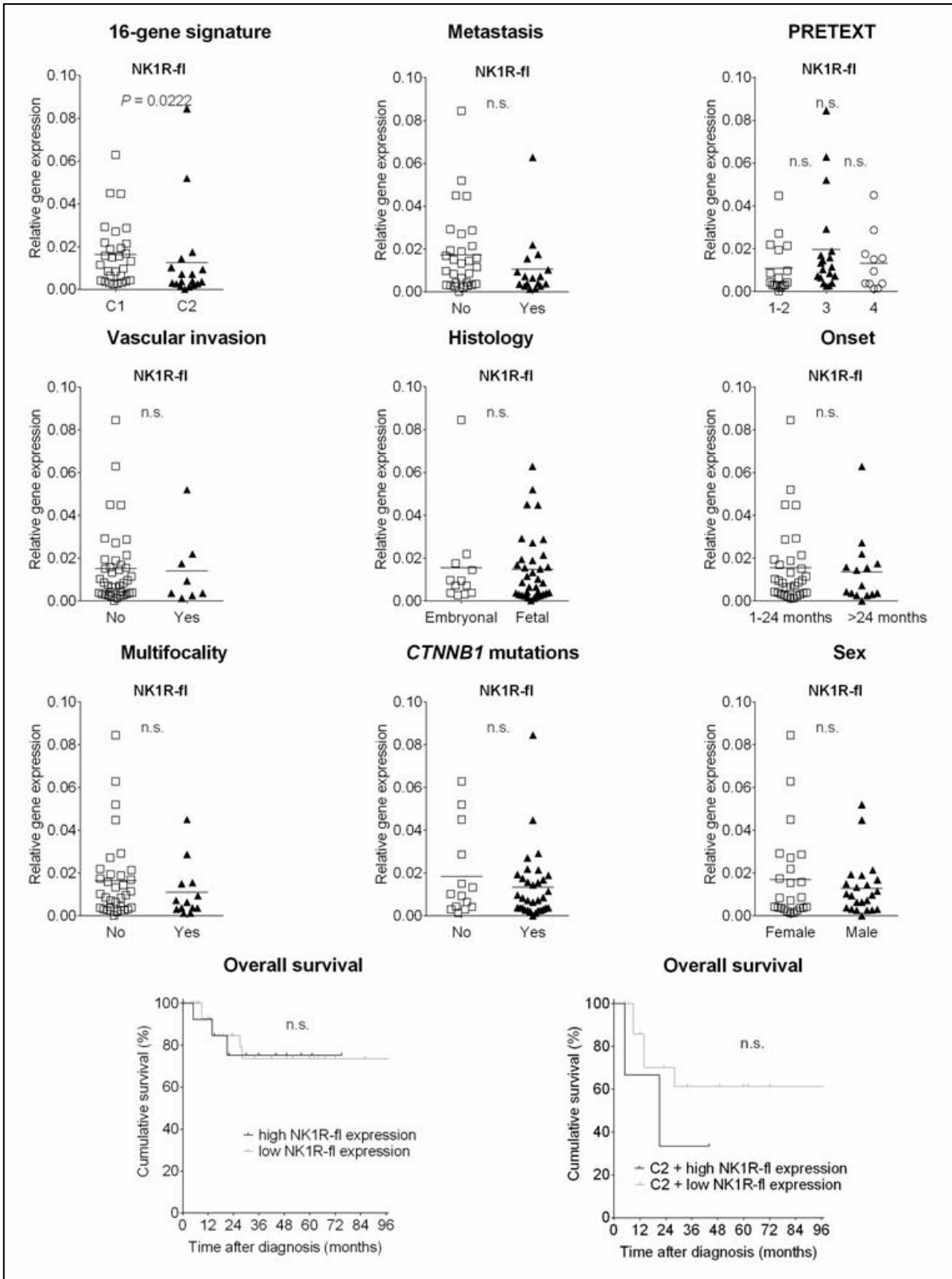


Figure 49: *NK1R-fl* expression displays no difference in biological, clinical, and histological features. Analogous to Figure 48, relative gene expression of *NK1R-fl* was compared to the same 10 parameters. The C2 signature (upper left) significantly correlated with a low gene expression of *NK1R-fl*. All other calculation of the p-values did not reveal any statistically relevant differences. High expression of *NK1R-fl* worsens outcome in hepatoblastoma tumors harboring the C2 signature, but the trend is not significant. n.s. = not significant. Figure taken from Garnier et al¹⁷⁹

RESULTS

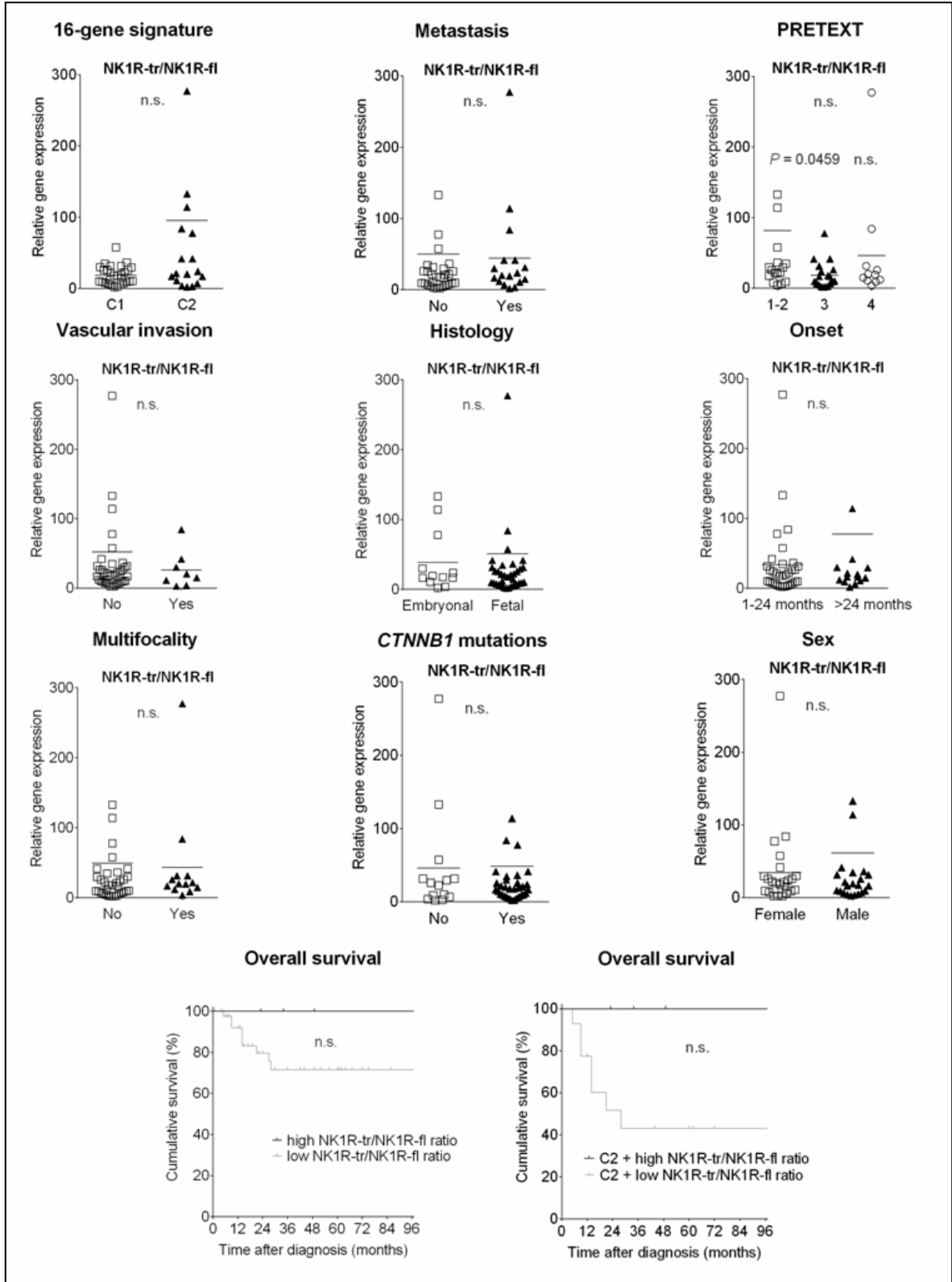


Figure 50: The ratio of *NK1R-tr* and *NK1R-fl* does not predict clinical prognosis.

As in Figures 48 and 49, ten different clinical features were analyzed with regards to the ratio of *NK1R-tr* vs. *NK1R-fl* gene expression. No significant difference could be detected in the 16-gene signature, metastasis, vascular invasion, histology, age of diagnosis, multifocality, *CTNNB1* status, sex or overall survival. PRETEXT 1-2 significantly correlated with a higher ratio compared to PRETEXT 3 (upper right panel). Low expression of the ratio of truncated / full length lowers overall survival in hepatoblastoma tumors harboring the C2 signature but the results are not significant. n.s. = not significant. Figure taken from Garnier et al¹⁷⁹

DISCUSSION

1. Hepatoblastoma cells express NK1R and can be growth inhibited by aprepitant *in vitro*

This study reports on a completely new approach for the treatment of hepatoblastoma based on the blockage of NK1R. We found that this receptor was highly expressed in hepatoblastoma cell lines and its inhibition by small molecules was responsible for a robust inhibition of proliferation with induction of apoptosis *in vitro*. However, aprepitant alone was not enough to eradicate HuH6 tumor *in vivo* but was efficient in significantly reducing tumor growth¹⁵⁶.

Combining aprepitant with cytostatics revealed very promising results: a synergistic effect was observed with the addition of aprepitant with doses as low as 1 μ M of doxorubicin. In line with these observations, osteosarcoma cell lines showed a similar effect with NK1R antagonists for mitomycin, ifosphamide, adriamycin and cisplatin¹⁵³. However, in this study results were obtained after one single treatment and are not representative of the clinical setting where several chemotherapy courses are needed. In a next step, it would be interesting to further investigate how combinations of low dose chemotherapy agents with aprepitant affect tumor growth *in vivo*. The ultimate goal would be to decrease the concentration of cytostatics because these molecules are responsible for severe side effects when given at high doses. Particularly, doxorubicin is responsible for cardiotoxicity¹²⁴, whereas cisplatin causes nephrotoxicity and ototoxicity⁸. Furthermore, aprepitant has successfully been used for the treatment of pain, migraine, and some psychiatric disorders including depression¹⁵². Therefore, the use of this molecule for future treatment strategies would be very interesting knowing that many patients with cancer suffer from these symptoms. Altogether these findings emphasize the relevance of conducting a clinical study with aprepitant in combination with cytostatics currently used for the treatment of hepatoblastoma.

Despite being highly expressed in neoplastic cells, the SP/NK1R complex has been recently incriminated as an important actor of the tumor microenvironment. For instance, high expression of NK1R in capillaries was recently linked to tumor neovascularization, which participates in the angiogenesis process¹⁸⁰. More precisely, SP which is highly expressed by the tumor itself but also by other structures such as peripheral terminal

DISCUSSION

nerves or infiltrated immune cells¹²⁷, was shown to induce the growth of capillary vessels *in vivo* and trigger the proliferation of endothelial cells *in vitro*. Additionally, SP acts as a pro-inflammatory compound, which potentially could contribute to tumor-promoted inflammations, a previously described hallmark of cancer¹⁸¹. The fact that cancer cells produce SP also suggests the presence of an autocrine growth stimulus pattern. Mayordomo et al. used a monoclonal, specific antibody against this agonist in isolated cultures of breast cancer and other cancer cell lines and observed an inhibition of cell growth and an increase of apoptosis¹⁸². Similarly, when using anti-SP or anti-NK1R antibodies, a significant growth inhibition was noted in our study. These findings converge to the fact that hepatoblastoma cells are capable of auto-stimulation, which therefore reinforces the preeminence of NK1R as a driver of hepatoblastoma growth.

Nevertheless, there are many unresolved questions concerning the true role of the SP/NK1R system in the development of cancer. For instance, until recently few attention has been given to the different splice variants of NK1R. Previous studies pointed out the central role of NK1R-tr in breast cancer^{183, 184}. Likewise, Gillespie et al. analyzed NK1R-tr and NK1R-fl in colitis-associated cancer and found that it was the expression of NK1R-tr alone that predicted the progression from quiescent colitis to high-grade dysplasia and cancer¹⁵⁷. Compared to NK1R-fl, the truncated variant is lacking residues at the cytoplasmic end of the receptor. Nonetheless, it seems to be able to couple to G proteins but shows reduced efficiency with respect to internalization and desensitization. The analysis of NK1R expression in hepatoblastoma cells revealed an overexpression of the truncated isoform whereas NK1R-fl was very little expressed. In comparison, human fibroblasts and non-malignant HEK293 cells expressed negligible levels of NK1R-tr. This receptor system seems to be of minor importance in human fibroblasts, since both splice variants were barely detectable. Interestingly, these cells showed the strongest resistance to aprepitant when analyzing cell survival whereas HEK293 cells, which expressed higher levels of NK1R-fl, displayed an increased response to aprepitant. Taking these results into account, it seems that the response to NK1R antagonists is selective and relies on the differential expression of the receptor within these cells. However, at the moment, these results do not permit us to establish clearly a causal relationship between the expression level of splice variants and the sensitivity to aprepitant. Nevertheless, as NK1R-tr is believed to be resistant to desensitization and internalization, one could suggest that this isoform is responsible for a constitutive growth stimulus.

DISCUSSION

This part of the study uncovered the SP/NK1R complex as an interesting therapeutic target in human hepatoblastoma. Aprepitant and other NK1R antagonists are capable of inducing a potent growth inhibition with induction of apoptosis in malignant cells harboring high level of NK1R-tr. Therefore, it would be interesting to realize complementary experiments such as NK1R knockdown, in order to investigate in detail the functional role of this specific isoform in hepatoblastoma development.

2. Targeting the NK1R compromises PI3K/AKT/mTOR pathway in hepatoblastoma

The next step of this study was to investigate the downstream mechanisms following inhibition of NK1R by aprepitant on hepatoblastoma cells. First, a robust inhibition of 4EBP1 and p70S6K was identified, which are both downstream members of the PI3K/AKT/mTOR pathway. This is really promising because this pathway is known to be involved in tumorigenesis and was identified as a potent target for the development of future anticancer strategies¹⁸⁵. In particular, previous work showed that the inhibition of hepatoblastoma cell growth could be achieved with the use of rapamycin through inhibition of the PI3K/AKT/mTOR pathway by dephosphorylating and deactivating p70S6K¹⁸⁶. Furthermore, the inhibition of both p70S6K and 4EBP1 in our study is in accordance with Mayordomo et al.¹⁸². This group treated breast, prostate and colon cancer cells with SP antibodies, which led to the inhibition of mTOR. Likewise, Garcia-Recio et al. showed that SP induced an activation of the pathway with an early increased expression of p-AKT in breast cancer cells¹⁸⁷.

When analyzing more in details the effect of aprepitant at the molecular level, we came across discrepancies by finding an unexpected increase of AKT phosphorylation (S473 and T308) suggesting an activation of the PI3K/AKT/mTOR pathway. This was confirmed by an increase of AKT substrate-specific phosphorylation of PRAS40 (T-246)¹⁸⁸ and GSK3 β (S9)⁸¹. However, activation of mTORC1 following aprepitant treatment is questionable for several reasons. Firstly, 4EBP1 was found phosphorylated at T37/T46 and although it is admitted that mTORC1 mediates this phosphorylation¹⁸⁹, other kinases have this ability. For instance, phosphorylation of 4EBP1 at these two distinct sites can be performed by CDK1 under conditions of reduced mTOR signaling¹⁹⁰. Likewise, PLK1 was shown to have similar effects in HepG2¹⁹¹. Furthermore, our data also indicated an increase in phosphorylation of mTOR at S2448 which, in this form, is known to be associated with mTORC1 complex¹⁹². At first, we speculated that it was an indicator of mTORC1 activity. However, mutation of

DISCUSSION

S2448 to A2448 has no discernible effect on the ability of mTOR to activate its downstream effectors. More interestingly, deletion of this region resulted in enhanced mTOR kinase activity suggesting that this region may actually act as a repressor domain¹⁹³. Therefore, the more grounded hypothesis would consider that mTORC1 is inhibited after aprepitant treatment (Figure 51).

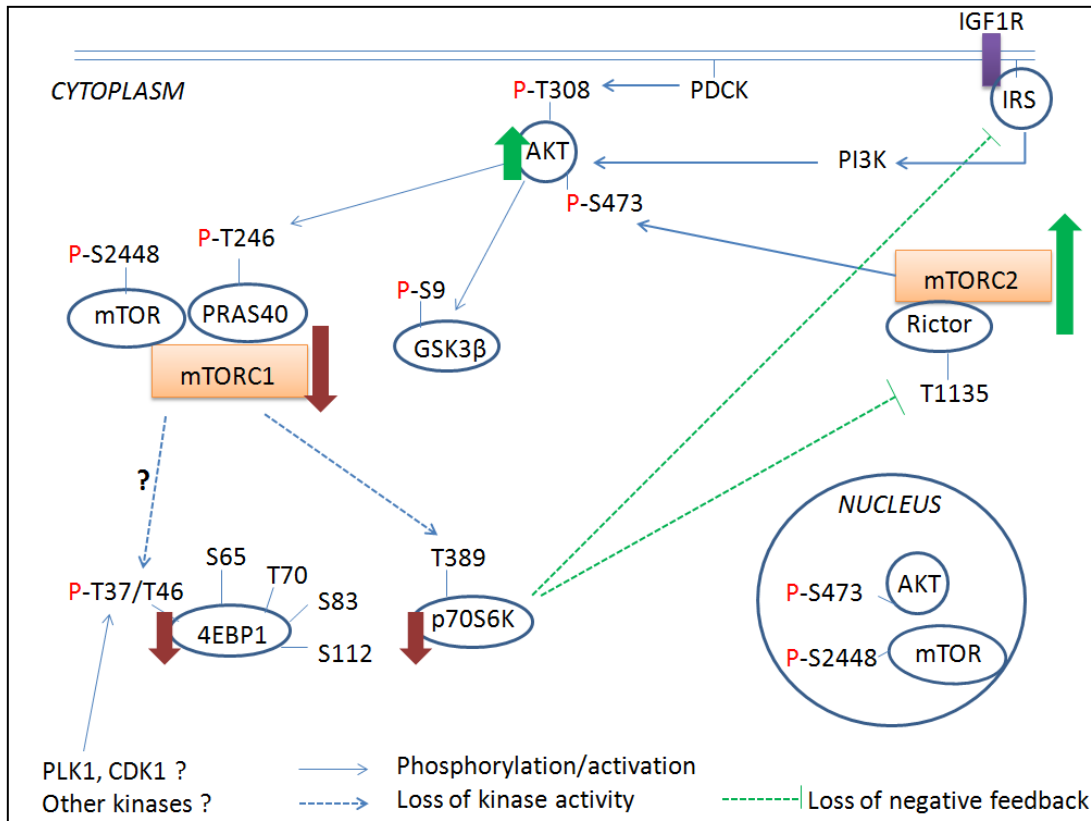


Figure 51: Schematic representation of aprepitant action on PI3K/AKT/mTOR pathway in hepatoblastoma based on RPPA and Western blot data

Following aprepitant treatment, mTORC1 is inhibited as proved by decrease of its downstream target p70S6K (T389) and 4EBP1 (S65). AKT becomes activated due to the loss of negative feedback of p70S6K on Rictor (decrease of phosphorylation at T1135), and on IRS protein. Activated AKT phosphorylates GSK3β (S9) and PRAS40 (T246) and promotes for instance cell survival.

Another indicator of mTORC1 inhibition is hyperactivation of mTORC2 as illustrated by increased phosphorylation of AKT at S473 and decreased phosphorylation of Rictor at T1135⁹⁷. We speculate as others that inhibition of mTORC1 complex suppresses the negative feedback of mTOR/p70S6K activation on IRS^{98, 194, 195} and Rictor (T1135)⁹⁵ (Figure 51). In the same manner, Western blots of AKT after short time treatment revealed first a decreased expression of phospho-AKT (S473) followed by a subsequent increase probably due to the loss of these negative feedbacks. Late AKT activation would therefore represent a rescue reaction of the tumor cells to escape cell death. This phenomenon was

DISCUSSION

already described after everolimus treatment where the negative feedback via p70S6K on mTORC2 is inhibited allowing AKT phosphorylation at S473 by mTORC2 complex¹⁹⁶. Importantly, it has been suggested that increased AKT signaling following mTORC1 inhibition could attenuate anticancer efficacy or over time, contribute to the development of resistance^{196, 197}.

Furthermore, we identified upon aprepitant treatment a nuclear localization of phospho-mTOR (S2448) and phospho-AKT (S473). mTOR is believed to be cytoplasmic¹⁹⁸ however our immunofluorescence staining in untreated cells revealed that mTOR was present in the cytoplasm but also to a lesser degree in the nucleus. Although no classic nuclear localization sequences have been found in mTOR, we think that this particular localization could be explained by the presence of a rapid nuclear export mechanism compared to the nuclear import, which could explain the strong nuclear accumulation of mTOR, AKT and FOXM1. Interestingly, Kim et al.¹⁹⁹ reported the same atypical localization of mTOR. Additionally, they observed an accumulation of nuclear mTOR upon Leptomycin B treatment, an inhibitor of CRM1-dependent nuclear export, which was associated with a decrease of p70S6K and 4EBP1 phosphorylation. It is possible to speculate that a perfect balance between cytoplasmic and nuclear mTOR is needed for maximal mTOR activity²⁰⁰. By disrupting a shuttling mechanism, aprepitant could induce a strong accumulation of mTOR in the nucleus, which therefore would inhibit cytoplasmic mTORC1 downstream targets such as p70S6K and 4EBP1.

Appart from this, increase of nuclear AKT was also detected upon aprepitant treatment. In the nucleus, active AKT can phosphorylate several intracellular substrates to promote cell survival or DNA repair²⁰¹. Furthermore, strong nuclear presence of AKT (S473) has been described in several cancer types, which corroborates the potential role of AKT in the development of drug resistance. Importantly, this phenomenon could explain our *in vivo* data. Despite the fact that aprepitant induced a significant reduction of tumor growth, we observed a slight increase in tumor volume over time growing from 75 to 200 mm³ after 20 days of treatment¹⁵⁶.

In sum, these findings clearly identify the PI3K/AKT/mTOR pathway as one major downstream mechanism responsible for NK1R-triggered growth inhibition in hepatoblastoma. However, several efforts have to be made in order to clearly understand the mechanisms involved in upregulation of AKT. This could lead to the development of

DISCUSSION

new approaches to abrogate completely this pathway pivotal in drug resistance. For instance, Wan et al. successfully suppressed reactivation of AKT by targeting mTOR but also IGF1R²⁰².

3. Targeting the NK1R compromises canonical Wnt signaling in hepatoblastoma

3.1 Aprepitant induces a downregulation of Wnt signaling

In this study, we also observed a striking reduction of Wnt activity as confirmed by reduced luciferase activity in SuperTOP/FOP assays and by decrease of Wnt target gene expression. Firstly, this effect seemed to be limited to cells with mutations of the Wnt pathway or cells in which the pathway was extrinsically activated, as demonstrated with the β -catenin wild-type cell lines HuH7 and HEK293 after lithium chloride stimulation. Further, the cell lines used in this study harbor β -catenin mutations indicating that the molecules upstream of the destruction complex should not be needed for pathway activation/modulation. Therefore, knowing that aprepitant more likely acts at the level of β -catenin, we made several assumptions on how NK1R inhibition could modulate Wnt signaling.

➤ Modulation of β -catenin/E-cadherin phosphorylation status

One of our intriguing results was the discovery of increased membrane bound β -catenin upon aprepitant treatment, that we believe could be the cause of Wnt inhibition. It is well established that E-cadherin/ β -catenin complex association is tightly regulated by a complex interplay of phosphorylations. Indeed, previous work reported that E-cadherin phosphorylation at specific sites promotes cell adhesion by increasing the E-cadherin/ β -catenin²⁰³ binding affinity. Particularly, the cytoplasmic domain of E-cadherin contains several phosphorylation sites for CKII and GSK3 β ²⁰³. However we found an increase of AKT dependent phosphorylation of GSK3 β (S9), which is known to completely suppress its kinase activity²⁰⁴. Therefore, it is unlikely that GSK3 β is responsible for the observed effect. Other phosphorylation sites have been characterized in β -catenin as being central for the binding to E-cadherin. Particularly, Y142, Y489 and Y654 are phosphorylated by Fyn/c-Met, Abl/Fer, and EGFR/Src, respectively, and enhanced activity of these kinases has been linked to a decrease of E-cadherin/ β -catenin binding affinity³⁷. However, our RPPA data revealed that total and phosphorylation levels of c-Met (Y1235), EGFR (Y1068/Y1173) and Src (Y416/Y527) were not affected. Therefore, at the moment our RPPA data doesn't allow

DISCUSSION

us to understand the underlying mechanisms responsible for the heightened level of β -catenin at the membrane. To perform this task, it would be worth investigating E-cadherin and β -catenin phosphorylation status and realize accordingly knockdown experiments of specific kinases coupled with co-immunoprecipitation and immunofluorescence experiments.

➤ Disruption of FOXM1/ β -catenin complex

In our study, we showed that FOXM1, a recognized shuttle protein for the translocation of β -catenin to the nucleus¹⁵⁹, was found inhibited at the mRNA and protein levels. Intriguingly, we also observed a loss of colocalization between these two proteins reflected by an increase of nuclear FOXM1 and membrane bound β -catenin. Disruption of this complex could therefore be the cause of Wnt inhibition in Wnt-dependent cancer cells leading to enhanced susceptibility for apoptosis and growth arrest. In accordance, Zhang et al. mentioned that FOXM1 mutation or nuclear import prevented β -catenin nuclear accumulation in tumor cells leading to decrease of Wnt activity¹⁵⁹. Nevertheless, these findings do not explain how exactly β -catenin accumulates at the membrane and further experiments need to be realized in this direction. This is indeed very interesting because it leads to the assumption that NK1R inhibition fortifies epithelial states of the cell, therefore indicating a potential role of NK1R in the regulation of epithelial-mesenchymal transition (EMT). This process confers mesenchymal properties on epithelial cells and has been associated with the acquisition of aggressive traits participating in the outgrowth of metastasis²⁰⁵. For this reason, approaches to reverse or inhibit this phenomenon in cancer cells are still intensively researched²⁰⁶. Additional experiments should thus focus on analyzing EMT regulation following aprepitant treatment, especially as Wnt and PI3K/AKT/mTOR pathways are important drivers^{206, 207}. For instance, an inquiry of EMT markers by qRT-PCR (*TWIST*, *SLUG*, *SNAIL*, *E-cadherin*)²⁰⁸, wound healing assay or Boyden chamber assays to assess invasiveness could be envisaged²⁰⁹.

3.2 Aprepitant targets cancer stem-like cells

Wnt signaling has been associated with stemness property¹⁶¹, which is considered as the final acquisition conferred by EMT²¹⁰. We were able to show *in vitro* that aprepitant not only diminished the sphere formation ability of hepatoblastoma cells when treated

DISCUSSION

simultaneously, but also sustainably altered their stemness potential as shown by sphere formation ability assays of pretreated hepatoblastoma cells and decreased expression of embryonic stemness genes. Interestingly, we found that high expression of embryonic stemness markers correlated with high expression of *NK1R-tr* in HepT1 and HuH7 spheres suggesting a mutual dependency. However, It seems unlikely that this mechanism solely rely on Wnt signaling as, contrary to HepT1, HuH7 spheres didn't overexpress members of the Wnt pathway (*LGR5*, *CTNNB1*, *AXIN2*). More interestingly, treatment of spheres with aprepitant only affected Wnt mutated cell lines when considering embryonic markers and *NK1R* expression. This suggests the presence of a positive retroaction loop in Wnt mutated cells between *NK1R-tr* and Wnt signaling, which is potentially pivotal in the acquisition of stem-like features. This highlights once again the central role of this isoform as a driver of hepatoblastoma and indicates that it could be used as a marker of aggressiveness. Taken together, we provide evidence that *NK1R* antagonism decreases canonical Wnt signaling and stemness property, especially in Wnt-dependent CSC-like cells. These results are of particular importance considering the assumption that CSC are responsible for cancer relapse and resistance²¹¹.

However, this is not to say that growth inhibition following treatment with *NK1R* antagonists in hepatoblastoma cells is necessarily triggered exclusively through this mechanism. For example, cancer cells that express little Wnt activity, such as HuH7 cells, still show a therapeutic effect in response to aprepitant. Often, this therapeutic response is in the same magnitude as in cancer cells with high Wnt activity. This goes along with our findings, which identify other important cancer pathways being significantly inhibited by *NK1R* antagonists, such as PI3K/AKT/mTOR. Overall, we find these results encouraging, because targeting two pathways involved in tumorigenesis might delay the development of escape mechanisms in the cancer cell.

3.3 Crosslinks between PI3K/AKT/mTOR and canonical Wnt signaling

Crosslinks between PI3K/AKT/mTOR and Wnt signaling have been well described, although not in the setting of *NK1R* inhibition. Wnt can inhibit GSK3 β in order to activate mTOR in the absence of β -catenin during regular cell growth. Inoki et al. reported that the kinases GSK3 β and AMPK cooperate in the activation of TSC2 to inhibit mTOR activity²¹². This work clearly showed that the phosphorylation of TSC2 by GSK3 β is significantly

DISCUSSION

suppressed by Wnt signaling. Furthermore, mTORC1 activity has been shown to facilitate nuclear translocation of Forkhead Box K1 (FOXK1), another member of the forkhead family which is predicted to contain an mTOR phosphorylation motif²¹³. We speculate here that FOXM1 might be modulated in a similar way since they share a common forkhead domain²¹⁴. Increase of nuclear mTOR (S2448) could therefore induce the sequestration of FOXM1 in the nucleus, which ultimately would inhibit Wnt signaling. Unfortunately, at this time our data do not permit us to fully answer this intriguing query. Inhibition of mTORC1 with rapamycin followed by immunofluorescence and phosphorylation status analysis of FOXM1 could be envisaged to elucidate this point.

Another crosslink between PI3K/AKT/mTOR and Wnt has been recently described. Gao et al. showed that autophagy negatively regulates Wnt signaling by promoting Dishevelled 2 degradation²¹⁵. Autophagy is an early mechanism set up by the cells under nutrient starvation, stress or reduced availability of growth factors to adjust the metabolism to survive. It is essentially activated upon mTORC1 inhibition^{216, 217}. However, we exclude this possibility as hepatoblastoma cells harbor β -catenin mutation and should theoretically be independent of upstream signals.

Taken together, these findings suggest that components of the PI3K/AKT/mTOR pathway can potentially be targets for diseases linked to hyperactive Wnt signaling, including cancer^{212, 218}.

4. Targeting the NK1R inhibits growth of human colon cancer cells

Colorectal cancer was found to be the consequence of an accumulation of genetic abnormalities including an overactivation of Wnt signaling in the early stages of tumorigenesis⁴⁷. New drugs have been developed to block this pathway. The use of antibody-based therapy, small molecules²¹⁹ or other direct and indirect inhibitors²²⁰ have all been studied in depth, but until now, no component has succeeded at a clinical level. We used colorectal cancer cell lines to assess whether aprepitant would have a similar effect, therefore reinforcing the action of aprepitant as a broad anti-cancer agent targeting Wnt signaling, and also providing new insights for the treatment of CRC.

Firstly, this work revealed that aprepitant triggered a robust inhibition of Wnt signaling activity and a growth inhibition of the two CRC cell lines DLD1 and LIM6. Aprepitant didn't clearly downregulate β -catenin at the protein or mRNA level, but induced an accumulation

DISCUSSION

in its membrane-bound state, as observed in the hepatoblastoma cell lines. These findings were confirmed by a significant inhibition of Wnt activity as measured by the luciferase reporter assay, and by the decrease of Wnt target genes *MYC*, *AXIN2* and *CCND1* at mRNA level and/or protein level.

With the results at hand, it is difficult to make other assumptions than the ones already exposed in the previous parts. Particularly, our work showed that *FOXM1* was significantly downregulated following treatment with aprepitant. Therefore, as observed in hepatoblastoma cells, *FOXM1* could also be responsible for the decreased Wnt activity in CRC cells. Indeed, in accordance with Zhang et al.¹⁵⁹, previous work showed that β -catenin activation directly correlates with *FOXM1* expression²²¹. They suggested also that *FOXM1* might be crucial for Wnt activity. This could be demonstrated in *Foxm1* knockout mice in which Wnt signaling was significantly reduced in *Foxm1*^{-/-} colon tumors²²². Furthermore, aprepitant also reduced sphere formation ability in CRC cell lines indicating that the inhibition effect of aprepitant on CSC is not restricted to hepatoblastoma cells, but englobes other Wnt-mutated cancers.

On the other hand, we found that aprepitant treatment resulted in growth inhibition of cells independently of their constitutional Wnt activity. For example, we observed the same therapeutic effect after separating colon cancer cells in Wnt^{high} and Wnt^{low} expressing cells. The treatment of pancreatic cancer cell line L3.6pl known to express minimal Wnt¹⁷⁶ showed furthermore a strong growth inhibition. One can give several explanations of these facts. Wnt signaling has a critical role for any cancer cell and its abrogation merely has detrimental effects on the cell, independently of its constitutional Wnt activity. Further, aprepitant has not only an anti-cancer effect by inhibiting Wnt but also by a downregulation of the PI3K/AKT/mTOR pathway, also observed in CRC cells. Therefore, aprepitant could actually be used as a broad spectrum anti-cancer agent, as already demonstrated *in vitro* in other cancer models¹⁵². The striking resemblance of aprepitant action with that of rapamycin, and the fact that even non Wnt-mutated cells are particularly susceptible to aprepitant, let us assume that NK1R inhibition modulates the PI3K/AKT/mTOR pathway at the level of mTORC1 and that the downregulation of Wnt signaling would be a fortunate side effect in a context of hyperactive Wnt (e.g. LiCl stimulated cells, hepatoblastoma cells, CRC cells). Therefore, understanding more in depth the crosslinks between PI3K/AKT/mTOR and Wnt signaling but also with other pathways (e.g. MAPK, p38) is essential in order to tackle the molecular basis of NK1R inhibition.

5. The NK1R is an ubiquitous anti-tumor target in hepatoblastoma and independent from tumor biology and stage

Very little is known regarding the expression profile of *NK1R* and its association with clinical outcome. *NK1R* is a crucial component of cancer development and progression and a promising anticancer target in a multitude of cancers¹⁵², including hepatoblastoma and colorectal cancer as demonstrated in this work. Here, we performed in depth analysis of the expression pattern of *NK1R* in hepatoblastoma and correlated our findings with patients' clinical tumor stage, biology and outcome.

We found that compared to tumor free liver tissue, tumorous tissue expressed significantly more truncated *NK1R*-tr, which is in accordance with our findings *in vitro*. Although not significant, hepatoblastoma tissues also tended to express slightly more of the full-length variant of *NK1R*. Within the tumorous tissues, expression of the full-length version correlated with the expression of the truncated version. Overall, our data provide evidence that hepatoblastoma ubiquitously expresses *NK1R*, supporting recent evidence that NK1R antagonist could be a promising anticancer agents against a wide variety of hepatoblastoma subsets²²³.

It has recently been suggested that a correlation exists between the expression rate of the SP/NK1R complex and prognosis^{187, 224-226}. Garcia-Recio et al. found that SP contributes to persistent transmodulation of the ErbB receptors, EGFR and HER2, in breast cancer, acting to enhance malignancy and therapeutic resistance¹⁸⁷. Both *NK1R* and *TAC1* (SP) were highly expressed in HER2+ primary breast tumors and correlated with poor prognosis factors. These findings are therefore in contradiction to our findings in hepatoblastoma, which showed worse prognosis with low expression of *NK1R*-tr. However, it must be noted that two completely separate tumor entities were investigated, and in their study, no distinction is made between the truncated and the full variant of the receptor. Interestingly, in their study, upon treatment of xenografted mice bearing HER2+ or HER2- human breast carcinoma, they found a therapeutic effect only for HER2+ tumors, suggesting that the anti-tumor effects of NK1R inhibition in carcinoma of the breast depended on the modulatory properties of NK1R signaling on the activity of HER2 and EGFR¹⁸⁷.

Cairo et al. recently described two tumor subclasses within hepatoblastoma resembling distinct phases of liver development and a discriminating 16-gene signature^{55, 227}. Intriguingly, when separated into the two groups by this 16-gene signature namely C1 and

DISCUSSION

C2, clinical prognosis could be predicted for these children with very high accuracy⁵⁵. By retrieving the C1/C2-status from our hepatoblastoma data base that classified each tumor according to this specific 16-gene signature, we found that *NK1R-fl* was lower in the C2 signature compared to C1. Further, we saw worse prognosis with low expression of *NK1R-tr* ($P = 0.0551$), although this was only a trend. Intriguingly, when further analyzing the C2 signature population separately, we again found worse prognosis with low expression of *NK1R-tr* ($P = 0.0377$). Therefore, in hepatoblastoma, *NK1R* alone cannot be used as a prognostic factor. However, *NK1R-tr* could possibly help to identify tumors with an advanced stage, potentially by itself and especially within the C2 signature patient population. More in depth analysis of such a C2 *NK1R-tr* low tumor cohort will be necessary in order to demonstrate the value of this distinction. Also, when making such a distinction, it needs to be understood that "low" expression here is in reference to "high", as a *NK1R-tr* low expressing tumor will on average express still significantly more *NK1R-tr* than non-tumorous tissue.

Another point, which has to be taken into account is that tumors, and especially tumors of the liver, have been shown to be significantly heterogeneous²²⁸. Typically, in our analysis we only analyzed one sample per tumor, which might not be representative for other areas of the cancer. Further, gene expression does not always correlate with the actual protein expression. It would be interesting to see whether an immunohistochemistry-based classification of hepatoblastoma could indicate prognosis. With regards to the SP/*NK1R* complex, immunohistochemical staining of its different splice variants remains a challenge and presents a major obstacle as no antibodies are currently available which distinguish both isoforms. Also, according to our current understanding of the SP/*NK1R* complex, having SP as its high affinity ligand is critical for its function¹²⁵. Here, we did not investigate SP gene expression within the tumor, which might be an interesting task for the future. And last, all but 4 patients enrolled into this retrospective study had received chemotherapy prior to surgery. Cairo et al. observed that the signature is stable irrespective of pretreatment, however we do not know in our setting if *NK1R* expression was altered. This is important to consider because the exposure to chemotherapy could potentially alter the expression pattern of *NK1R* and its splice variants. Therefore, the influence of systemic chemotherapy on the expression of the *NK1R* complex remains an unsolved question to this point.

In conclusion, our findings do not show that the *NK1R* expression pattern depends on or predicts the clinical stage and behavior, but that the two splice variants of *NK1R* are

DISCUSSION

ubiquitously overexpressed in hepatoblastoma. Overall, our data further support the potential of the SP/NK1R complex as an ideal target in a wide variety of hepatoblastoma.

SUPPLEMENTAL FIGURE

Table S1: Ratio of phospho/total protein values (RPPA) in comparison to untreated cells

		<div style="display: flex; justify-content: space-between; font-size: 0.8em; font-weight: normal;"> <div style="width: 15%;">4E-BP1_pS65-R-V_GBL9033952</div> <div style="width: 15%;">4E-BP1_pT37_T46-R-V_GBL9033953</div> <div style="width: 15%;">ACC_pS79-R-V_GBL9033954</div> <div style="width: 15%;">Akt_pS473-R-V_GBL9033956</div> <div style="width: 15%;">Akt_pT308-R-V_GBL9034077</div> <div style="width: 15%;">AMPK_pT172-R-V_GBL9034503</div> <div style="width: 15%;">c-Met_pY1235-R-V_GBL9034016</div> <div style="width: 15%;">C-Raf_pS338-R-V_GBL9033973</div> <div style="width: 15%;">Chk1_pS345-R-C_GBL9034038</div> <div style="width: 15%;">Chk2_pT68-R-C_GBL9033970</div> <div style="width: 15%;">EGFR_pY1173-R-V_GBL9033976</div> <div style="width: 15%;">ER-alpha_pS118-R-V_GBL9033977</div> <div style="width: 15%;">FOXO3a_pS318_S321-R-C_GBL9034506</div> <div style="width: 15%;">GSK3-alpha-beta_pS21_S9-R-V_GBL9033980</div> <div style="width: 15%;">GSK3_pS9-R-V_GBL9034057</div> <div style="width: 15%;">HER2_pY1248-R-C_GBL9034054</div> <div style="width: 15%;">HER3_pY1289-R-C_GBL9034017</div> </div>																	
HepT1	Ap20	0.81	1.19	1.23	1.39	1.28	1.19	1.05	1.06	1.10	1.05	1.03	0.90	1.01	1.23	1.16	1.04	1.16	
	Ap40	0.68	1.34	1.43	0.97	1.56	1.17	1.01	1.09	1.32	1.09	1.00	0.92	0.99	1.72	1.33	1.04	1.29	
	SP	1.04	1.01	0.86	1.16	0.97	1.03	1.00	0.97	1.09	1.09	1.03	0.94	1.05	1.11	1.13	1.03	0.97	
HepG2	Ap20	1.03	1.40	1.28	0.99	1.07	1.05	0.93	1.07	1.18	1.05	1.01	0.99	1.01	1.02	1.12	0.96	1.12	
	Ap40	0.88	1.16	1.91	0.96	1.14	0.96	1.02	1.00	1.39	1.16	1.07	0.99	1.01	1.02	1.20	0.90	1.18	
	SP	0.97	1.03	1.10	0.91	0.94	0.96	0.96	1.02	1.01	1.01	0.97	0.88	0.98	0.97	1.08	1.02	1.24	
HUH6	Ap20	0.87	1.21	1.64	1.13	1.22	1.31	1.08	0.84	1.17	1.07	1.09	1.18	0.93	1.06	1.08	0.98	1.15	
	Ap40	0.71	1.02	1.70	1.43	1.66	1.41	1.08	0.99	1.21	1.15	1.08	0.98	1.13	1.41	1.36	1.07	1.35	
	SP	1.03	1.01	1.08	0.96	0.99	1.23	1.04	1.00	0.99	1.10	1.11	0.98	1.04	1.06	1.10	0.94	1.00	
		<div style="display: flex; justify-content: space-between; font-size: 0.8em; font-weight: normal;"> <div style="width: 15%;">JNK_pT183_pY185-R-V_GBL9034034</div> <div style="width: 15%;">MEK1_pS217_S221-R-V_GBL9034055</div> <div style="width: 15%;">mTOR_pS2448-R-C_GBL9033987</div> <div style="width: 15%;">p27_pT157-R-C_GBL9034031</div> <div style="width: 15%;">p27_pT198-R-V_GBL9034033</div> <div style="width: 15%;">p38_pT180_Y182-R-V_GBL9033991</div> <div style="width: 15%;">p70S6K_pT389-R-V_GBL9033994</div> <div style="width: 15%;">p90RSK_pT359_S363-R-C_GBL9034022</div> <div style="width: 15%;">PDK1_pS241-R-V_GBL9033997</div> <div style="width: 15%;">PEA15_pS116-R-V_GBL9034048</div> <div style="width: 15%;">PKC-alpha_pS657-R-C_GBL9033999</div> <div style="width: 15%;">Rb_pS807_S811-R-V_GBL9034001</div> <div style="width: 15%;">Rictor_pT1135-R-V_GBL9034071</div> <div style="width: 15%;">Src_pY416-R-C_GBL9034006</div> <div style="width: 15%;">Src_pY527-R-V_GBL9034007</div> <div style="width: 15%;">Tuberin_pT1462-R-V_GBL9034011</div> <div style="width: 15%;">YAP_pS127-R-E_GBL9034520</div> <div style="width: 15%;">YB-1_pS102-R-V_GBL9034030</div> </div>																	
HepT1	Ap20	0.98	0.95	1.10	1.05	1.02	1.33	0.62	1.00	1.01	1.19	0.97	0.72	0.80	1.03	1.10	1.29	0.72	1.29
	Ap40	1.11	0.87	1.07	0.93	0.98	1.79	0.58	0.79	1.06	1.19	0.78	0.54	0.74	0.92	0.93	1.32	1.35	1.58
	SP	1.01	0.93	0.90	0.99	0.99	1.04	0.95	1.02	1.02	1.03	0.97	1.04	1.01	1.09	1.10	1.08	0.84	0.95
HepG2	Ap20	0.97	1.00	1.06	0.99	1.05	1.38	1.02	1.19	1.01	1.04	1.01	0.77	0.93	1.09	0.91	1.07	1.00	1.72
	Ap40	0.96	0.97	1.13	0.91	1.02	1.69	0.84	1.03	1.05	1.03	1.03	0.58	0.75	1.12	1.01	1.16	0.94	1.84
	SP	1.01	0.99	1.21	1.02	1.05	1.00	1.01	0.96	0.97	1.07	1.00	0.91	0.89	0.96	0.95	1.08	0.95	0.96
HUH6	Ap20	0.95	0.84	0.96	0.98	1.00	1.32	0.89	1.00	1.04	1.02	0.98	0.99	1.09	1.30	1.17	1.30	0.92	1.01
	Ap40	1.17	0.90	1.01	1.05	0.98	1.76	0.91	0.84	1.08	0.93	0.99	0.84	1.03	1.43	0.90	1.45	1.07	0.96
	SP	1.05	0.95	0.95	1.01	1.03	1.05	1.01	0.94	1.06	1.02	1.01	1.09	1.03	0.95	1.02	1.05	0.97	0.86

ABSTRACT

The neurokinin-1 receptor (NK1R) has recently been described as being pivotal in the development of cancer. NK1R antagonists, such as the clinical drug aprepitant, are therefore under current investigation as future innovative anticancer agents. However, little is known about the NK1R complex as a potential target in hepatoblastoma and colon cancer cells. Thus, we aimed at investigating the impact of NK1R inhibition with aprepitant on cell growth, apoptosis, downstream mechanisms and cancer stem cells in three human hepatoblastoma cell lines HepT1, HepG2 and HuH6 and the human colon cancer cell lines LiM6 and DLD1. Finally, mRNA from 47 children with hepatoblastoma were analysed regarding both full length and truncated forms of NK1R.

NK1R is highly expressed in human hepatoblastoma cell lines predominantly in its truncated version. Following NK1R blockage by aprepitant, a significant growth inhibition of hepatoblastoma cells and colon cancer cells as well as induction of apoptosis was detected, which was associated with the downregulation of two critical signaling pathways, namely Wnt and PI3K/AKT/mTOR. Further, treatment of colon cancer or hepatoblastoma cells grown under cancer stem cell conditions reduced sphere formation in number and size as well as expression of the stemness markers *SOX2*, *NANOG*, and *OCT4*. From a clinical perspective, both forms of NK1R were generally overexpressed in hepatoblastoma cases, without any correlation with clinicopathological parameters indicating that aprepitant might be used in a wide variety of hepatoblastoma.

Taken together, these findings give important insight into the molecular mechanisms of the NK1R as a critical component in tumorigenesis and can help in the development of future anticancer therapies for Wnt-activated cancers such as hepatoblastoma and colon cancer.

ZUSAMMENFASSUNG

Der Neurokinin-Rezeptor 1 spielt eine wichtige Rolle in der Tumorentwicklung. Daher besteht gegenwärtig ein großes Forschungsinteresse an der Untersuchung von NK1R-Antagonisten wie z.B. Aprepitant, welches bereits klinisch angewendet wird, als mögliche neue innovative Anti-Krebstherapie. Allerdings ist aktuell noch wenig bekannt über den NK1-R Komplex als potentieller Zielkandidat bei Hepatoblastomen und Kolonkarzinomen. Ziel dieser Arbeit war deshalb, die Auswirkungen einer NK1R-Inhibierung bei den drei humanen Hepatoblastomzelllinien HepT1, HepG2 und HUH6 sowie den Kolonkarzinomzelllinien LIM6 und DLD1 zu untersuchen. Schließlich sollte auch die Genexpression der full length und truncated Formen von NK1R in 47 Hepatoblastoma-Fällen gemessen werden.

Als Resultat fanden wir in den Hepatoblastoma-Fällen eine Überexpression des NK1R vor allem in der truncated Form. Aprepitant als NK1R Antagonist bewirkt sowohl eine signifikante Wachstumsinhibierung als auch Apoptoseinduktion bei Hepatoblastom- und Kolonkarzinomzellen, was mit der Herunterregulierung zweier entscheidender Signalwege, dem WNT und PI3K/AKT/mTOR Signalweg, assoziiert ist. Nach Behandlung der Hepatoblastom- und Kolonkarzinomzelllinien mit Aprepitant unter Tumorstammzell-Wachstumsbedingungen zeigten diese sowohl eine generell verringerte Anzahl und Größe der Sphären als auch eine reduzierte Expression der Tumorstammzellmarker SOX2, NANOG und OCT4. Betrachtet man die Forschungsergebnisse zusammen mit dem Krankheitsverlauf der einzelnen Patienten, werden zwar in den HB-Fällen beide Formen des NK1R-1 Rezeptors überexprimiert, jedoch ohne mit klinisch-pathologischen Parametern zu korrelieren. Daraus ließe sich ableiten, dass Aprepitant bei einer Vielzahl von Hepatoblastom-Fällen Anwendung finden könnte. Zusammenfassend geben die Forschungsergebnisse einen wichtigen Einblick in die molekularen Mechanismen von NK1R als wichtiger Faktor in der Tumorgenese des Hepatoblastoms und dessen Bedeutung für die zukünftige Entwicklung von Krebstherapien bezüglich Wnt-aktivierter Tumoren wie dem Hepatoblastom- und des Kolonkarzinoms.

ACKNOWLEDGMENT

Thanks, first and foremost, must go to Prof. Dr. med. Dietrich von Schweinitz, the director of the Department of Pediatric Surgery at the Dr. von Hauner Children's Hospital in Munich where I realized my PhD.

I am deeply grateful to Prof. Dr. rer. nat. Roland Kappler for accepting me as a member of his lab and for introducing me to the fascinating field of hepatoblastoma, for helpful discussions and guidance during my PhD project.

I am indebted to PD Dr. med. Michael Berger for giving me the opportunity to start this exciting and challenging project in the Pediatric Surgery Research Laboratories. Thank you for your friendship, your patience and unremitting help in many scientific, technical and personal matters.

Further, I would like to thank Dr. med. Matthias Ilmer for providing important scientific input during my thesis and for his guidance during my stay in MD Anderson Cancer Center in Houston. I take this opportunity to thank the Translational Molecular Pathology group of MD Anderson and Prof. Dr. med. Eckhard Alt for their generous support.

Special thanks to Corinna Weber, a fellow PhD student, who helped me several times during my project and to Fatemeh Promoli for technical support of qPCR and cell culture.

I am particularly grateful to all the members of the Kappler lab (Corinna Weber, Alexander Beck, Björn Krietemeyer, Fatemeh Promoli, Tatiana Schmid, Iva Mikulić and Jakob Mühling) for the warm and open welcome, for their numerous assistance, for providing a stimulating and joyful lab atmosphere and for all the shared activities.

I am very grateful to my family, particularly to my brother Dr. Ilias Garnier, and my friends for their unlimited help, support and understanding during this long journey in Munich.

REFERENCES

1. Allan, B.J. *et al.* Predictors of survival and incidence of hepatoblastoma in the paediatric population. *HPB : the official journal of the International Hepato Pancreato Biliary Association* **15**, 741-746 (2013).
2. Schnater, J.M., Kohler, S.E., Lamers, W.H., von Schweinitz, D. & Aronson, D.C. Where do we stand with hepatoblastoma? A review. *Cancer* **98**, 668-678 (2003).
3. DeBaun, M.R. & Tucker, M.A. Risk of cancer during the first four years of life in children from The Beckwith-Wiedemann Syndrome Registry. *The Journal of pediatrics* **132**, 398-400 (1998).
4. Hughes, L.J. & Michels, V.V. Risk of hepatoblastoma in familial adenomatous polyposis. *American journal of medical genetics* **43**, 1023-1025 (1992).
5. Ikeda, H., Matsuyama, S. & Tanimura, M. Association between hepatoblastoma and very low birth weight: a trend or a chance? *The Journal of pediatrics* **130**, 557-560 (1997).
6. von Schweinitz, D. *et al.* [Results of the HB-89 Study in treatment of malignant epithelial liver tumors in childhood and concept of a new HB-94 protocol]. *Klinische Padiatrie* **206**, 282-288 (1994).
7. Perilongo, G. *et al.* Hepatoblastoma presenting with lung metastases: treatment results of the first cooperative, prospective study of the International Society of Paediatric Oncology on childhood liver tumors. *Cancer* **89**, 1845-1853 (2000).
8. Herzog, C.E., Andrassy, R.J. & Eftekhari, F. Childhood cancers: hepatoblastoma. *The oncologist* **5**, 445-453 (2000).
9. Haas, J.E., Feusner, J.H. & Finegold, M.J. Small cell undifferentiated histology in hepatoblastoma may be unfavorable. *Cancer* **92**, 3130-3134 (2001).
10. Maibach, R. *et al.* Prognostic stratification for children with hepatoblastoma: the SIOPEL experience. *Eur J Cancer* **48**, 1543-1549 (2012).
11. Hishiki, T. Current therapeutic strategies for childhood hepatic tumors: surgical and interventional treatments for hepatoblastoma. *International journal of clinical oncology* **18**, 962-968 (2013).
12. Haeberle, B. & Schweinitz, D. Treatment of hepatoblastoma in the German cooperative pediatric liver tumor studies. *Front Biosci (Elite Ed)* **4**, 493-498 (2012).
13. Malogolowkin, M.H., Katzenstein, H.M., Krailo, M. & Meyers, R.L. Treatment of hepatoblastoma: the North American cooperative group experience. *Front Biosci (Elite Ed)* **4**, 1717-1723 (2012).
14. Czauderna, P. *et al.* Hepatoblastoma state of the art: pathology, genetics, risk stratification, and chemotherapy. *Current opinion in pediatrics* **26**, 19-28 (2014).
15. Roebuck, D.J. *et al.* 2005 PRETEXT: a revised staging system for primary malignant liver tumours of childhood developed by the SIOPEL group. *Pediatric radiology* **37**, 123-132; quiz 249-150 (2007).
16. Khaderi, S. *et al.* Role of liver transplantation in the management of hepatoblastoma in the pediatric population. *World journal of transplantation* **4**, 294-298 (2014).
17. Purcell, R. *et al.* Potential biomarkers for hepatoblastoma: results from the SIOPEL-3 study. *Eur J Cancer* **48**, 1853-1859 (2012).
18. Klaus, A. & Birchmeier, W. Wnt signalling and its impact on development and cancer. *Nature reviews. Cancer* **8**, 387-398 (2008).
19. Nusse, R. & Varmus, H.E. Many tumors induced by the mouse mammary tumor virus contain a provirus integrated in the same region of the host genome. *Cell* **31**, 99-109 (1982).
20. Rijsewijk, F. *et al.* The Drosophila homolog of the mouse mammary oncogene int-1 is identical to the segment polarity gene wingless. *Cell* **50**, 649-657 (1987).
21. Nusse, R. *et al.* A new nomenclature for int-1 and related genes: the Wnt gene family. *Cell* **64**, 231 (1991).
22. Barker, N. & Clevers, H. Mining the Wnt pathway for cancer therapeutics. *Nature reviews. Drug discovery* **5**, 997-1014 (2006).
23. Liu, C. *et al.* Control of beta-catenin phosphorylation/degradation by a dual-kinase mechanism. *Cell* **108**, 837-847 (2002).

REFERENCES

24. Aberle, H., Bauer, A., Stappert, J., Kispert, A. & Kemler, R. beta-catenin is a target for the ubiquitin-proteasome pathway. *The EMBO journal* **16**, 3797-3804 (1997).
25. Daniels, D.L. & Weis, W.I. Beta-catenin directly displaces Groucho/TLE repressors from Tcf/Lef in Wnt-mediated transcription activation. *Nature structural & molecular biology* **12**, 364-371 (2005).
26. Bilic, J. *et al.* Wnt induces LRP6 signalosomes and promotes dishevelled-dependent LRP6 phosphorylation. *Science* **316**, 1619-1622 (2007).
27. Behrens, J. *et al.* Functional interaction of beta-catenin with the transcription factor LEF-1. *Nature* **382**, 638-642 (1996).
28. He, T.C. *et al.* Identification of c-MYC as a target of the APC pathway. *Science* **281**, 1509-1512 (1998).
29. Leyns, L., Bouwmeester, T., Kim, S.H., Piccolo, S. & De Robertis, E.M. Frzb-1 is a secreted antagonist of Wnt signaling expressed in the Spemann organizer. *Cell* **88**, 747-756 (1997).
30. Glinka, A. *et al.* Dickkopf-1 is a member of a new family of secreted proteins and functions in head induction. *Nature* **391**, 357-362 (1998).
31. Mao, B. *et al.* Kremen proteins are Dickkopf receptors that regulate Wnt/beta-catenin signalling. *Nature* **417**, 664-667 (2002).
32. Kazanskaya, O. *et al.* R-Spondin2 is a secreted activator of Wnt/beta-catenin signaling and is required for *Xenopus* myogenesis. *Developmental cell* **7**, 525-534 (2004).
33. Jamora, C. & Fuchs, E. Intercellular adhesion, signalling and the cytoskeleton. *Nature cell biology* **4**, E101-108 (2002).
34. Orsulic, S., Huber, O., Aberle, H., Arnold, S. & Kemler, R. E-cadherin binding prevents beta-catenin nuclear localization and beta-catenin/LEF-1-mediated transactivation. *Journal of cell science* **112** (Pt 8), 1237-1245 (1999).
35. Huber, O., Bierkamp, C. & Kemler, R. Cadherins and catenins in development. *Current opinion in cell biology* **8**, 685-691 (1996).
36. Huber, A.H., Stewart, D.B., Laurents, D.V., Nelson, W.J. & Weis, W.I. The cadherin cytoplasmic domain is unstructured in the absence of beta-catenin. A possible mechanism for regulating cadherin turnover. *The Journal of biological chemistry* **276**, 12301-12309 (2001).
37. Lilien, J. & Balsamo, J. The regulation of cadherin-mediated adhesion by tyrosine phosphorylation/dephosphorylation of beta-catenin. *Current opinion in cell biology* **17**, 459-465 (2005).
38. Monga, S.P. *et al.* Hepatocyte growth factor induces Wnt-independent nuclear translocation of beta-catenin after Met-beta-catenin dissociation in hepatocytes. *Cancer research* **62**, 2064-2071 (2002).
39. Apte, U. *et al.* beta-Catenin is critical for early postnatal liver growth. *American journal of physiology. Gastrointestinal and liver physiology* **292**, G1578-1585 (2007).
40. Tan, X. *et al.* Beta-catenin deletion in hepatoblasts disrupts hepatic morphogenesis and survival during mouse development. *Hepatology* **47**, 1667-1679 (2008).
41. Monga, S.P. Role and regulation of beta-catenin signaling during physiological liver growth. *Gene expression* **16**, 51-62 (2014).
42. Monga, S.P., Padiaditakis, P., Mule, K., Stolz, D.B. & Michalopoulos, G.K. Changes in WNT/beta-catenin pathway during regulated growth in rat liver regeneration. *Hepatology* **33**, 1098-1109 (2001).
43. Michalopoulos, G.K. Liver regeneration after partial hepatectomy: critical analysis of mechanistic dilemmas. *The American journal of pathology* **176**, 2-13 (2010).
44. Michalopoulos, G.K. & DeFrances, M.C. Liver regeneration. *Science* **276**, 60-66 (1997).
45. Polakis, P. Wnt signaling and cancer. *Genes & development* **14**, 1837-1851 (2000).
46. Bodmer, W.F. *et al.* Localization of the gene for familial adenomatous polyposis on chromosome 5. *Nature* **328**, 614-616 (1987).
47. Fearhead, N.S., Britton, M.P. & Bodmer, W.F. The ABC of APC. *Human molecular genetics* **10**, 721-733 (2001).
48. Rubinfeld, B. *et al.* Binding of GSK3beta to the APC-beta-catenin complex and regulation of complex assembly. *Science* **272**, 1023-1026 (1996).

REFERENCES

49. Ikeda, S. *et al.* Axin, a negative regulator of the Wnt signaling pathway, forms a complex with GSK-3 β and β -catenin and promotes GSK-3 β -dependent phosphorylation of β -catenin. *The EMBO journal* **17**, 1371-1384 (1998).
50. Koch, A. *et al.* Childhood hepatoblastomas frequently carry a mutated degradation targeting box of the β -catenin gene. *Cancer research* **59**, 269-273 (1999).
51. Koesters, R. & von Knebel Doeberitz, M. The Wnt signaling pathway in solid childhood tumors. *Cancer letters* **198**, 123-138 (2003).
52. Jeng, Y.M., Wu, M.Z., Mao, T.L., Chang, M.H. & Hsu, H.C. Somatic mutations of β -catenin play a crucial role in the tumorigenesis of sporadic hepatoblastoma. *Cancer letters* **152**, 45-51 (2000).
53. Takayasu, H. *et al.* Frequent deletions and mutations of the β -catenin gene are associated with overexpression of cyclin D1 and fibronectin and poorly differentiated histology in childhood hepatoblastoma. *Clinical cancer research : an official journal of the American Association for Cancer Research* **7**, 901-908 (2001).
54. Wei, Y. *et al.* Activation of β -catenin in epithelial and mesenchymal hepatoblastomas. *Oncogene* **19**, 498-504 (2000).
55. Cairo, S. *et al.* Hepatic stem-like phenotype and interplay of Wnt/ β -catenin and Myc signaling in aggressive childhood liver cancer. *Cancer cell* **14**, 471-484 (2008).
56. Taniguchi, K. *et al.* Mutational spectrum of β -catenin, AXIN1, and AXIN2 in hepatocellular carcinomas and hepatoblastomas. *Oncogene* **21**, 4863-4871 (2002).
57. Koch, A. *et al.* Mutations and elevated transcriptional activity of conductin (AXIN2) in hepatoblastomas. *The Journal of pathology* **204**, 546-554 (2004).
58. Oda, H., Imai, Y., Nakatsuru, Y., Hata, J. & Ishikawa, T. Somatic mutations of the APC gene in sporadic hepatoblastomas. *Cancer research* **56**, 3320-3323 (1996).
59. Aretz, S. *et al.* Should children at risk for familial adenomatous polyposis be screened for hepatoblastoma and children with apparently sporadic hepatoblastoma be screened for APC germline mutations? *Pediatric blood & cancer* **47**, 811-818 (2006).
60. Koch, A. *et al.* Elevated expression of Wnt antagonists is a common event in hepatoblastomas. *Clinical cancer research : an official journal of the American Association for Cancer Research* **11**, 4295-4304 (2005).
61. Cavard, C. *et al.* Wnt/ β -catenin pathway in hepatocellular carcinoma pathogenesis and liver physiology. *Future Oncol* **4**, 647-660 (2008).
62. Burke, Z.D. *et al.* Liver zonation occurs through a β -catenin-dependent, c-Myc-independent mechanism. *Gastroenterology* **136**, 2316-2324 e2311-2313 (2009).
63. Testa, J.R. & Tsichlis, P.N. AKT signaling in normal and malignant cells. *Oncogene* **24**, 7391-7393 (2005).
64. Hartmann, W. *et al.* Activation of phosphatidylinositol-3'-kinase/AKT signaling is essential in hepatoblastoma survival. *Clinical cancer research : an official journal of the American Association for Cancer Research* **15**, 4538-4545 (2009).
65. Polivka, J., Jr. & Janku, F. Molecular targets for cancer therapy in the PI3K/AKT/mTOR pathway. *Pharmacology & therapeutics* **142**, 164-175 (2014).
66. Altomare, D.A. & Testa, J.R. Perturbations of the AKT signaling pathway in human cancer. *Oncogene* **24**, 7455-7464 (2005).
67. Engelman, J.A. Targeting PI3K signalling in cancer: opportunities, challenges and limitations. *Nature reviews. Cancer* **9**, 550-562 (2009).
68. Lemmon, M.A. & Schlessinger, J. Cell signaling by receptor tyrosine kinases. *Cell* **141**, 1117-1134 (2010).
69. Gschwind, A., Fischer, O.M. & Ullrich, A. The discovery of receptor tyrosine kinases: targets for cancer therapy. *Nature reviews. Cancer* **4**, 361-370 (2004).
70. Schlessinger, J. Cell signaling by receptor tyrosine kinases. *Cell* **103**, 211-225 (2000).
71. Cantley, L.C. The phosphoinositide 3-kinase pathway. *Science* **296**, 1655-1657 (2002).

REFERENCES

72. Sun, X.J. *et al.* Structure of the insulin receptor substrate IRS-1 defines a unique signal transduction protein. *Nature* **352**, 73-77 (1991).
73. Wymann, M.P., Zvelebil, M. & Laffargue, M. Phosphoinositide 3-kinase signalling--which way to target? *Trends in pharmacological sciences* **24**, 366-376 (2003).
74. Katso, R. *et al.* Cellular function of phosphoinositide 3-kinases: implications for development, homeostasis, and cancer. *Annual review of cell and developmental biology* **17**, 615-675 (2001).
75. Engelman, J.A., Luo, J. & Cantley, L.C. The evolution of phosphatidylinositol 3-kinases as regulators of growth and metabolism. *Nature reviews. Genetics* **7**, 606-619 (2006).
76. Klippel, A., Kavanaugh, W.M., Pot, D. & Williams, L.T. A specific product of phosphatidylinositol 3-kinase directly activates the protein kinase Akt through its pleckstrin homology domain. *Molecular and cellular biology* **17**, 338-344 (1997).
77. Alessi, D.R. *et al.* Characterization of a 3-phosphoinositide-dependent protein kinase which phosphorylates and activates protein kinase Balpha. *Current biology : CB* **7**, 261-269 (1997).
78. Stokoe, D. *et al.* Dual role of phosphatidylinositol-3,4,5-trisphosphate in the activation of protein kinase B. *Science* **277**, 567-570 (1997).
79. Sarbassov, D.D., Guertin, D.A., Ali, S.M. & Sabatini, D.M. Phosphorylation and regulation of Akt/PKB by the rictor-mTOR complex. *Science* **307**, 1098-1101 (2005).
80. Calnan, D.R. & Brunet, A. The FoxO code. *Oncogene* **27**, 2276-2288 (2008).
81. Cross, D.A., Alessi, D.R., Cohen, P., Andjelkovich, M. & Hemmings, B.A. Inhibition of glycogen synthase kinase-3 by insulin mediated by protein kinase B. *Nature* **378**, 785-789 (1995).
82. Datta, S.R. *et al.* Akt phosphorylation of BAD couples survival signals to the cell-intrinsic death machinery. *Cell* **91**, 231-241 (1997).
83. Ashworth, R.E. & Wu, J. Mammalian target of rapamycin inhibition in hepatocellular carcinoma. *World journal of hepatology* **6**, 776-782 (2014).
84. Ma, X.M. & Blenis, J. Molecular mechanisms of mTOR-mediated translational control. *Nature reviews. Molecular cell biology* **10**, 307-318 (2009).
85. Peterson, T.R. *et al.* DEPTOR is an mTOR inhibitor frequently overexpressed in multiple myeloma cells and required for their survival. *Cell* **137**, 873-886 (2009).
86. Wang, L., Harris, T.E., Roth, R.A. & Lawrence, J.C., Jr. PRAS40 regulates mTORC1 kinase activity by functioning as a direct inhibitor of substrate binding. *The Journal of biological chemistry* **282**, 20036-20044 (2007).
87. Huang, J. & Manning, B.D. A complex interplay between Akt, TSC2 and the two mTOR complexes. *Biochemical Society transactions* **37**, 217-222 (2009).
88. Pullen, N. & Thomas, G. The modular phosphorylation and activation of p70s6k. *FEBS letters* **410**, 78-82 (1997).
89. Richter, J.D. & Sonenberg, N. Regulation of cap-dependent translation by eIF4E inhibitory proteins. *Nature* **433**, 477-480 (2005).
90. Buchkovich, N.J., Yu, Y., Zampieri, C.A. & Alwine, J.C. The TORrid affairs of viruses: effects of mammalian DNA viruses on the PI3K-Akt-mTOR signalling pathway. *Nature reviews. Microbiology* **6**, 266-275 (2008).
91. Sabatini, D.M. mTOR and cancer: insights into a complex relationship. *Nature reviews. Cancer* **6**, 729-734 (2006).
92. Yang, Q., Inoki, K., Ikenoue, T. & Guan, K.L. Identification of Sin1 as an essential TORC2 component required for complex formation and kinase activity. *Genes & development* **20**, 2820-2832 (2006).
93. Huang, J., Dibble, C.C., Matsuzaki, M. & Manning, B.D. The TSC1-TSC2 complex is required for proper activation of mTOR complex 2. *Molecular and cellular biology* **28**, 4104-4115 (2008).
94. Guertin, D.A. *et al.* Ablation in mice of the mTORC components raptor, rictor, or mLST8 reveals that mTORC2 is required for signaling to Akt-FOXO and PKCalpha, but not S6K1. *Developmental cell* **11**, 859-871 (2006).
95. Julien, L.A., Carriere, A., Moreau, J. & Roux, P.P. mTORC1-activated S6K1 phosphorylates Rictor on threonine 1135 and regulates mTORC2 signaling. *Molecular and cellular biology* **30**, 908-921 (2010).

REFERENCES

96. Huang, J., Wu, S., Wu, C.L. & Manning, B.D. Signaling events downstream of mammalian target of rapamycin complex 2 are attenuated in cells and tumors deficient for the tuberous sclerosis complex tumor suppressors. *Cancer research* **69**, 6107-6114 (2009).
97. Treins, C., Warne, P.H., Magnuson, M.A., Pende, M. & Downward, J. Rictor is a novel target of p70 S6 kinase-1. *Oncogene* **29**, 1003-1016 (2010).
98. Tzatsos, A. & Kandror, K.V. Nutrients suppress phosphatidylinositol 3-kinase/Akt signaling via raptor-dependent mTOR-mediated insulin receptor substrate 1 phosphorylation. *Molecular and cellular biology* **26**, 63-76 (2006).
99. Goel, A. *et al.* Frequent inactivation of PTEN by promoter hypermethylation in microsatellite instability-high sporadic colorectal cancers. *Cancer research* **64**, 3014-3021 (2004).
100. Samuels, Y. *et al.* High frequency of mutations of the PIK3CA gene in human cancers. *Science* **304**, 554 (2004).
101. Carpten, J.D. *et al.* A transforming mutation in the pleckstrin homology domain of AKT1 in cancer. *Nature* **448**, 439-444 (2007).
102. Gray, S.G. *et al.* Altered expression of members of the IGF-axis in hepatoblastomas. *British journal of cancer* **82**, 1561-1567 (2000).
103. Rosen, C.J. & Pollak, M. Circulating IGF-I: New Perspectives for a New Century. *Trends in endocrinology and metabolism: TEM* **10**, 136-141 (1999).
104. Rainier, S., Dobry, C.J. & Feinberg, A.P. Loss of imprinting in hepatoblastoma. *Cancer research* **55**, 1836-1838 (1995).
105. Akmal, S.N., Yun, K., MacLay, J., Higami, Y. & Ikeda, T. Insulin-like growth factor 2 and insulin-like growth factor binding protein 2 expression in hepatoblastoma. *Human pathology* **26**, 846-851 (1995).
106. Li, X. *et al.* Expression, promoter usage and parental imprinting status of insulin-like growth factor II (IGF2) in human hepatoblastoma: uncoupling of IGF2 and H19 imprinting. *Oncogene* **11**, 221-229 (1995).
107. Regel, I. *et al.* IGFBP3 impedes aggressive growth of pediatric liver cancer and is epigenetically silenced in vascular invasive and metastatic tumors. *Molecular cancer* **11**, 9 (2012).
108. Eichenmuller, M. *et al.* Blocking the hedgehog pathway inhibits hepatoblastoma growth. *Hepatology* **49**, 482-490 (2009).
109. Litten, J.B. *et al.* Activated NOTCH2 is overexpressed in hepatoblastomas: an immunohistochemical study. *Pediatric and developmental pathology : the official journal of the Society for Pediatric Pathology and the Paediatric Pathology Society* **14**, 378-383 (2011).
110. Lopez-Terrada, D. *et al.* Histologic subtypes of hepatoblastoma are characterized by differential canonical Wnt and Notch pathway activation in DLK+ precursors. *Human pathology* **40**, 783-794 (2009).
111. Sakamoto, L.H., B, D.E.C., Cajaiba, M., Soares, F.A. & Vettore, A.L. MT1G hypermethylation: a potential prognostic marker for hepatoblastoma. *Pediatric research* **67**, 387-393 (2010).
112. Weber, R.G., Pietsch, T., von Schweinitz, D. & Lichter, P. Characterization of genomic alterations in hepatoblastomas. A role for gains on chromosomes 8q and 20 as predictors of poor outcome. *The American journal of pathology* **157**, 571-578 (2000).
113. Ortega, J.A. *et al.* Randomized comparison of cisplatin/vincristine/fluorouracil and cisplatin/continuous infusion doxorubicin for treatment of pediatric hepatoblastoma: A report from the Children's Cancer Group and the Pediatric Oncology Group. *Journal of clinical oncology : official journal of the American Society of Clinical Oncology* **18**, 2665-2675 (2000).
114. Aronson, D.C., Czauderna, P., Maibach, R., Perilongo, G. & Morland, B. The treatment of hepatoblastoma: Its evolution and the current status as per the SIOPEL trials. *Journal of Indian Association of Pediatric Surgeons* **19**, 201-207 (2014).
115. Meyers, R.L., Tiao, G., de Ville de Goyet, J., Superina, R. & Aronson, D.C. Hepatoblastoma state of the art: pre-treatment extent of disease, surgical resection guidelines and the role of liver transplantation. *Current opinion in pediatrics* **26**, 29-36 (2014).

REFERENCES

116. Kremer, N., Walther, A.E. & Tiao, G.M. Management of hepatoblastoma: an update. *Current opinion in pediatrics* **26**, 362-369 (2014).
117. Malogolowkin, M.H. *et al.* Complete surgical resection is curative for children with hepatoblastoma with pure fetal histology: a report from the Children's Oncology Group. *Journal of clinical oncology : official journal of the American Society of Clinical Oncology* **29**, 3301-3306 (2011).
118. D'Antiga, L. *et al.* Features predicting unresectability in hepatoblastoma. *Cancer* **110**, 1050-1058 (2007).
119. Browne, M. *et al.* Survival after liver transplantation for hepatoblastoma: a 2-center experience. *Journal of pediatric surgery* **43**, 1973-1981 (2008).
120. Meyers, R.L. *et al.* Predictive power of pretreatment prognostic factors in children with hepatoblastoma: a report from the Children's Oncology Group. *Pediatric blood & cancer* **53**, 1016-1022 (2009).
121. Warmann, S. *et al.* The role of the MDR1 gene in the development of multidrug resistance in human hepatoblastoma: clinical course and in vivo model. *Cancer* **95**, 1795-1801 (2002).
122. Kimura, Y., Morita, S.Y., Matsuo, M. & Ueda, K. Mechanism of multidrug recognition by MDR1/ABC1. *Cancer science* **98**, 1303-1310 (2007).
123. Morland, B. Commentary on hepatoblastoma minisymposium. *Pediatric radiology* **36**, 175 (2006).
124. Ichikawa, Y. *et al.* Cardiotoxicity of doxorubicin is mediated through mitochondrial iron accumulation. *The Journal of clinical investigation* **124**, 617-630 (2014).
125. Pennefather, J.N. *et al.* Tachykinins and tachykinin receptors: a growing family. *Life sciences* **74**, 1445-1463 (2004).
126. Tsuchida, K., Shigemoto, R., Yokota, Y. & Nakanishi, S. Tissue distribution and quantitation of the mRNAs for three rat tachykinin receptors. *European journal of biochemistry / FEBS* **193**, 751-757 (1990).
127. Ho, W.Z., Lai, J.P., Zhu, X.H., Uvaydova, M. & Douglas, S.D. Human monocytes and macrophages express substance P and neurokinin-1 receptor. *J Immunol* **159**, 5654-5660 (1997).
128. Patacchini, R. & Maggi, C.A. Peripheral tachykinin receptors as targets for new drugs. *European journal of pharmacology* **429**, 13-21 (2001).
129. Saffroy, M., Torrens, Y., Glowinski, J. & Beaujouan, J.C. Autoradiographic distribution of tachykinin NK2 binding sites in the rat brain: comparison with NK1 and NK3 binding sites. *Neuroscience* **116**, 761-773 (2003).
130. Page, N.M. Characterization of the gene structures, precursor processing and pharmacology of the endokinin peptides. *Vascular pharmacology* **45**, 200-208 (2006).
131. Otsuka, M. & Yoshioka, K. Neurotransmitter functions of mammalian tachykinins. *Physiological reviews* **73**, 229-308 (1993).
132. Almeida, T.A. *et al.* Tachykinins and tachykinin receptors: structure and activity relationships. *Current medicinal chemistry* **11**, 2045-2081 (2004).
133. Gerard, N.P. *et al.* Human substance P receptor (NK-1): organization of the gene, chromosome localization, and functional expression of cDNA clones. *Biochemistry* **30**, 10640-10646 (1991).
134. Roush, E.D. & Kwatra, M.M. Human substance P receptor expressed in Chinese hamster ovary cells directly activates G(alpha q/11), G(alpha s), G(alpha o). *FEBS letters* **428**, 291-294 (1998).
135. Mitsuhashi, M. *et al.* Multiple intracellular signaling pathways of the neuropeptide substance P receptor. *Journal of neuroscience research* **32**, 437-443 (1992).
136. Sagan, S., Chassaing, G., Pradier, L. & Lavielle, S. Tachykinin peptides affect differently the second messenger pathways after binding to CHO-expressed human NK-1 receptors. *The Journal of pharmacology and experimental therapeutics* **276**, 1039-1048 (1996).
137. Takeda, Y. *et al.* Ligand binding kinetics of substance P and neurokinin A receptors stably expressed in Chinese hamster ovary cells and evidence for differential stimulation of inositol 1,4,5-trisphosphate and cyclic AMP second messenger responses. *Journal of neurochemistry* **59**, 740-745 (1992).

REFERENCES

138. Khawaja, A.M. & Rogers, D.F. Tachykinins: receptor to effector. *The international journal of biochemistry & cell biology* **28**, 721-738 (1996).
139. Holst, B., Hastrup, H., Raffetseder, U., Martini, L. & Schwartz, T.W. Two active molecular phenotypes of the tachykinin NK1 receptor revealed by G-protein fusions and mutagenesis. *The Journal of biological chemistry* **276**, 19793-19799 (2001).
140. Ramkissoon, S.H., Patel, H.J., Taborga, M. & Rameshwar, P. G protein-coupled receptors in haematopoietic disruption. *Expert opinion on biological therapy* **6**, 109-120 (2006).
141. Nakajima, Y., Tsuchida, K., Negishi, M., Ito, S. & Nakanishi, S. Direct linkage of three tachykinin receptors to stimulation of both phosphatidylinositol hydrolysis and cyclic AMP cascades in transfected Chinese hamster ovary cells. *The Journal of biological chemistry* **267**, 2437-2442 (1992).
142. Mantyh, P.W. *et al.* Rapid endocytosis of a G protein-coupled receptor: substance P evoked internalization of its receptor in the rat striatum in vivo. *Proceedings of the National Academy of Sciences of the United States of America* **92**, 2622-2626 (1995).
143. Garland, A.M. *et al.* Mechanisms of desensitization and resensitization of G protein-coupled neurokinin1 and neurokinin2 receptors. *Molecular pharmacology* **49**, 438-446 (1996).
144. Roosterman, D., Cottrell, G.S., Schmidlin, F., Steinhoff, M. & Bunnett, N.W. Recycling and resensitization of the neurokinin 1 receptor. Influence of agonist concentration and Rab GTPases. *The Journal of biological chemistry* **279**, 30670-30679 (2004).
145. Fong, T.M., Anderson, S.A., Yu, H., Huang, R.R. & Strader, C.D. Differential activation of intracellular effector by two isoforms of human neurokinin-1 receptor. *Molecular pharmacology* **41**, 24-30 (1992).
146. Page, N.M. New challenges in the study of the mammalian tachykinins. *Peptides* **26**, 1356-1368 (2005).
147. Li, H. *et al.* A substance P (neurokinin-1) receptor mutant carboxyl-terminally truncated to resemble a naturally occurring receptor isoform displays enhanced responsiveness and resistance to desensitization. *Proceedings of the National Academy of Sciences of the United States of America* **94**, 9475-9480 (1997).
148. Tuluc, F., Lai, J.P., Kilpatrick, L.E., Evans, D.L. & Douglas, S.D. Neurokinin 1 receptor isoforms and the control of innate immunity. *Trends in immunology* **30**, 271-276 (2009).
149. Harrison, S. & Geppetti, P. Substance p. *The international journal of biochemistry & cell biology* **33**, 555-576 (2001).
150. Tattersall, F.D. *et al.* The novel NK1 receptor antagonist MK-0869 (L-754,030) and its water soluble phosphoryl prodrug, L-758,298, inhibit acute and delayed cisplatin-induced emesis in ferrets. *Neuropharmacology* **39**, 652-663 (2000).
151. Dando, T.M. & Perry, C.M. Aprepitant: a review of its use in the prevention of chemotherapy-induced nausea and vomiting. *Drugs* **64**, 777-794 (2004).
152. Munoz, M., Rosso, M. & Covenas, R. A new frontier in the treatment of cancer: NK-1 receptor antagonists. *Current medicinal chemistry* **17**, 504-516 (2010).
153. Munoz, M. *et al.* Antitumor activity of neurokinin-1 receptor antagonists in MG-63 human osteosarcoma xenografts. *International journal of oncology* **44**, 137-146 (2014).
154. Pietsch, T. *et al.* Characterization of the continuous cell line HepT1 derived from a human hepatoblastoma. *Laboratory investigation; a journal of technical methods and pathology* **74**, 809-818 (1996).
155. Bresalier, R.S. *et al.* Mucin production by human colonic carcinoma cells correlates with their metastatic potential in animal models of colon cancer metastasis. *The Journal of clinical investigation* **87**, 1037-1045 (1991).
156. Berger, M. *et al.* Hepatoblastoma cells express truncated neurokinin-1 receptor and can be growth inhibited by aprepitant in vitro and in vivo. *Journal of hepatology* **60**, 985-994 (2014).
157. Gillespie, E. *et al.* Truncated neurokinin-1 receptor is increased in colonic epithelial cells from patients with colitis-associated cancer. *Proceedings of the National Academy of Sciences of the United States of America* **108**, 17420-17425 (2011).

REFERENCES

158. Ilmer, M. *et al.* Targeting the Neurokinin-1 Receptor Compromises Canonical Wnt Signaling in Hepatoblastoma. *Molecular cancer therapeutics* **14**, 2712-2721 (2015).
159. Zhang, N. *et al.* FoxM1 promotes beta-catenin nuclear localization and controls Wnt target-gene expression and glioma tumorigenesis. *Cancer cell* **20**, 427-442 (2011).
160. Stambolic, V., Ruel, L. & Woodgett, J.R. Lithium inhibits glycogen synthase kinase-3 activity and mimics wingless signalling in intact cells. *Current biology : CB* **6**, 1664-1668 (1996).
161. Reya, T. & Clevers, H. Wnt signalling in stem cells and cancer. *Nature* **434**, 843-850 (2005).
162. Rattis, F.M., Voermans, C. & Reya, T. Wnt signaling in the stem cell niche. *Current opinion in hematology* **11**, 88-94 (2004).
163. Lonardo, E. *et al.* Nodal/Activin signaling drives self-renewal and tumorigenicity of pancreatic cancer stem cells and provides a target for combined drug therapy. *Cell stem cell* **9**, 433-446 (2011).
164. Haraguchi, N. *et al.* CD13 is a therapeutic target in human liver cancer stem cells. *The Journal of clinical investigation* **120**, 3326-3339 (2010).
165. Akita, M. *et al.* Detection of CD133 (prominin-1) in a human hepatoblastoma cell line (HuH-6 clone 5). *Microscopy research and technique* **76**, 844-852 (2013).
166. Kim, H. *et al.* Human hepatocellular carcinomas with "Stemness"-related marker expression: keratin 19 expression and a poor prognosis. *Hepatology* **54**, 1707-1717 (2011).
167. de Boer, C.J., van Krieken, J.H., Janssen-van Rhijn, C.M. & Litvinov, S.V. Expression of Ep-CAM in normal, regenerating, metaplastic, and neoplastic liver. *The Journal of pathology* **188**, 201-206 (1999).
168. Cheung, S.T., Cheung, P.F., Cheng, C.K., Wong, N.C. & Fan, S.T. Granulin-epithelin precursor and ATP-dependent binding cassette (ABC)B5 regulate liver cancer cell chemoresistance. *Gastroenterology* **140**, 344-355 (2011).
169. Brabletz, T. *et al.* Variable beta-catenin expression in colorectal cancers indicates tumor progression driven by the tumor environment. *Proceedings of the National Academy of Sciences of the United States of America* **98**, 10356-10361 (2001).
170. Yang, J. *et al.* Adenomatous polyposis coli (APC) differentially regulates beta-catenin phosphorylation and ubiquitination in colon cancer cells. *The Journal of biological chemistry* **281**, 17751-17757 (2006).
171. Garnier, A. *et al.* Targeting the neurokinin-1 receptor inhibits growth of human colon cancer cells. *International journal of oncology* **47**, 151-160 (2015).
172. Bossy-Wetzel, E., Bakiri, L. & Yaniv, M. Induction of apoptosis by the transcription factor c-Jun. *The EMBO journal* **16**, 1695-1709 (1997).
173. Leppa, S. & Bohmann, D. Diverse functions of JNK signaling and c-Jun in stress response and apoptosis. *Oncogene* **18**, 6158-6162 (1999).
174. Gespach, C. Increasing potential of HER3 signaling in colon cancer progression and therapy. *Clinical cancer research : an official journal of the American Association for Cancer Research* **18**, 917-919 (2012).
175. Taylor, W.R. & Stark, G.R. Regulation of the G2/M transition by p53. *Oncogene* **20**, 1803-1815 (2001).
176. Ilmer, M. *et al.* RSPO2 Enhances Canonical Wnt Signaling to Confer Stemness-Associated Traits to Susceptible Pancreatic Cancer Cells. *Cancer research* **75**, 1883-1896 (2015).
177. Vermeulen, L. *et al.* Wnt activity defines colon cancer stem cells and is regulated by the microenvironment. *Nature cell biology* **12**, 468-476 (2010).
178. Fuerer, C. & Nusse, R. Lentiviral vectors to probe and manipulate the Wnt signaling pathway. *PLoS one* **5**, e9370 (2010).
179. Garnier, A. *et al.* Truncated neurokinin-1 receptor is an ubiquitous antitumor target in hepatoblastoma, and its expression is independent of tumor biology and stage. *Oncology Letters* **11** (2015).
180. Rosso, M., Munoz, M. & Berger, M. The role of neurokinin-1 receptor in the microenvironment of inflammation and cancer. *TheScientificWorldJournal* **2012**, 381434 (2012).

REFERENCES

181. Colotta, F., Allavena, P., Sica, A., Garlanda, C. & Mantovani, A. Cancer-related inflammation, the seventh hallmark of cancer: links to genetic instability. *Carcinogenesis* **30**, 1073-1081 (2009).
182. Mayordomo, C. *et al.* Targeting of substance P induces cancer cell death and decreases the steady state of EGFR and Her2. *Journal of cellular physiology* **227**, 1358-1366 (2012).
183. Patel, H.J., Ramkissoon, S.H., Patel, P.S. & Rameshwar, P. Transformation of breast cells by truncated neurokinin-1 receptor is secondary to activation by preprotachykinin-A peptides. *Proceedings of the National Academy of Sciences of the United States of America* **102**, 17436-17441 (2005).
184. Ramkissoon, S.H., Patel, P.S., Taborga, M. & Rameshwar, P. Nuclear factor-kappaB is central to the expression of truncated neurokinin-1 receptor in breast cancer: implication for breast cancer cell quiescence within bone marrow stroma. *Cancer research* **67**, 1653-1659 (2007).
185. Alayev, A. & Holz, M.K. mTOR signaling for biological control and cancer. *Journal of cellular physiology* **228**, 1658-1664 (2013).
186. Wagner, F. *et al.* Rapamycin blocks hepatoblastoma growth in vitro and in vivo implicating new treatment options in high-risk patients. *Eur J Cancer* **48**, 2442-2450 (2012).
187. Garcia-Recio, S. *et al.* Substance P autocrine signaling contributes to persistent HER2 activation that drives malignant progression and drug resistance in breast cancer. *Cancer research* **73**, 6424-6434 (2013).
188. Kovacina, K.S. *et al.* Identification of a proline-rich Akt substrate as a 14-3-3 binding partner. *The Journal of biological chemistry* **278**, 10189-10194 (2003).
189. Gingras, A.C. *et al.* Regulation of 4E-BP1 phosphorylation: a novel two-step mechanism. *Genes & development* **13**, 1422-1437 (1999).
190. Shuda, M. *et al.* CDK1 substitutes for mTOR kinase to activate mitotic cap-dependent protein translation. *Proceedings of the National Academy of Sciences of the United States of America* **112**, 5875-5882 (2015).
191. Shang, Z.F. *et al.* 4E-BP1 participates in maintaining spindle integrity and genomic stability via interacting with PLK1. *Cell Cycle* **11**, 3463-3471 (2012).
192. Copp, J., Manning, G. & Hunter, T. TORC-specific phosphorylation of mammalian target of rapamycin (mTOR): phospho-Ser2481 is a marker for intact mTOR signaling complex 2. *Cancer research* **69**, 1821-1827 (2009).
193. Sekulic, A. *et al.* A direct linkage between the phosphoinositide 3-kinase-AKT signaling pathway and the mammalian target of rapamycin in mitogen-stimulated and transformed cells. *Cancer research* **60**, 3504-3513 (2000).
194. Shah, O.J., Wang, Z. & Hunter, T. Inappropriate activation of the TSC/Rheb/mTOR/S6K cassette induces IRS1/2 depletion, insulin resistance, and cell survival deficiencies. *Current biology : CB* **14**, 1650-1656 (2004).
195. Harrington, L.S. *et al.* The TSC1-2 tumor suppressor controls insulin-PI3K signaling via regulation of IRS proteins. *The Journal of cell biology* **166**, 213-223 (2004).
196. Breuleux, M. *et al.* Increased AKT S473 phosphorylation after mTORC1 inhibition is rictor dependent and does not predict tumor cell response to PI3K/mTOR inhibition. *Molecular cancer therapeutics* **8**, 742-753 (2009).
197. Chen, K.F. *et al.* Activation of phosphatidylinositol 3-kinase/Akt signaling pathway mediates acquired resistance to sorafenib in hepatocellular carcinoma cells. *The Journal of pharmacology and experimental therapeutics* **337**, 155-161 (2011).
198. Betz, C. & Hall, M.N. Where is mTOR and what is it doing there? *The Journal of cell biology* **203**, 563-574 (2013).
199. Kim, J.E. & Chen, J. Cytoplasmic-nuclear shuttling of FKBP12-rapamycin-associated protein is involved in rapamycin-sensitive signaling and translation initiation. *Proceedings of the National Academy of Sciences of the United States of America* **97**, 14340-14345 (2000).
200. Bachmann, R.A., Kim, J.H., Wu, A.L., Park, I.H. & Chen, J. A nuclear transport signal in mammalian target of rapamycin is critical for its cytoplasmic signaling to S6 kinase 1. *The Journal of biological chemistry* **281**, 7357-7363 (2006).

REFERENCES

201. Martelli, A.M. *et al.* The emerging multiple roles of nuclear Akt. *Biochimica et biophysica acta* **1823**, 2168-2178 (2012).
202. Wan, X., Harkavy, B., Shen, N., Grohar, P. & Helman, L.J. Rapamycin induces feedback activation of Akt signaling through an IGF-1R-dependent mechanism. *Oncogene* **26**, 1932-1940 (2007).
203. Lickert, H., Bauer, A., Kemler, R. & Stappert, J. Casein kinase II phosphorylation of E-cadherin increases E-cadherin/beta-catenin interaction and strengthens cell-cell adhesion. *The Journal of biological chemistry* **275**, 5090-5095 (2000).
204. McCubrey, J.A. *et al.* GSK-3 as potential target for therapeutic intervention in cancer. *Oncotarget* **5**, 2881-2911 (2014).
205. Scheel, C. & Weinberg, R.A. Cancer stem cells and epithelial-mesenchymal transition: concepts and molecular links. *Seminars in cancer biology* **22**, 396-403 (2012).
206. Larue, L. & Bellacosa, A. Epithelial-mesenchymal transition in development and cancer: role of phosphatidylinositol 3' kinase/AKT pathways. *Oncogene* **24**, 7443-7454 (2005).
207. Heuberger, J. & Birchmeier, W. Interplay of cadherin-mediated cell adhesion and canonical Wnt signaling. *Cold Spring Harbor perspectives in biology* **2**, a002915 (2010).
208. Lamouille, S., Xu, J. & Derynck, R. Molecular mechanisms of epithelial-mesenchymal transition. *Nature reviews. Molecular cell biology* **15**, 178-196 (2014).
209. Hulkower, K.I. & Herber, R.L. Cell migration and invasion assays as tools for drug discovery. *Pharmaceutics* **3**, 107-124 (2011).
210. Wu, K.J. & Yang, M.H. Epithelial-mesenchymal transition and cancer stemness: the Twist1-Bmi1 connection. *Bioscience reports* **31**, 449-455 (2011).
211. Yu, Y., Ramena, G. & Elble, R.C. The role of cancer stem cells in relapse of solid tumors. *Front Biosci (Elite Ed)* **4**, 1528-1541 (2012).
212. Inoki, K. *et al.* TSC2 integrates Wnt and energy signals via a coordinated phosphorylation by AMPK and GSK3 to regulate cell growth. *Cell* **126**, 955-968 (2006).
213. Bowman, C.J., Ayer, D.E. & Dynlacht, B.D. Foxk proteins repress the initiation of starvation-induced atrophy and autophagy programs. *Nature cell biology* **16**, 1202-1214 (2014).
214. Partridge, L. & Bruning, J.C. Forkhead transcription factors and ageing. *Oncogene* **27**, 2351-2363 (2008).
215. Gao, C. *et al.* Autophagy negatively regulates Wnt signalling by promoting Dishevelled degradation. *Nature cell biology* **12**, 781-790 (2010).
216. Jung, C.H., Ro, S.H., Cao, J., Otto, N.M. & Kim, D.H. mTOR regulation of autophagy. *FEBS letters* **584**, 1287-1295 (2010).
217. Noda, T. & Ohsumi, Y. Tor, a phosphatidylinositol kinase homologue, controls autophagy in yeast. *The Journal of biological chemistry* **273**, 3963-3966 (1998).
218. Vadlakonda, L., Pasupuleti, M. & Pallu, R. Role of PI3K-AKT-mTOR and Wnt Signaling Pathways in Transition of G1-S Phase of Cell Cycle in Cancer Cells. *Frontiers in oncology* **3**, 85 (2013).
219. Lepourcelet, M. *et al.* Small-molecule antagonists of the oncogenic Tcf/beta-catenin protein complex. *Cancer cell* **5**, 91-102 (2004).
220. Moon, R.T., Kohn, A.D., De Ferrari, G.V. & Kaykas, A. WNT and beta-catenin signalling: diseases and therapies. *Nature reviews. Genetics* **5**, 691-701 (2004).
221. Gong, A. & Huang, S. FoxM1 and Wnt/beta-catenin signaling in glioma stem cells. *Cancer research* **72**, 5658-5662 (2012).
222. Yoshida, Y., Wang, I.C., Yoder, H.M., Davidson, N.O. & Costa, R.H. The forkhead box M1 transcription factor contributes to the development and growth of mouse colorectal cancer. *Gastroenterology* **132**, 1420-1431 (2007).
223. Munoz, M. & Covenas, R. Neurokinin-1 receptor: a new promising target in the treatment of cancer. *Discovery medicine* **10**, 305-313 (2010).
224. Esteban, F., Munoz, M., Gonzalez-Moles, M.A. & Rosso, M. A role for substance P in cancer promotion and progression: a mechanism to counteract intracellular death signals following oncogene activation or DNA damage. *Cancer metastasis reviews* **25**, 137-145 (2006).

REFERENCES

225. Castro, T.A., Cohen, M.C. & Rameshwar, P. The expression of neurokinin-1 and preprotachykinin-1 in breast cancer cells depends on the relative degree of invasive and metastatic potential. *Clinical & experimental metastasis* **22**, 621-628 (2005).
226. Misawa, K. *et al.* Frequent promoter hypermethylation of tachykinin-1 and tachykinin receptor type 1 is a potential biomarker for head and neck cancer. *Journal of cancer research and clinical oncology* **139**, 879-889 (2013).
227. Cairo, S., Armengol, C. & Buendia, M.A. Activation of Wnt and Myc signaling in hepatoblastoma. *Front Biosci (Elite Ed)* **4**, 480-486 (2012).
228. Nault, J.C. & Villanueva, A. Intratumor molecular and phenotypic diversity in hepatocellular carcinoma. *Clinical cancer research : an official journal of the American Association for Cancer Research* **21**, 1786-1788 (2015).

LIST OF ABBREVIATIONS

4EBP1	4E binding protein 1
AC	Adenylate cyclase
AFP	Alpha feto protein
AMPK	AMP-activated protein kinase
APC	Adenomatous polyposis coli
bFGF	Basic fibroblast growth factor
BWS	Beckwith-Wiedemann syndrome
BSA	Bovine serum albumin
cAMP	Cyclic adenosine monophosphate
CDK1	Cyclin-dependent kinase 1
CHK1	Checkpoint kinase 1
CK1 α	Casein kinase 1 α
CKII	Casein kinase II
COG	Children's oncology group
CSC	Cancer stem cells
DAG	Diacylglycerol
DAPI	4,6-diamidino-2-phenylindole
DEPTOR	DEP domain-containing mTOR-interacting protein
DKK	Dickkopfs
DLK1	Delta-Like 1 Homolog
DTT	Dithiothreitol
DMSO	Dimethyl sulfoxide
EDTA	Ethylendiamintetraacetate
EGF	Epidermal growth factor
EGFR	Epidermal growth factor receptor
EGTA	ethylene glycol tetraacetic acid
EMT	Epithelial-mesenchymal transition
EpCAM	Epithelial cell adhesion molecule
FACS	Fluorescence activated cell sorting
FAP	Familial adenomatosis polyposis
FCS	Fetal calf serum

LIST OF ABBREVIATIONS

FDA	Food and drug administration
FOXM1	Forkhead box M1
FO XK1	Forkhead box K1
GAP	GTPase activating protein
GDP	Guanosine 5'-diphosphate
GEP	Granulin/epithelin precursor
GFP	Green fluorescent protein
GPCR	G-protein coupled receptors
GPOH	German pediatric oncology hematology group
GSK3 β	Glycogen synthase kinase 3 β
GTP	Guanosine 5'-triphosphate
HGF	Hepatocyte growth factor
IGF	Insulin like growth factor
IGF1R	Insulin-like growth factor 1 receptor
IGFBP	Insulin-like growth factor binding proteins
HHIP	Hedgehog-interacting protein
Int1	Integration 1
IRS	Insulin receptor substrate
KLF4	Kruppel-like factor 4
LEF	Lymphoid enhancer-binding factor
LiCl	Lithium chloride
LRP	Low-density lipoprotein receptor-related protein
MAPK	Mitogen-activated protein kinases
MDR	Multidrug resistance
mLST8	Mammalian Sec13 protein with lethal 8
MnK1	Mitogen-activated protein kinase-interacting kinase 1
mTOR	Mammalian target of rapamycin
mTORC	Mammalian target of rapamycin complex
MTT	1-(4,5-dimethylthiazol-2-yl)-3,5-diphenylformazan
NK1R	Neurokinin-1 receptor
NK2R	Neurokinin-2 receptor
NK3R	Neurokinin-3 receptor
NK1R-fl	Full length form of NK1R

LIST OF ABBREVIATIONS

NK1R-tr	Truncated form of NK1R
OCT4	Octamer-binding transcription factor 4
p70S6K	p70 ribosomal S6 kinase
PARP	poly ADP ribose polymerase
PBS	Phosphate-buffered saline
PDK1	Phosphoinositide-dependent kinase-1
PH	Pleckstrin homology
PI	Propidium iodide
PI3K	Phosphatidylinositol 3-kinase
PIKK	Phosphatidylinositol 3-kinase-related kinase
PIP2	Phosphatidylinositol-4,5-diphosphate
PIP3	Phosphatidylinositol-3,4,5-triphosphate
PKA	Protein kinase A
PKC α	Protein kinase C α
PLC	Phospholipase C
PLK1	Polo-Like Kinase 1
POSTTEXT	POST-Treatment EXTent of Tumor
PRAS40	Proline-rich AKT substrate of 40kDa
PRETEXT	PRE-Treatment tumor EXTension
PTEN	Phosphatase and tensin homologue
JAK	Janus kinase
JPLT	Japanese study group for pediatric liver tumor
RAPTOR	Regulatory-associated rotein to mTOR
Rheb	Ras homolog enriched in brain
Rictor	Rapamycin-insensitive companion of TOR
RPPA	Reverse-phase protein array
RTK	Receptor tyrosine kinase
SDS	Sodium dodecyl sulfate
SFA	Sphere formation ability
SFRP	Secreted frizzled-related proteins
SGK1	Serum and glucocorticoid-induced protein kinase 1
SH2	Src Homology 2
SIN1	Stress-activated map kinase-interacting protein 1

LIST OF ABBREVIATIONS

SIOPEL	International society of pediatric oncology group
SOX2	SRY-related HMG-box 2
SP	Substance P
STAT	Signal transducer and activator of transcription
STF	Super TOP/FOP
TBE	Tris, Borate, EDTA
TBP	TATA box binding protein
TCF	T-cell factor
TSC	Tuberous sclerosis complex

Eidesstattliche Versicherung

Garnier, Agnès

Ich erkläre hiermit an Eides statt, dass ich die vorliegende Dissertation mit dem Thema

Neurokinin-1 receptor as a therapeutic target in hepatoblastoma

selbständig verfasst, mich außer der angegebenen keiner weiteren Hilfsmittel bedient und alle Erkenntnisse, die aus dem Schrifttum ganz oder annähernd übernommen sind, als solche kenntlich gemacht und nach ihrer Herkunft unter Bezeichnung der Fundstelle einzeln nachgewiesen habe.

Ich erkläre des Weiteren, dass die hier vorgelegte Dissertation nicht in gleicher oder in ähnlicher Form bei einer anderen Stelle zur Erlangung eines akademischen Grades eingereicht wurde.

Ort, Datum

Unterschrift Doktorand